Government of **Western Australia**
Department of **Mines and Petroleum**

RECORD 2012/13

FINE-FRACTION GEOCHEMISTRY OF REGOLITH FROM THE EAST WONGATHA AREA, WESTERN AUSTRALIA: TRACING BEDROCK AND MINERALIZATION THROUGH COVER

by
PA Morris



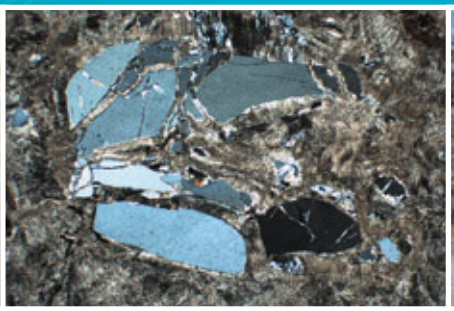


Geological Survey of Western Australia

Government of **Western Australia**
Department of **Mines and Petroleum**

Record 2012/13

FINE-FRACTION GEOCHEMISTRY OF REGOLITH FROM THE EAST WONGATHA AREA, WESTERN AUSTRALIA: TRACING BEDROCK AND MINERALIZATION THROUGH COVER

by
PA Morris

Perth 2012

Geological Survey of Western Australia

MINISTER FOR MINES AND PETROLEUM
Hon. Norman Moore MLC

DIRECTOR GENERAL, DEPARTMENT OF MINES AND PETROLEUM
Richard Sellers

EXECUTIVE DIRECTOR, GEOLOGICAL SURVEY OF WESTERN AUSTRALIA
Rick Rogerson

REFERENCE
The recommended reference for this publication is:
Morris, PA 2012, Fine-fraction geochemistry of regolith from the east Wongatha area, Western Australia: tracing bedrock and mineralization through cover: Geological Survey of Western Australia, Record 2012/13, 58p.

National Library of Australia Card Number and ISBN 978-1-74168-468-1

Grid references in this publication refer to the Geocentric Datum of Australia 1994 (GDA94). Locations mentioned in the text are referenced using Map Grid Australia (MGA) coordinates, Zone 51. All locations are quoted to at least the nearest 100 m.

Published 2013 by Geological Survey of Western Australia
This Record is published in digital format (PDF) and is available online at <http://www.dmp.wa.gov.au/GSWApublications>.

Further details of geological products and maps produced by the Geological Survey of Western Australia are available from:
Information Centre
Department of Mines and Petroleum
100 Plain Street
EAST PERTH WESTERN AUSTRALIA 6004
Telephone: +61 8 9222 3459 Facsimile: +61 8 9222 3444
www.dmp.wa.gov.au/GSWApublications

Contents

Figures

Tables

Appendices (CD-ROM)

1. Sample duplicate analyses
2. Site duplicate analyses
3. Reference materials and blank analyses

Fine-fraction geochemistry of regolith from the east Wongatha area, Western Australia: tracing bedrock and mineralization through cover

by

PA Morris

Abstract

In areas of thick and allochthonous regolith, there is usually no genetic relationship between surface soil (regolith) and bedrock or bedrock-hosted mineralization. Furthermore, regolith composition may not be a proxy for underlying bedrock, and have limited application for regional geochemical surveys. However, in the east Wongatha area of central south Western Australia, where cover is thick and transported, both bedrock and bedrock-hosted mineralization can be identified by analysis of the fine (<50 μm; silt to clay) fraction of regolith using a partial digest. Dry screening out the coarse fraction excludes the potentially barren, eolian-derived quartz sand, whereas the partial digest releases the introduced (i.e. exogenic) component of bedrock or mineralization of the regolith, and further minimizes the input of the eolian component. Analysis of 50 samples following deionized water digestion shows that this exogenic component is either labile and/or microparticulate. The results of this study indicate that the fine fraction of thick and allochthonous regolith can be used to detect both bedrock and bedrock-hosted mineralization through thick cover.

KEYWORDS: regolith, partial digest, silt, clay, geochemistry, mineralization.

Introduction

In areas of thick regolith cover, the composition of surface regolith may provide few clues about either the composition of the underlying bedrock or bedrock-hosted mineralization. This is especially the case in areas of transported (i.e. allochthonous) regolith. However, regolith is commonly the only universally available sample medium for regional geochemical surveys. In this Record, the methodology and results of a multi-element regolith geochemistry program undertaken in the sandplain-dominated east Wongatha area of central south Western Australia are discussed. The purpose of this program was to examine the suitability of the fine-fraction (<50 μm; silt and clay) chemistry of regolith as an exploration tool in detecting bedrock and bedrock-hosted mineralization through thick cover, much of which is allochthonous. Here, 'cover' can include unmineralized bedrock as well as regolith.

The east Wongatha area, located approximately 250 km east-northeast of Kalgoorlie (Fig. 1), spans the Yilgarn Craton, Albany–Fraser Orogen, and Gunbarrel Basin (Fig. 2). Of these, the Yilgarn Craton and Albany–Fraser Orogen have demonstrated bedrock-hosted mineralization. Uranium, base metal, and gold mineralization has also been reported from the Gunbarrel Basin, close to the margin with the Yilgarn Craton and Albany–Fraser Orogen (Energy and Minerals Australia, 2010a), as shown in Figure 3.

The east Wongatha project area covers six 1:100 000 map sheets on the eastern part of MINIGWAL[1] (SH 51-7; Bunting and Boegli, 1977) and the western part of PLUMRIDGE (SH 51-8; Van De Graaff and Bunting, 1977) 1:250 000 sheets between latitudes 29°00'S and 30°00'S, and longitudes 123°00'E and 125°00'E (Figs 1 and 3). Regolith from 835 sites at a nominal density of 1/16 km^2 has been collected, with all but seven of these samples from the MINIGWAL, NARNOO, KAKAROOK, BOWDEN and MEINYA 1:100 000 map sheets. The total area encompassed is approximately 12 500 km^2 (Fig. 3). Seventeen samples were collected by vehicle in November 2009, and the remainder were collected by helicopter between 6 March and 20 March 2010.

Access to the east Wongatha area is by unsealed roads from either Kalgoorlie (via Pinjin Station), or via the access road to the Trans Australia Railway (known as the Transline). Apart from Pinjin Station to the west of the project area, there are no permanent inhabitants and few

[1] Capitalized map names refer to 1:100 000 Geological Series maps, unless otherwise indicated. Map numbers of the form SH 51-7 refer to 1:250 000 Geological Series.

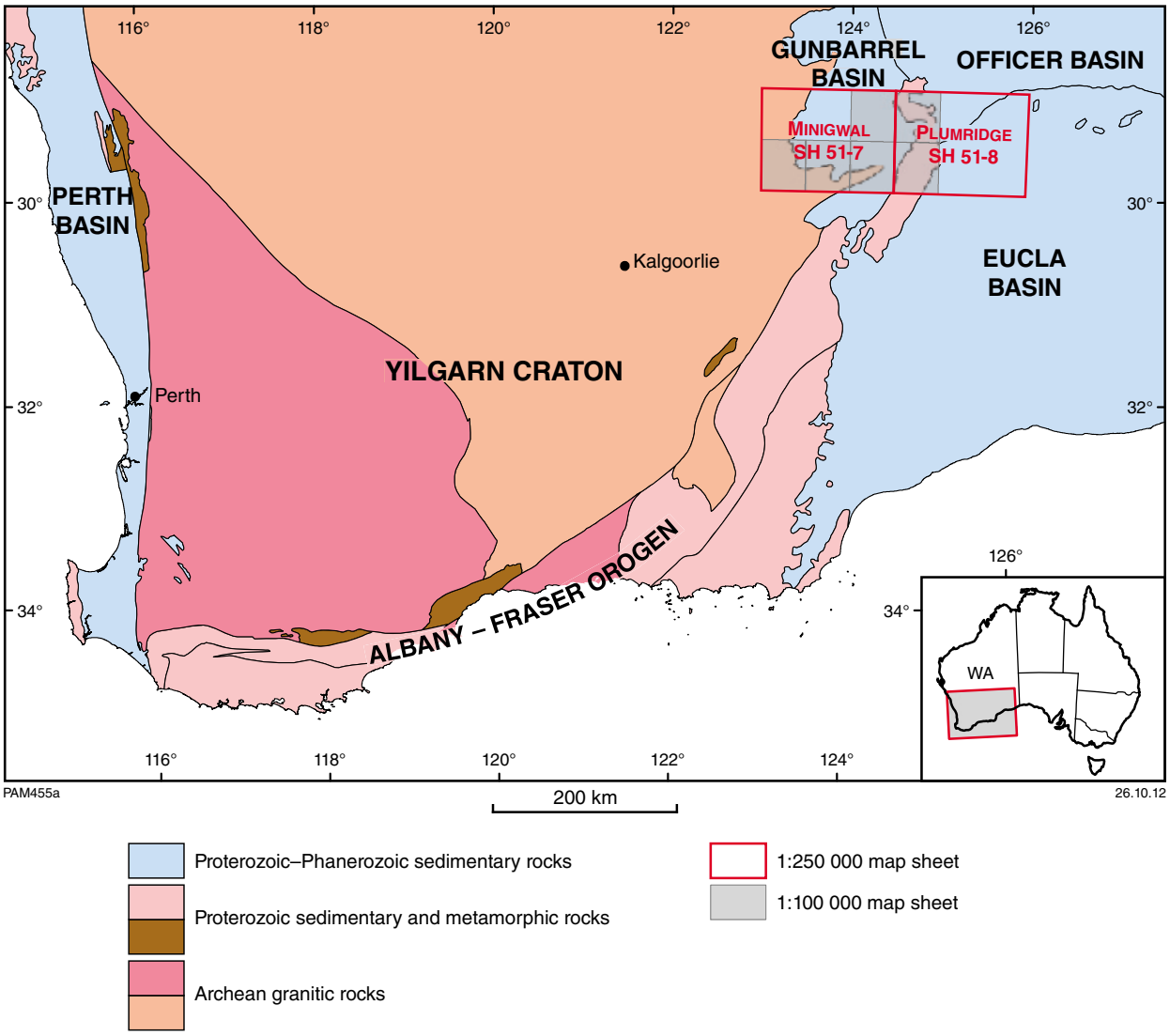

Figure 1. Location of the east Wongatha project area (six 1:100 000 map sheets shaded grey) and simplified geology of southern Western Australia.

roads and tracks, although the increased level of mineral exploration activity has resulted in upgrading of existing roads and tracks and development of new ones. Away from roads and tracks, access is slow and difficult due to the extensive cover of soft sand and the localized development of sand dunes (Fig. 4a,b).

Prior to commencement of the sampling program, consultation with Traditional Owners from the east Wongatha area was facilitated by the Central Desert Native Title Services Limited. This culminated in an on-site heritage survey being carried out on 4–5 March 2010.

Climate

The east Wongatha area is semi-arid to arid, with the majority of rainfall (on average, about 200 mm/year) resulting from summer thunderstorms, but rain can fall throughout the year. The area is classed as desert, as rainfall is exceeded by an annual evaporation rate of more than 2700 mm (Bunting and Boegli, 1977).

Data collected by Energy and Minerals Australia Ambassador climate monitoring station at their Mulga Rock exploration camp during the period of soil sampling (6–20 March 2010) showed a temperature range of 7.7 – 39°C (average 23°C; n = 460), an average humidity of 45% (range 5 to 90%; n = 460), and total rainfall of 0.1 mm, which fell between midday and 1.00 pm on Wednesday 17 March.

Vegetation

MINIGWAL (SH 51-7) and PLUMRIDGE (SH 51-8) lie in the Helms Botanical District, in the northern part of the Nullarbor area of Beard (1975), and close to the southern

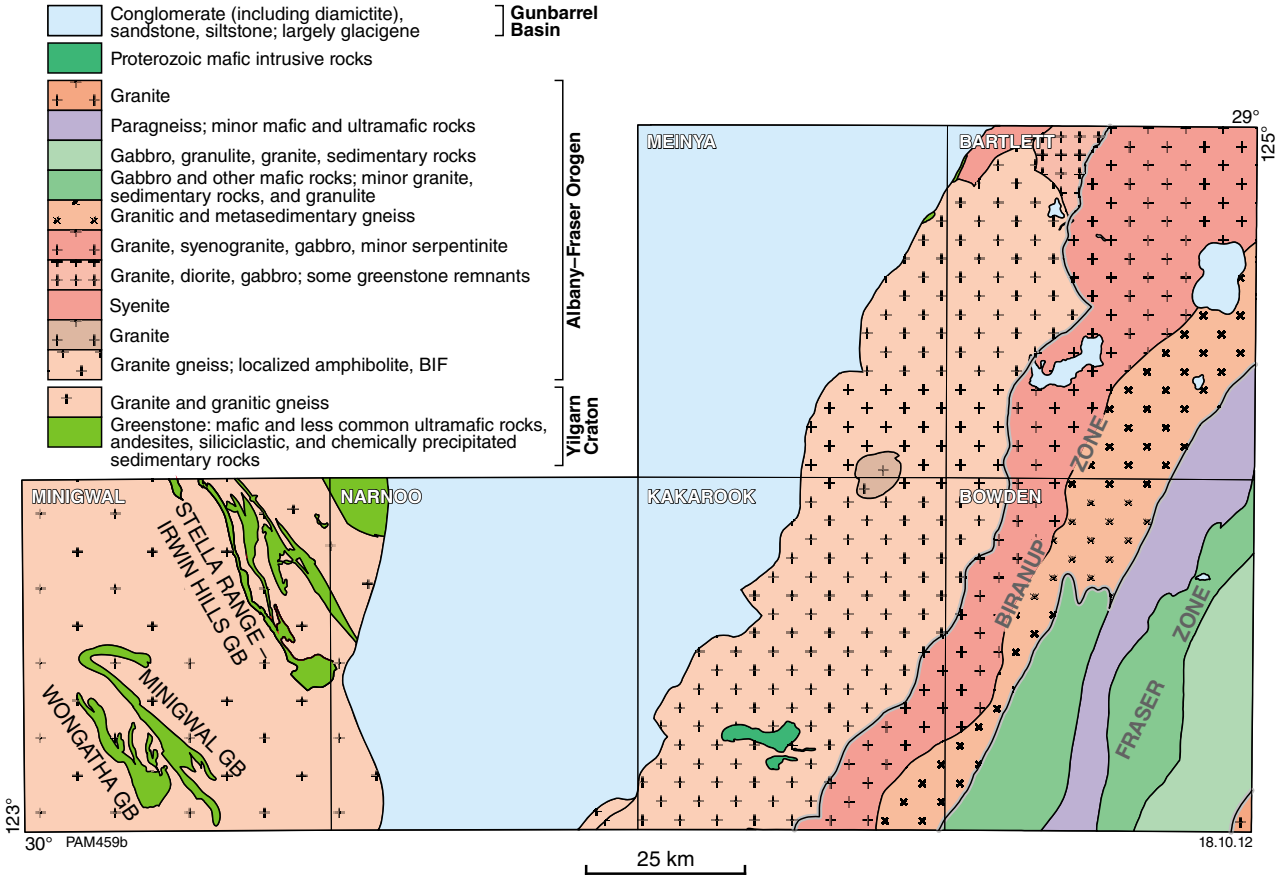

Figure 2. Simplified 1:500 000 interpreted bedrock geology (after Spaggiari et al., 2011) underlying the project area.

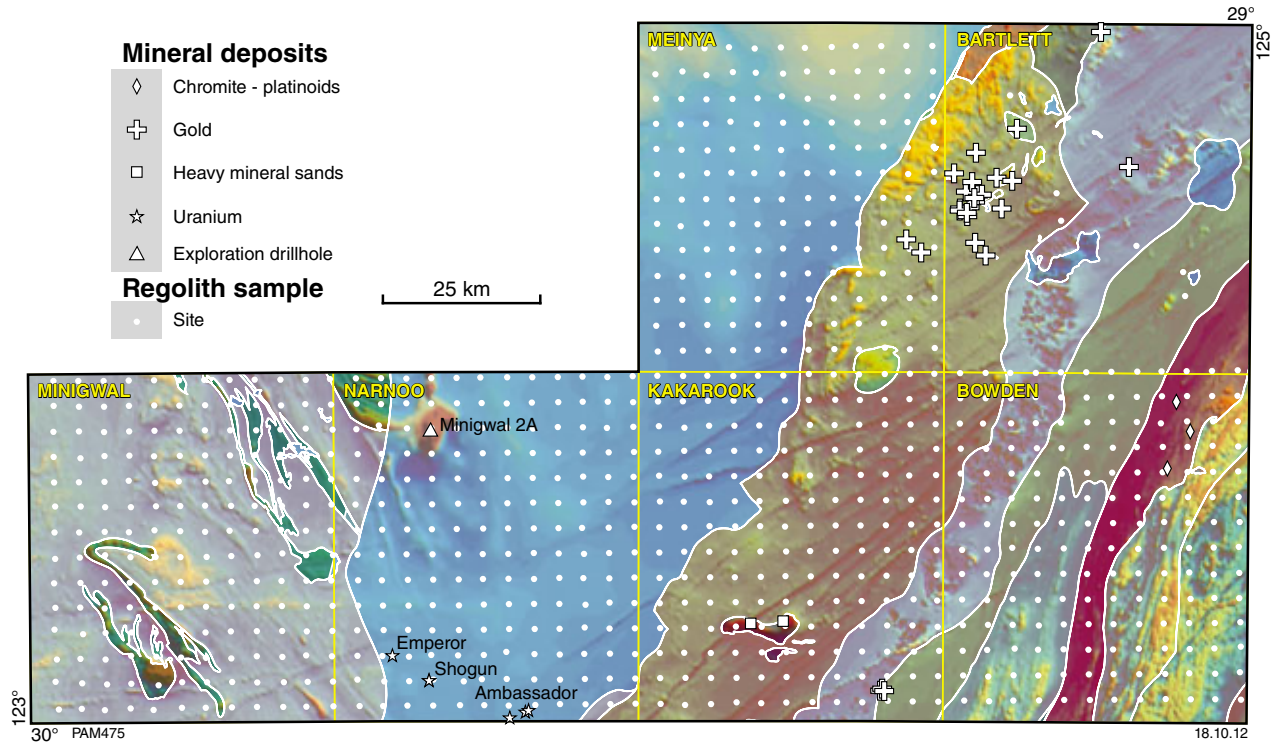

Figure 3. Sample sites spaced at one per 16 km² shown against interpreted bedrock geology and total magnetic intensity reduced to pole. Also shows locations of known sites of bedrock mineralization, extracted from the Department of Mines and Petroleum's MINEDEX database.

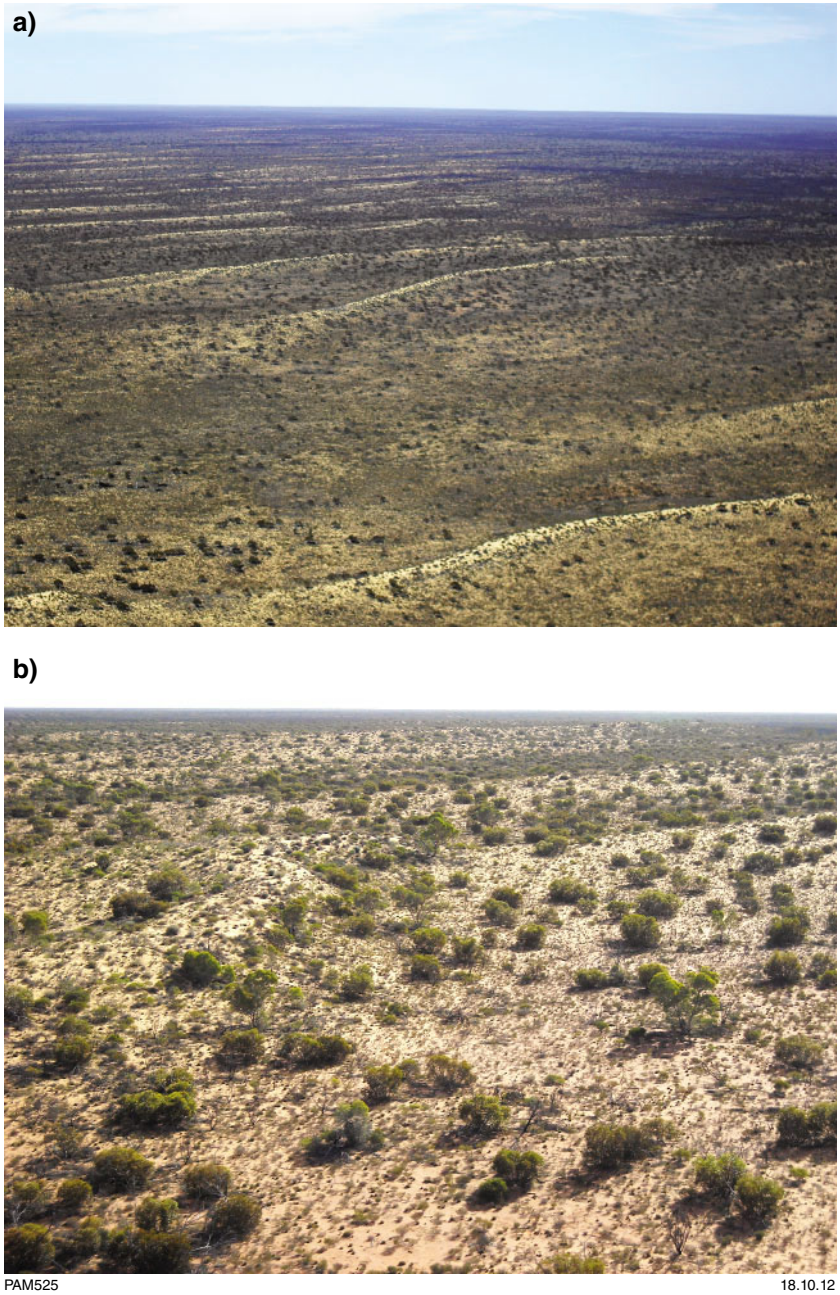

Figure 4. a) and b) Oblique aerial photographs of typical sandplain-dominated country of the east Wongatha area.

margin of the Great Victoria Desert area of Beard (1974). The most comprehensive description of vegetation throughout the Helms Botanical District is provided by Beard (1974), who noted that vegetation is dominated by *Eucalyptus gongylocarpa* (marble gum) and *Triodia basedowii* (spinifex). Bunting and Boegli (1977) noted that the most common vegetation association on MINIGWAL (SH 51-7) is spinifex (*Triodia*) and mallee (*Eucalyptus spp*), with less common marble gums and native pine (*Callistris*), which occupy sandplain, some of which supports sand dunes. Van de Graaff and Bunting (1977) noted that sandplain areas on PLUMRIDGE (SH 51-8) also support mulga (*Acacia aneura*). Sheetwash and less common areas of in-situ soils support mulga (*Acacia spp*), whereas salt-tolerant plants such as saltbush (*Atriplex*), bluebush (*Kochia*), and samphire (*Arthrocnemum*) are found close to Lake Minigwal in the northwestern part of the sampling area. Grass trees (*Xanthorrea thorntonii*) form scattered groups.

Vegetation has been used as a sample medium for regional geochemical surveys (e.g. Reid et al., 2010), and information about the distribution of different vegetation types was collected during the present study. Spinifex is the most abundant vegetation type at 459 sites (55% of all sites; Fig. 5a), but was not recorded at 175 (21%) of

sites, most of which are either close to lake systems in the northwest part of MINIGWAL, or over parts of the Yilgarn Craton. Mulga was not recorded at 212 sites (25%), but was the dominant vegetation type at 116 sites (14%) (Fig. 5b). Eucalypts were the least abundant vegetation type (Fig. 5c), dominant at only 43 (5%) of sites, and not observed at 477 sites (57%).

Regional geology

The east Wongatha project area spans three tectonic units, the Archean Yilgarn Craton, the Proterozoic Albany–Fraser Orogen, and the Paleozoic Gunbarrel Basin (Figs 1 and 2), with a small portion of the Eucla basin encroaching on the southeastern edge of BOWDEN. Determining the actual extent of these units and their lithology is made difficult by the small area of exposed bedrock, and the extensive and contiguous cover of regolith. Widespread development of sandplain, some of which supports dunes, indicates that most of the regolith is allochthonous (i.e. transported), so it may not be a reliable indicator of the extent or composition of the underlying bedrock. Instead, determining the bedrock geology has relied heavily on extrapolating from the few outcrops and available drillhole data, and using remotely-sensed datasets, in particular geophysics (Fig. 3). The interpreted bedrock geology used here is that of Spaggiari et al. (2011; Figs 2, 3).

Yilgarn Craton

The Archean Yilgarn Craton hosts world-class gold and nickel mineralization, as well as base metal deposits (e.g. Barley et al., 1998; Blewett et al., 2010; McCuaig et al., 2010), and there is a well-established relationship between mineralization and greenstone belts. Accordingly, Yilgarn Craton greenstones found in the western part of the east Wongatha area have been actively explored for nickel and gold mineralization.

The Yilgarn Craton in the project area is part of the Burtville Terrane, the easternmost of the six terranes identified in the Yilgarn Craton by Cassidy et al. (2006), based on lithological associations, structural analysis, isotopic data, geochronology, and seismic interpretation. In the east Wongatha area, the Yilgarn Craton is dominated by variably metamorphosed granitic rocks, with two broad belts of northwest-trending greenstones. In the northeast of MINIGWAL is the Stella Range – Irwin Hills greenstone belt, and in the southwest of MINIGWAL are two subparallel greenstone belts, informally referred to here as the Minigwal and Wongatha greenstone belts.

Due to the lack of outcrop, the lithological content of these greenstone belts is not well understood, but rock types including basalt, komatiite, and siliciclastic and chemical sedimentary rocks have been recorded by Spaggiari et al. (2011). For this project, a variety of variably metamorphosed granitic rocks and gneisses have been collectively described as 'Yilgarn Craton granitic rocks'. Similarly, variably deformed and metamorphosed mafic or felsic volcanic rocks, intrusive mafic igneous rocks, and siliciclastic and chemically precipitated sedimentary rocks are collectively referred to as 'Yilgarn Craton greenstones'.

Albany–Fraser Orogen

The Albany–Fraser Orogen consists of a series of northeast-trending lithological associations, including metagranitic rocks, metagabbro, granulites, quartz- and feldspar-rich gneisses, syenogranitic rocks, and greenstones. The orogen has been a focus of recent mineral exploration activity following discovery of significant gold mineralization at the Tropicana–Havana (Doyle et al., 2009; Spaggiari et al., 2011; Fig. 3). Combining regional geophysical data, information from key outcrops, geochronology, and lithogeochemistry (Kirkland et al., 2010; Spaggiari et al., 2010; Spaggiari et al., 2011) has resulted in a better understanding of the geological history of the Albany–Fraser Orogen (cf. Myers, 1990), including its relationship to the Yilgarn Craton. The orogen is now seen as comprising reworked parts of the Yilgarn Craton and crustal fragments accreted on to the craton margin, but the extent and intensity of metamorphism and deformation, and the paucity of outcrop, has created difficulties in reconstructing the geological history. Zircon U–Pb geochronology and Hf isotope data (Kirkland et al., 2010) have made an important contribution to the interpretation.

In the east Wongatha area, the Albany–Fraser Orogen is mainly represented by reworked parts of the Yilgarn Craton margin, as indicated in part by the presence of greenstone selvedges. Lithologies include granite and gneiss, gabbro, syenite, and fine-grained mafic rocks. Aeromagnetic data have been useful in identifying more highly magnetized rocks (likely to be more mafic in composition), including an 11-km long east–west intrusion of Proterozoic mafic rocks in the southern part of KAKAROOK.

Officer and Gunbarrel Basins

Elements of both the Yilgarn Craton and Albany–Fraser Orogen are unconformably overlain by Neoproterozoic to ?mid-Cambrian sedimentary rocks of the Officer Basin (Iasky, 1990). The east Wongatha area spans part of the westernmost Officer Basin, where Paleozoic to Mesozoic rocks were assigned by Hocking (1994) to the Gunbarrel Basin. The thickness of these sedimentary rocks is not well known. Elongate troughs of Permian glacigene rocks more than 300 m deep are inferred from geophysical data and from drilling (Spaggiari et al., 2011). In Minigwal 2A (Fig. 3), about 8 m of unconsolidated red sand overlies 410 m of Cenozoic sedimentary rock, consisting mainly of clay and shale, with lesser amounts of breccia and conglomerate (Perincek, 1998). This succession unconformably overlies a banded iron-formation (BIF), interpreted to represent Yilgarn Craton basement, which coincides with an area of more magnetized rock (Fig. 3). Uranium, gold, REE (rare earth elements: La – Lu), and base metal mineralization has been discovered in Phanerozoic sedimentary rocks in the southern part of the Gunbarrel Basin close to the Yilgarn Craton margin.

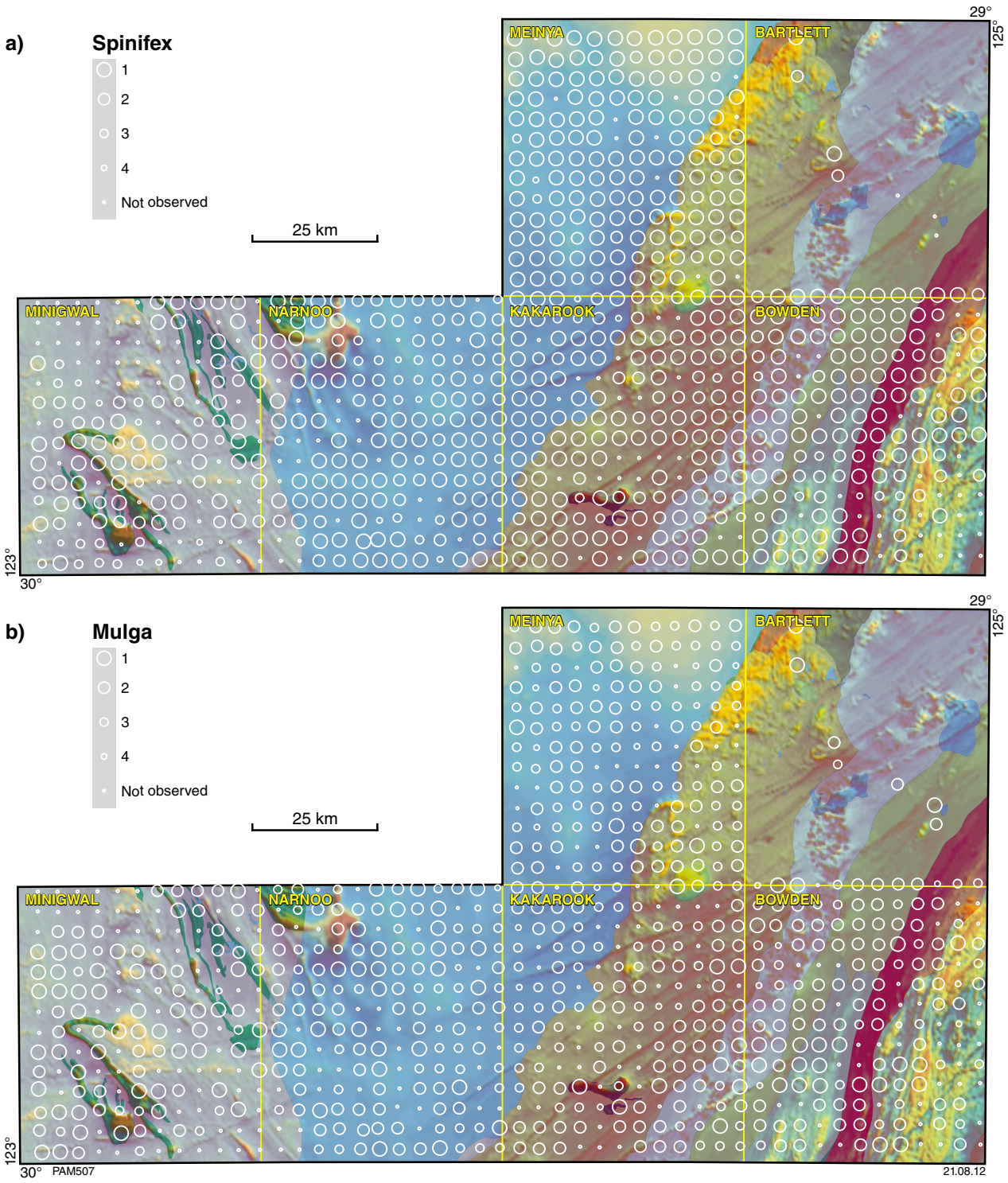

Figure 5. Relative abundance of different vegetation types in the east Wongatha project area: a) Spinifex; b) mulga; c) eucalypt. 1 is most abundant and 4 is least abundant; dots – not observed.

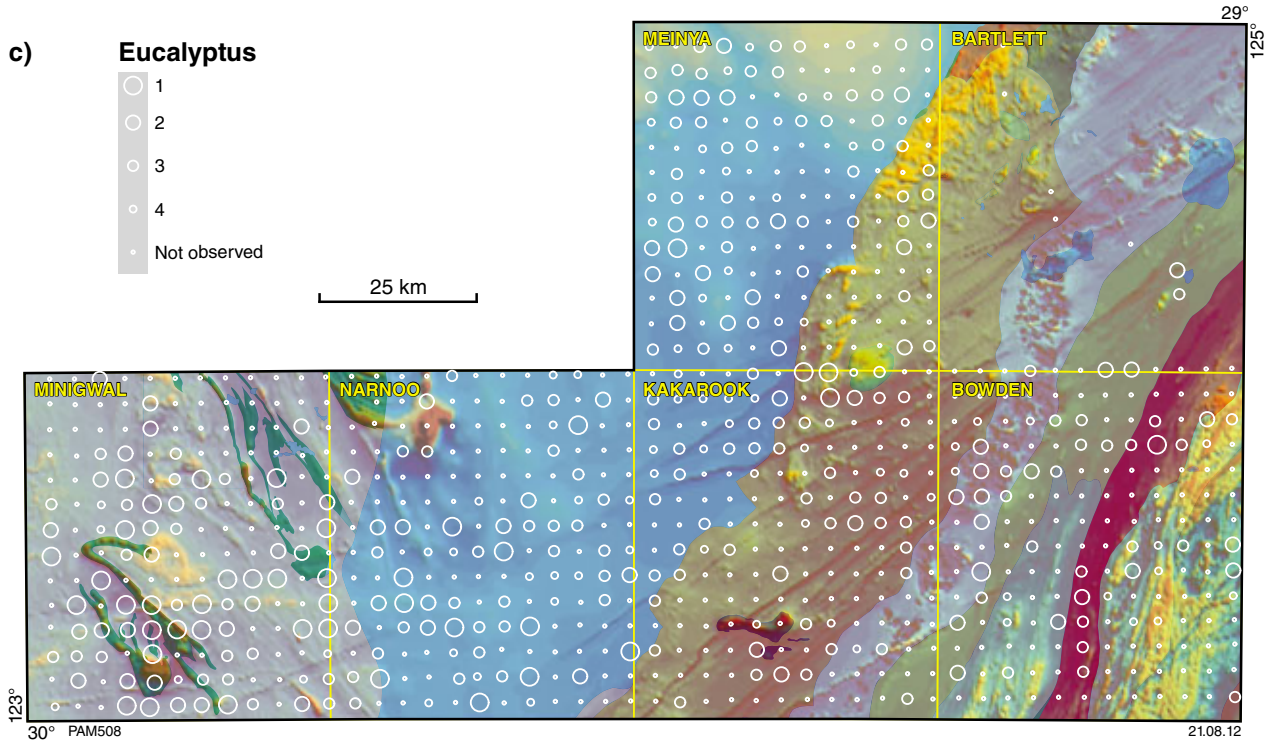

Figure 5. continued

Mineralization and exploration activity

An extract from the Department of Mines and Petroleum's (DMP) MINEDEX database <http:www.dmp.wa.gov.au/minedex> (Fig. 3) shows a concentration of gold deposits on BARTLETT, related to the Tropicana mineralization. Recent data indicate a resource of 78.6 million tonnes grading at 2.12 g/t for 5.36 Moz of gold (Spaggiari et al., 2011). Mineralization is hosted in reworked Archean rocks of the Yilgarn Craton that have undergone fluid-present granulite facies metamorphism (Doyle et al., 2009). The gold deposits are found in a 1.2 x 5 km long, northeast-trending belt, consisting of a main ore zone and several subordinate zones between 2 and 50 m thick. The Tropicana deposits are hosted in garnet gneiss, whereas the dominant rock type hosting mineralization at Havana is quartzofeldspathic gneiss. Free gold is typically 10–30 µm diameter and hosted in pyrite, although is also less commonly found along fractures in silicate minerals. Gold mineralization has been attributed to shearing, which post-dated development of a gneissic fabric. Precipitation of sulfides and gold took place from a silica-undersaturated fluid at about 350°C. Extensive and contiguous Permian to contemporary cover up to 15 m thick is reported, effectively obscuring the host rocks. Depletion of gold in saprolite has resulted in only subtle surface soil anomalies with a maximum of 31 ppb (Doyle et al., 2009).

Mineralization in the Mulga Rocks area (Emperor, Shogun, Ambassador; Fig. 3) has been summarized in a series of stock exchange reports released by Energy and Minerals Australia Limited (Energy and Minerals Australia, 2010a,b,c), and in a paper by Douglas et al. (2011). Uranium mineralization is found both as a lignite- and sandstone-hosted resource in mid-Eocene sedimentary rocks of the Narnoo Basin, a part of the Eucla Basin succession (Energy and Minerals Australia, 2010b, figure 3). A mid-Eocene stratigraphy comprising three units (upper lignite, lower lignite, sandstone) has been delineated, unconformably overlying Cretaceous rocks and Permian glacigene sedimentary rocks of the Paterson Formation, both of which are part of the Gunbarrel Basin. The mineralized succession is fault bounded and forms a series of horsts and grabens.

Other instances of mineralization are found in more confined parts of the stratigraphy. Most base metal mineralization is confined to organic-rich units, whereas gold and silver mineralization is hosted along with uranium in the underlying reduced sandstone. Along with uranium, elevated concentrations of vanadium, scandium, and rare earth elements (REE) are found, possibly as compounds adsorbed onto organic material, together with base metals hosted in finely disseminated sulfides. Gold grades up to 6.5 g/t and silver up to 28 g/t Au (Energy and Minerals Australia, 2010c). Gold is in its native form and typically less than 5 µm in diameter.

Douglas et al. (2003) noted that there is no surface regolith expression of the Mulga Rocks mineral deposit, apart from anomalous radon (see discussion by Butt and Gole, 1985), although Gray (2001) noted some enrichment of elements such as HCO_3-, PO_4^{3-}, barium and tungsten in some groundwaters

Regolith-landform mapping

A regolith landform map for the east Wongatha area (McGuinness, 2010) has been compiled using Landsat™ imagery, 1:250 000-scale geological maps for MINIGWAL (SH 51-7; Bunting and Boegli, 1977) and PLUMRIDGE (SH 51-8; van de Graaff and Bunting, 1977), orthophotographs, GoogleEarth™ imagery, digital elevation model (DEM) data, open-file company reports, and radiometric data. Field checking of selected areas was carried out in November 2009.

A simplified version of this map (Fig. 6) shows that in situ (i.e. residual) regolith developed over bedrock, or regolith representing remnants of previous landforms (relict regolith), accounts for only three percent by area. Only relict or residual regolith may provide any direct link to bedrock lithologies. Most of it is found as either calcrete (commonly spatially associated with paleodrainages) or silcrete, the latter usually overlying, or adjacent to, rocks of the Permian Paterson Formation in the Gunbarrel Basin. Thus, of the two, only silcrete can be directly related to bedrock, although minor silcrete and silica-rich sand is spatially associated with some Yilgarn Craton granitic rocks.

Colluvium (14% by area) occupies several different landscape positions. In sandplain depressions, colluvium is dominantly quartz-rich sand, with less common silt, clay, ferromagnesian granules, silcrete, and calcrete. Colluvium close to exposed or poorly outcropping bedrock and duricrust is more ferruginous and siliceous, whereas calcrete-dominated colluvium (three percent by area) is mostly restricted to the eastern part of the project area over parts of the Albany–Fraser Orogen. Sheetwash is found in paleodrainages, as fan deposits adjacent to some lake systems, and as reworked parts of sandplain. A calcrete layer between 20 and 60 cm depth, patchily distributed mainly in the eastern part of the area, has been interpreted as a sheetwash deposit.

Alluvial deposits are confined to drainage depressions, and account for two percent of regolith. Most contemporary streams are ephemeral and contain sand (most likely reworked eolian material), silt, and clay. Elongate drainage depressions found in sandplain, interpreted as paleochannels, contain sand, silt, and clay, as well as ferruginous and calcareous material. Lacustrine deposits (approximately five percent by area) are largely confined to lake systems in the northwest part of MINIGWAL and on parts of BARTLETT.

The majority of the east Wongatha area is a mixture of residual and eolian sandplain, which accounts for approximately 70% of regolith by area, or greater than 11 400 km^2. In some areas, east-southeast trending dunes between 5 and 10 m high, and spaced from 50 m to 2 km, are developed. In these areas, the regolith is dominated by well-sorted, frosted, and polished quartz sand indicative of some eolian transport, with a few percent clay- and silt-grade material. This is typical of eolian sandplain deposits. In other areas, dunes are less common and, although the sandplain is still dominated by quartz-rich sand, the regolith is more heterogeneous, in terms of the amount of quartzofeldspathic, ferruginous, and calcareous material. This suggests some influence from underlying bedrock. The undulating nature of the sandplain in some areas may reflect the proximity of bedrock to the surface.

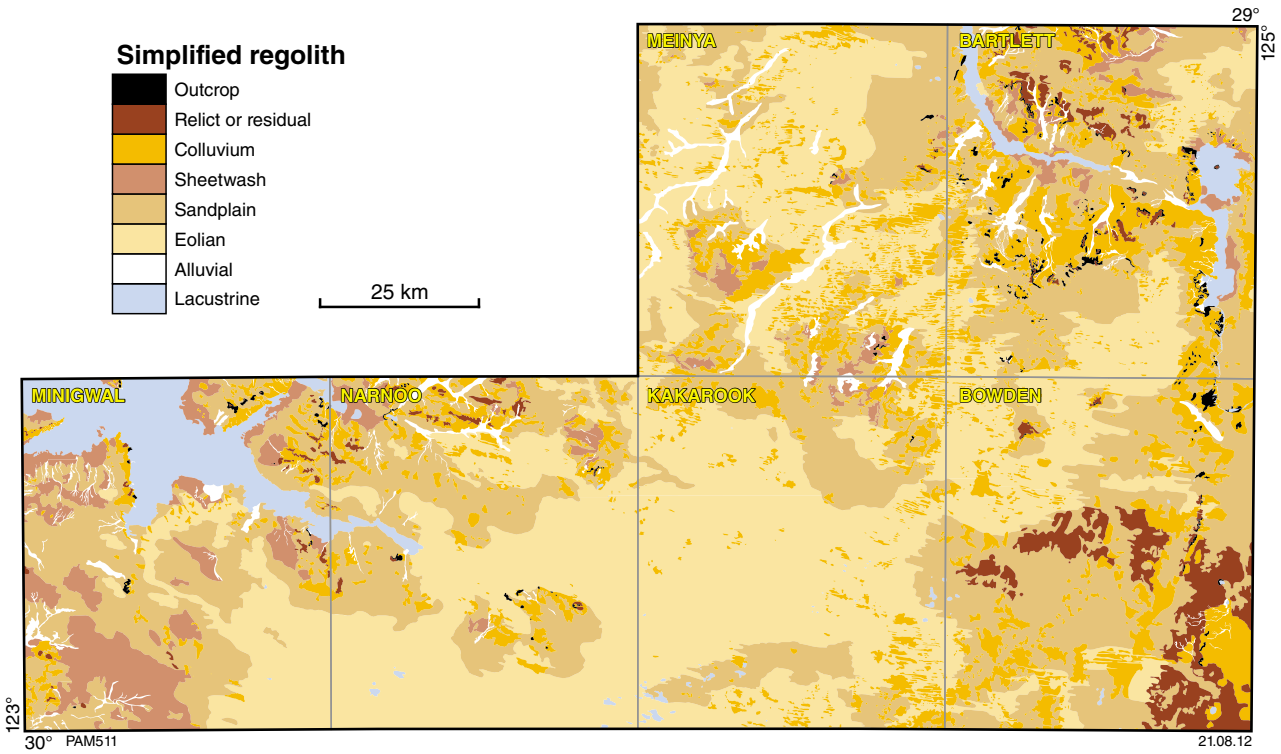

Figure 6. Simplified regolith-landform map (McGuinness, 2010).

Thickness of cover

In most parts of Western Australia, 'cover' refers to the typically thick and extensive blanket of regolith, but it can also include barren rock successions that cover mineralized bedrock. In the east Wongatha area, Phanerozoic sedimentary rocks that cover parts of the Yilgarn Craton may fall into this category. The thickness of the sedimentary rocks is only known from drillhole Minigwal 2A (Perincek, 1998; Fig. 3), where the succession is greater than 400 m thick.

Some knowledge of the thickness of regolith, and whether all or part of the regolith has been developed in situ or has been transported, are important factors when planning regional geochemical surveys, or when interpreting the results of such surveys (e.g. Gray et al., 1999; Anand and Butt, 2010). Information about regolith thickness is available from some reports provided by exploration companies to DMP as part of reporting requirements. An extract of data for 950 drillholes, largely from Narnoo (but extending onto Minigwal, Lightfoot, and Moonyoora), is largely confined to the Irwin Hills – Stella Range greenstone belt on the Yilgarn Craton, close to the Gunbarrel Basin margin (Fig. 7). These drillholes contain sufficient information (i.e. trend and plunge, collar coordinates, recorded depth to regolith–bedrock interface) to allow an estimate of the regolith–bedrock interface depth. From these data, the average depth of the this interface is 55 m, with a range of 5–121 m (Fig. 8). Closer examination (Geological Survey of Western Australia, 2009) of these data shows that this interface can vary markedly over a short distance, indicating a rugged basement topography.

Other open-file exploration company data (Geological Survey of Western Australia, 2009) are less definitive, in that in some cases, the depth to the regolith–bedrock interface has not been recorded. Instead, the total depth for RAB drilling, for example, is given. Data for 197 holes

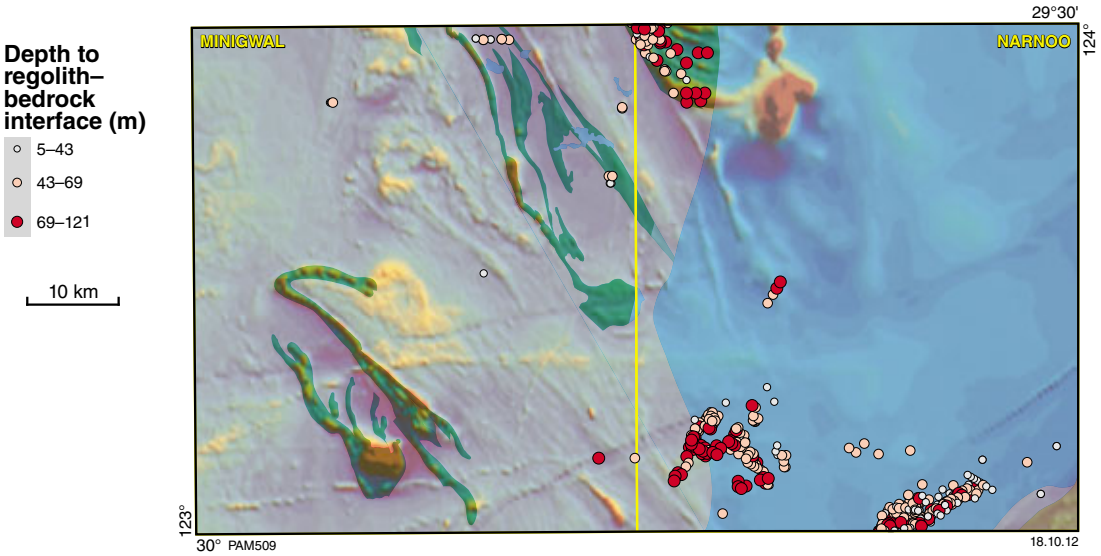

Figure 7. Depth to regolith–bedrock interface (metres) for open-file data from DMP's WAMEX mineral exploration database. All depths have been corrected for the plunge of the drillhole.

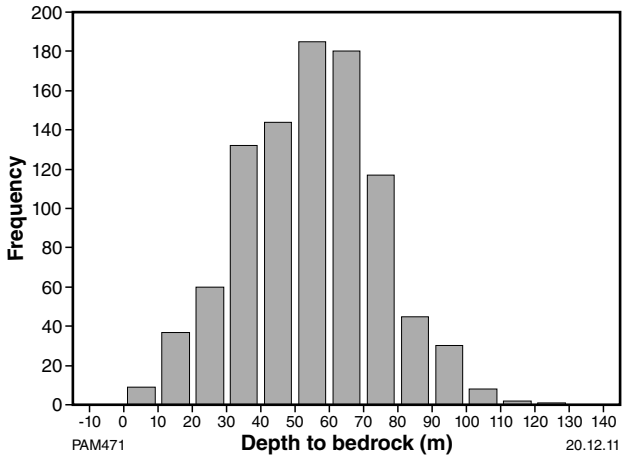

Figure 8. Frequency histogram for depth to regolith–bedrock interface (metres) for both closed- and open-file data held in WAMEX database.

drilled using a variety of techniques (reverse circulation (RC), rotary air blast (RAB), aircore, diamond) show that most activity is focused on Yilgarn Craton greenstones (Fig. 9). The depth range of these holes is 5–201 m, with most holes between 20 and 80 m (Fig. 10). The average depth of 58 m is similar to that for other data (cf. Fig. 8).

Regolith sampling

Most regolith samples (based on a 4 x 4 km grid) in the east Wongatha area were collected in March 2010 by a two-person sampling team (geologist and field assistant), transported by a Bell Jetranger B206 helicopter (Australian National Helicopters). In most cases, the sample was collected within 100 m of the pre-determined site, apart from areas of dense vegetation, where the sample site was moved to ensure the safety of the helicopter, pilot, and sampling team.

At each site, two holes approximately 50 cm apart were drilled using a Tanaka® single-operator earth auger fitted with a 10 cm diameter auger bit (Fig. 11). The power auger is preferable to excavation by either spade or shovel, as the friable nature of the regolith results in collapse of excavated pit walls. In each hole, regolith between the surface and 40 cm was rejected, and the holes drilled to a maximum depth of 80–90 cm, if possible. A composite sample of approximately 5 kg was collected from the bottom part of the two holes. The sample was placed in a uniquely numbered plastic bag, which was then placed in an identically numbered drawstring calico bag. Holes were then rehabilitated with unsampled material. At some sites, consolidated or impervious layers — usually calcrete or dense layers of calcrete or ferricrete nodules, locally lateritic ducricrust — prevented augering to the target depth of 90 cm. In these cases, the sample was collected immediately above the impervious later, and the target depth, and the reason for shallow sampling, were noted. Fourteen samples consisting of damp to wet, clay-dominated regolith were collected in or close to lake systems in the northwest part of MINIGWAL. Regolith sampled at a few other sites was also damp.

A standard form was completed at each sample site (Fig. 12), to record the sample location, and information about vegetation, landforms, surface and downhole regolith characteristics (e.g. colour, sorting, grain size), the proximity and composition of outcropping rocks or secondary units, and any unique features of the site (e.g. damp or wet samples). At each site, two photographs were taken: one recording the regolith in the immediate proximity of the augered holes, and a second showing the local context of the sample site (Fig. 13a,b). At every fifteenth site, a second sample was taken from two holes drilled approximately 50 cm to 1 m from the original holes. These 50 site duplicates, collected to test within-site homogeneity, were labelled with the same sample

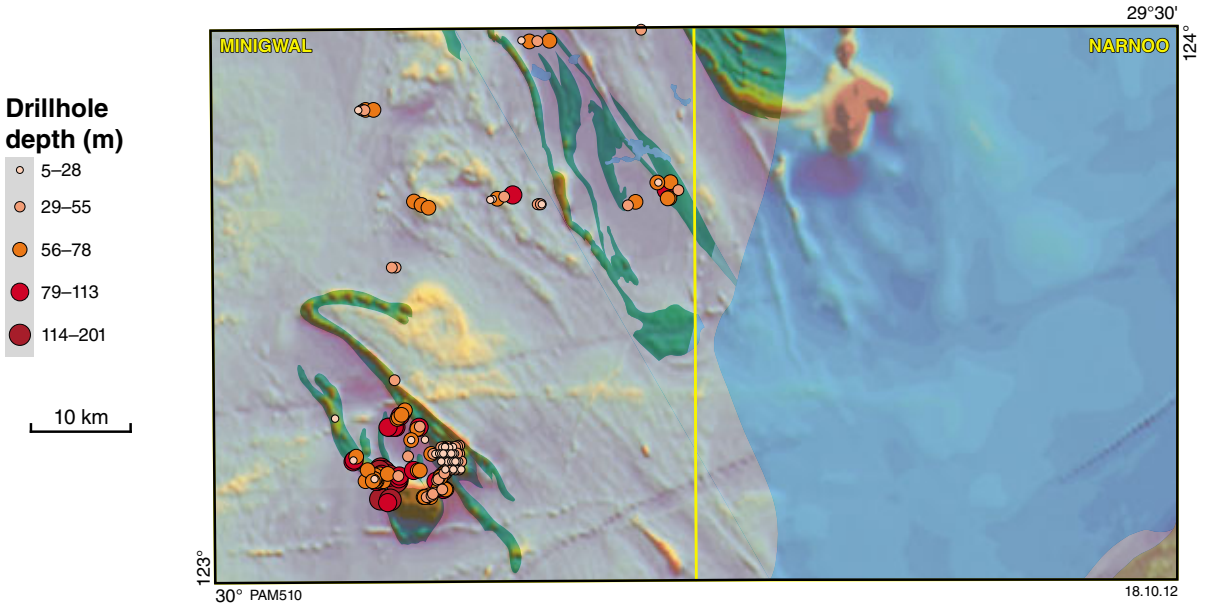

Figure 9. Drillhole depth (metres) as a proxy for depth to regolith–bedrock interface. From open-file data (Geological Survey of WA, 2009).

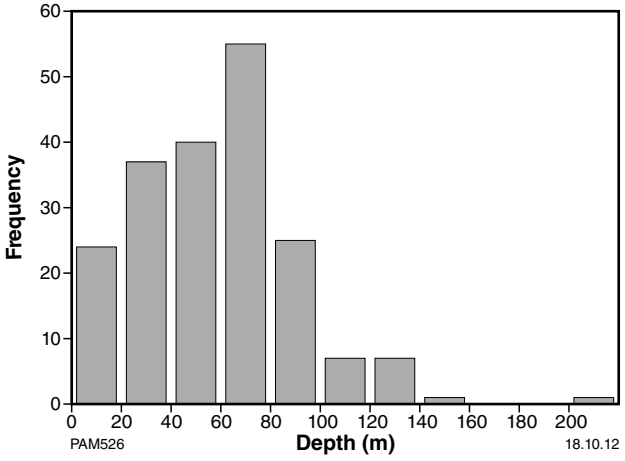

Figure 10. Frequency histogram for open-file drilling data extracted from open-file data (Geological Survey of WA, 2009).

Figure 11. Sample collection using Tanaka® power auger.

EAST WONGATHA SOIL SAMPLING PROGRAM

GSWA No		***Site No***	
EASTING		***NORTHING***	

Sampler		Date		Time	

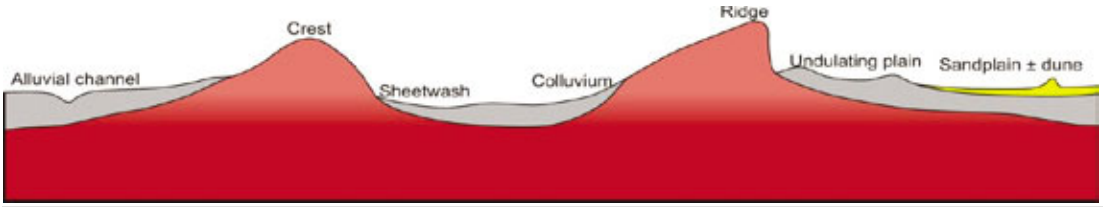

REGOLITH-LANDFORM					
Sandplain	Colluvium	Sheetwash			
REGOLITH-COLOUR					
Red	**Brown**	**Yellow**	**Orange**	**Grey**	**Other**
VEGETATION					
Spinifex	Mulga	Eucalypt	Grass	Shrubs	
SURFACE REGOLITH					
%	Fe-rich	CO3	Lithic	Quartz	Other
Nod/grans					
Sand					
Silt/clay					
DOWNHOLE REGOLITH					
%	Fe-rich	CO3	Lithic	Quartz	Depth-cm
Nod/grans					
Sand					
Silt/clay					
LITHIC MATERIAL					
%	Surface	Downhole	Outcrop	Dist (m)	Dirn (bearing)
Mafic					
Fg felsic					
Granitic					
Sedimentary					
Schistose					
Gneissose					
Vein quartz					
Other					
Secondary coating	Fe	Mn	Si	CO3	Other

Units nearby	Sand dune	Lake	Saprock	Saprolite	Other
Sample features	HCl reaction		Dry?	Damp?	
Photo taken?					

Comments

PAM528 18.10.12

Figure 12. Sample site form used for the east Wongatha program. See Table 1 for description.

Table 1. Description of fields in site sample form, east Wongatha program. See Figure 12.

Field	*Type*	*Description*	*Example*
GSWA No	Numeric	Geological Survey of Western Australia sample number. A unique number for samples held in the GSWA collection.	200056
Site No	Text	Site identifier for collection of soil sample. 'EW' is for East Wongatha. Numbers are non-consecutive between 51 and 1136.	EW216
Easting	Numeric	GDA east coordinate for sample site.	504438
Northing	Numeric	GDA north coordinate for sample site.	6683431
Sampler	Text	Initials of the geologist who made the site observations. SW – Stephen White, SM – Sarah Martin, PM – Paul Morris.	SM
Date	Text	Date on which the sample was collected.	
Time	Numeric	Time at which the sample was taken (24 hour format). These data are useful in calculating the total sampling time/site.	
REGOLITH-LANDFORM	Text	Regolith-landform type from Hocking et al. (2007) to describe the site and an area of approximately 50 m radius. Apart from those shown, sites in the northwest of the program area include lake, and playa.	Sheetwash
REGOLITH-COLOUR	Numeric (text)	Colour of the regolith within a 50 m radius of the site. Predominant colour designated 1, with subordinate or modifying colours designated 2, 3, 4, etc. 'Other' category allows text entry of other colours.	Brownish-red is designated red (1), brown (3). Brown-red designated red (1) brown (2).
VEGETATION	Numeric (text)	Vegetation types shown in decreasing order of abundance from 1 (most abundant) to 4, 5, etc. (least abundant). Broad groupings only are shown (e.g. eucalypts), with grasses undivided, and shrubs including bluebush, samphire, Casuarina, unless otherwise shown. 'Other' category allows text entry of specific vegetation types.	
SURFACE REGOLITH	Numeric/text	Percentage values of components seen within a 50 m radius of the designated sample site. Clay is designated as Lithic – Silt/clay unless otherwise shown. 'Other' allows text entry of unlisted components. Estimates probably accurate to within 10%. Trace amounts shown as 2%. If any Lithic component is listed for nodules or granules (Nod/grains) then identification must be entered in LITHIC MATERIAL part of form.	
DOWNHOLE REGOLITH	Numeric/text	As for surface regolith, but Depth-cm column allows entry of depth downhole to component listed in table. If no depth is entered, the implication is that the component is found throughout the sampled interval. Estimates probably accurate to within 10%. Trace amounts shown as 2%. If any lithic component is listed for nodules or granules (Nod/grains), then identification must be entered in LITHIC MATERIAL part of form.	
LITHIC MATERIAL	Numeric/text	Percentage of Lithic material identified in either surface or downhole regolith part of form. Facility also for entry of outcrop, and its distance and bearing from the sample site. 'Other' allows for entry of lithic type not listed. Estimates probably accurate to within 10%. Trace amounts shown as 2%.	
Secondary coating	Numeric/text	Coating observed on regolith material (e.g. iron staining, clay). 'Other' allows for entry of coatings not listed.	
Units nearby	Numeric/text	Allows designation of any secondary units seen close to the site. Estimated distance can be entered in Comments. 'Other ' allows listing of units not listed.	
Sample features		HCl reaction is whether the sample releases CO_2 following application of 10% HCl, indicative of reactive carbonate content. Originally planned to be tested at the site, but subsequently tested either at base camp or Perth. Dry? And Damp? Indicate whether the sample has noticeable moisture which may inhibit its ability to be dry sieved, requiring air drying or alternative pre-analysis preparation.	Strong (effusive CO_2 release), moderate (noticeable CO_2 release), weak (some CO_2 release), none (no reaction).
Photo taken?	Numeric	Whether a series of two digital photographs (one of the sample site and bag, and one of the sample in the foreground with the bag for scale) have been taken.	

Table 1. continued

Field	*Type*	*Description*	*Example*
Comments	Text	Information unique to the site.	Depth of sample holes if less than the required 85–90 cm (e.g. due to encountering resistant layers, such as carbonate, Fe-nodules, etc.). Distance to secondary features (e.g. sand dunes), presence of animal droppings, unusually extensive consolidated colluvial layers.

number as the original sample suffixed with 'R' (Fig. 13c). Samples collected from five sites by vehicle in November 2009 were also uplifted by helicopter, and included as site duplicates, resulting in a total of 55 site duplicates, or 6.5% of all samples collected.

Analysis

Reconnaissance in November 2009, sample collection in March 2010, and regolith-landform mapping (McGuinness, 2010) indicated that regolith in the east Wongatha area is dominated by quartz-rich sand. Although there is evidence that some areas of sandplain deposits may have local input from bedrock (e.g. higher proportion of quartzofeldspathic material, minor Fe-rich lag), these areas are uncommon and localized, and the presence of sand dunes, together with the frosting of quartz sand, indicates that most areas of sandplain have had some eolian input. Inclusion of any potentially barren quartz sand in an analytical fraction could result in dilution of elements related to mineralization. For this reason, the sand fraction was excluded from analysis.

The results of several studies show that the finer fraction (i.e. silt and clay; <50 μm) has advantages as a sample medium for geochemical surveys. According to Hawkes and Webb (1962), the ability of soils to adsorb ions is related to the nature of soil particles and grain size. Significant levels of adsorption are usually restricted to clays, although organic compounds and colloids can also adsorb ions. The ability of clays to adsorb ions is related to their unsatisfied electric charges both on and within layers. This base-exchange capacity of clays (cf. cation exchange capacity or CEC; Hall, 1998) can therefore be important in the generation of geochemical anomalies. Hall (1998) noted that labile elements in soils are usually associated with hydrous Fe and Mn oxides, humic and fulvic components of humus, and clay minerals. Components are variably bound by such processes as physical and chemical adsorption on the surface, occlusions within structures, chelation, complexation, and coprecipitation. Hall (1998) recommended that phases capable of scavenging were found in the clay fraction, and samples should be sieved to <63 μm. The cation exchange capacity of soil is a measure of its capability for non-specific adsorption, with CEC measured in meq/100 g (where meq is milliequivalents). Generally, a solid soil phase with a high surface area has a high CEC. Clays have elevated CEC values due their high surface area. For example, montmorillonite and vermiculite have surface areas of 700–800 m^2/g, and CEC values of 70–150 meq/100 g (Hall, 1998).

Although screening out the coarser fraction excludes the input of potentially barren quartz sand, quartz-rich eolian material can be present in the finer fraction of soils. Grain size analysis, mineralogy, and geochemistry identified an eolian component in soils in part of New South Wales, with this component predominant in the finer particle range (Tate et al., 2007). The mineralogy and chemistry of several grain size fractions of regolith from the Beasley Creek gold deposit in Western Australia contain a significant eolian component, especially the 75–710 μm (silt to fine sand) and 4–75 μm (clay to silt) fractions according to Robertson (1999). He argued that the 710–4000 μm (coarse sand – granule/pebble) fraction could be related to gold mineralization, but finer fractions were less effective due to dilution by eolian material. However, analytical results for gold, arsenic, cadmium, and copper in the <4 μm fraction proved more reliable. Notably, the analytical approach for this study used X-ray fluorescence (XRF) spectrometry, instrumental neutron activation (INAA) analysis, and inductively coupled plasma mass spectrometry (ICP-MS), all of which are 'total' analytical approaches.

Chao (1984) discussed the importance for analysis of the fine grain-size fraction in mineral exploration, in relation to the application of partial extraction techniques. He noted the importance of the clay-size aluminosilicate fraction of soils in terms of the high proportion of reaction sites (i.e. sites where elements released during weathering are held). This fraction can retain any mineralization component present as either loosely bound or weakly bonded particles (known as the exogenic component), or that directly related to the sample medium (Cameron et al., 2004). Partial or selective digests can bring into solution this exogenic component, at the same time minimizing the input of the same elements which may be occult in the sample medium but unrelated to mineralization (the endogenic component; Cameron et al., 2004). Approaches that maximize the exogenic to endogenic ratio have been shown to be effective in detecting mineralization through thick transported overburden over several styles of mineralization in Chile, the USA, Canada, and China (e.g. Smee, 1998; Hamilton, 1998; Wang et al., 2007; Cameron et al., 2010).

Dry sieving of regolith samples from the east Wongatha area shows that, for the majority of samples, the <50 μm fraction comprises less than 2% by volume (Fig. 14). This compilation excludes samples collected in, or close to, lake systems, because those samples became consolidated following collection. Unconsolidated samples were dry-screened for 30 minutes using new 50 μm nylon mesh for

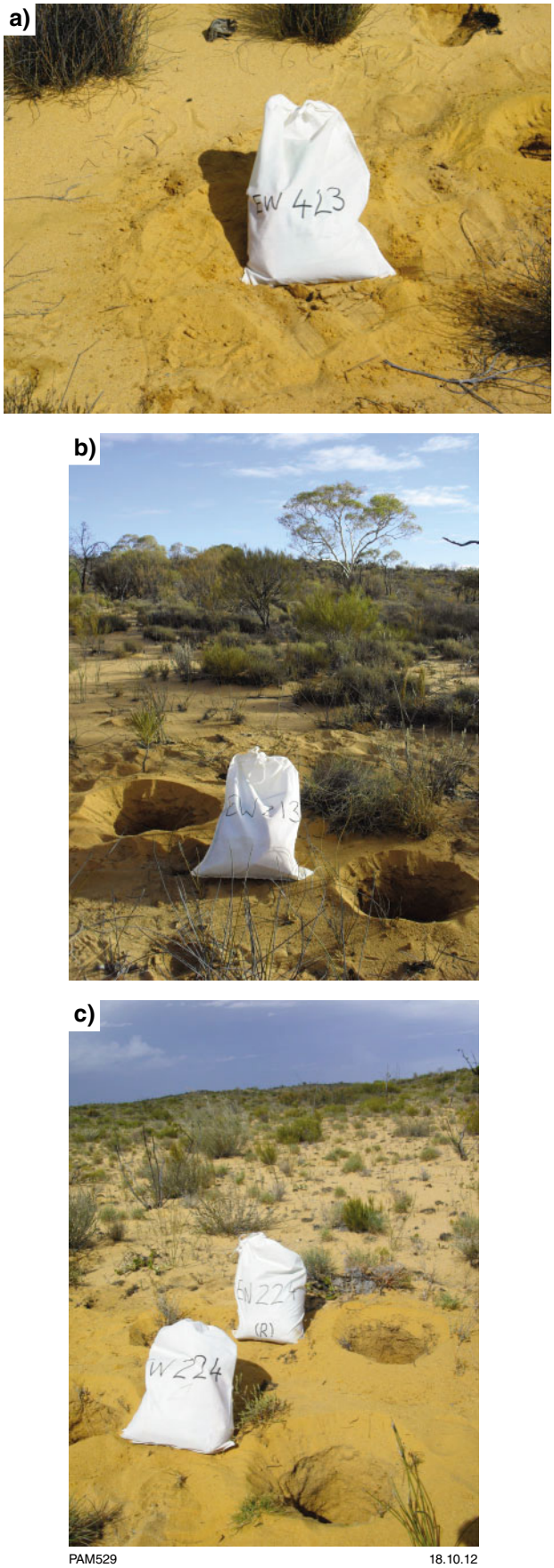

Figure 13. Bagged composite regolith samples at sites EW 423 (a), EW 413 (b), and EW 224 (c; site duplicate). Photographs also illustrate the visual record made of the context of each sample site.

each sample, in plastic flexi-stack frames loaded onto a Retsch AS2000 sieve shaker. Consolidated samples were disaggregated using a roller, then milled to <75 µm.

To further minimize the input of any quartz-rich eolian component, one gram of the fine fraction of each sample was digested with aqua regia, a 3:1 mixture of hydrochloric (HCl) and nitric (HNO_3) acids, which is a non-selective partial digest (Mann, 2010). This digest is capable of attacking both organic and inorganic phases (Chao, 1984), and is effective for decomposing sulphides and oxides, but is largely ineffective in dissolving silicates (Fletcher, 1981; Chao and Sanzolone, 1992). Following digestion, 55 elements were measured by either ICP-MS or inductively coupled plasma optical emission spectrometry (ICP-OES) in eleven batches, ten of which were unconsolidated samples. Included in these ten batches were 89 sample duplicates, 55 site duplicates, seven reference materials, and blank solutions (i.e. a solution containing elements at less than the lower level of detection for all elements). Samples with relatively high gold contents were checked using electrothermal atomisation (ETA). The <50 µm fractions of 40 samples were digested with aqua regia and analysed by ICP-MS and ICP-OES at a second laboratory (Ultratrace Laboratories, Canning Vale, Perth).

Quality control

Analytical precision for sample duplicates and site duplicates was assessed by calculating the Half Relative Deviation (HRD):

HRD = 100 x [(assay1 – assay2)/(assay1 + assay2)] (Shaw et al., 1998)

There is no specific level below which HRD is acceptable, but for GSWA's regolith geochemistry program (e.g. Morris and Verren, 2001), a value of <20 was taken as good agreement, provided the analyte concentration was greater than three times the lower level of detection.

Sample duplicates

Of the 89 sample duplicates, 81 (91%) have <10 elements for which HRD >20, and 26 sample duplicates (29%) have HRD values of <20 for all elements (Appendix 1). Twenty sample duplicates have HRD >20 for Al, Li, and Nb, and 10 sample duplicates have HRD values >20 for Ni, Rb, Sn, Sr, and Zn. These elements can be broadly divided into two groups. Aluminium, Li, Rb, and Sr are lithophile elements usually found at elevated concentrations in clay minerals. The poor duplication could reflect variable digestion of the silt-clay fraction. Poor duplication for Nb, Ni, and Sn could result from incomplete dissolution of resistate minerals such as rutile, metal oxides, or native metals. Zirconium is usually found in the resistate mineral zircon, which is commonly resistant to acid attack. However, for east Wongatha samples, there is usually good agreement between parent and duplicate, which could mean that zircon is homogeneously distributed, it is not a common resistate phase, or it is sufficiently fine grained that it has been partially or completely digested.

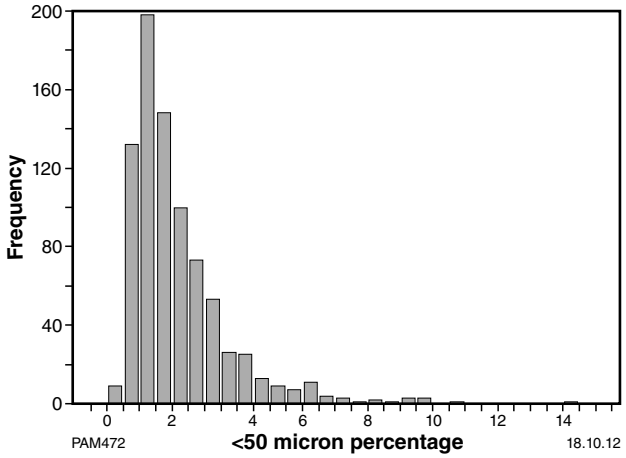

Figure 14. Frequency histogram showing percentage of fine fraction (i.e. <50 micron) dry screened from unconsolidated regolith samples in the east Wongatha program (n = 821).

In terms of individual samples, the poorest agreement between parent and duplicate is for sheetwash sample GSWA 200620 (35 elements with HRD >20) and sandplain sample GSWA 200140 (22 elements have HRD >20). Site information shows that both samples are dominated by quartz-sand with trace amounts of ferruginous material. In both cases, there is poor agreement for most of the rare earth elements (REE; La–Lu), Ba, Sr, and Al, which can be attributed to inhomogeneous distribution of REE-bearing accessory minerals and variable dissolution of clay. Poor agreement for Ca, Cr, Cu, Fe, Mn, Ni, Pb, Sb, and V in GSWA 200620 may reflect uneven distribution of secondary oxides and possibly sulphides.

Site duplicates

At 50 of the 55 sites where a duplicate was collected, both samples were collected during helicopter sampling from holes augered within 1 m of each other. For the five remaining sites, the 'site duplicate' is composed of a sample collected by vehicle in November 2009, and a sample collected by helicopter in March 2010. In these cases, the helicopter and vehicle sites can be separated by as much as 650 m (Appendix 2).

Between 10 and 21 site duplicates have HRD >20 for Al, Ba, Be, Ca, Dy, Er, Gd, La, Li, Mn, Nb, Nd, Pr, Rb, Sr, and Tb, and the amount of the <50 µm fraction (Appendix 2), which may be due to any of the following: inhomogeneity at the site scale; variable digestion of the silt and clay fraction (Al, Li, Rb); variable amounts of carbonate (Ca, Sr); secondary oxides (Mn); REE-bearing minerals (Dy, Er, Gd, La, Nd, Pr, Tb); resistate minerals (Nb); the amount of clay and silt present. For most of the remaining sites, HRD is <5 for most elements, but at six sites (602, 171, 496, 175, 983 and 926) between 23 and 36 elements have HRD >20. The elements that show the least within-site agreement indicate inhomogeneous distribution of REE-bearing minerals and resistate minerals, such as chromite, rutile, and zircon (Cr, Nb, Zr), iron oxides (Fe, Mn, Co), and silt to clay (<50 µm) content (Al, Rb). Three of the five sites sampled by vehicle and helicopter have HRD >20 for more than ten elements, and HRD is >20 for 33 elements at site 494 (GSWA 197335 and GSWA 200428).

Reference materials and blanks

Monitoring of precision and accuracy has been undertaken by analysis of seven reference materials (Kane, 1990) inserted by Genalysis Laboratory Services Pty Ltd. These are SYN26 (high-Au standard with base metals), AE18 (low-level aqua regia base metal and Au standard), AE19 (low-level aqua regia base metal and Au standard), CMM-08 (high-Ca, low-Au standard), NGL-23 (low-level Au and base metal standard), PL-16 (low-level aqua regia base metal and Au standard with higher Fe), and MPL-3 (multi-element major and trace element standard).

In assessing the results of reference material analysis, two factors need to be taken into account. Firstly, obtaining consensus values against which assays can be compared requires repeated analysis under controlled conditions. As there are few such data for aqua regia digestion of these seven reference materials (R Holdsworth, written communication, 2010), reference values are indicative rather than certified. Secondly, as aqua regia is a partial digest, small variations in digestion conditions (e.g. temperature, time) could result in variable release of elements into solution.

In most cases, indicative and obtained values for reference materials result in HRD values <10 when analyte concentrations are in the order of ten times the lower level of detection (Appendix 3). Elements that show less acceptable agreement between indicative and obtained values in more than one batch include: Ag, As, Sb, and Zr in CMM-08; Gd and Mo in PL-16; Nb, Sb, and Tb in SYN-26; Sb and Sn in NGL-23. There is generally poor agreement for several elements for the reference material MPL-3, but good agreement for indicative and obtained values for Au in all reference materials, spanning a concentration range from 11 to greater than 22 000 ppb.

Precision has been assessed by calculating the percent relative standard deviation (RSD%; i.e. 100 x [average/standard deviation], also known as the percent covariance) for reference materials that have been analysed more than twice (Appendix 3). Where the analyte concentration is greater than three times the lower level of detection, RSD% >20 is found for silver and niobium in four reference materials, gold and palladium in three materials, and higher values are also found in some reference materials for elements such as Dy, Li, Cr, Er, Ge, Hf, Sb, Sn, Tb, Rb, Tl, W, and Yb. In general, a high level of precision has been achieved over all batches. Elements such as Dy, Er, Tb, and Yb are found in more resistant REE minerals, which may indicate incomplete digestion. A similar argument may account for the behaviour of Cr, Sn, and V.

Blank determinations have been compared to a value equal to three times the lower level of detection for the analyte and, apart from isolated occurrences, all blank determinations were below this level. The most consistent divergences were for Ce, Sn, and Sr (Appendix 3).

Umpire laboratory analysis

Analyses of a second aliquot of the <50 µm fraction of 40 samples by Ultratrace-Bureau Veritas, Canning Vale have been compared to analyses carried out by Genalysis Laboratory Services (Appendix 3). Apart from Al, Li, Rb and in some cases Sr, there is good overall agreement between data from the two laboratories. For these four elements, when HRD >20, concentrations are higher for determinations at Genalysis. As all four elements are common constituents of clays, it is possible that the higher concentrations determined at Genalysis result from slightly more aggressive sample digestion conditions.

Quality control summary for the determination of fine-fraction gold

Parent and duplicate analyses of fine-fraction gold (i.e. analysis of two separate pulp digests from the one sample) show a positive correlation (Fig. 15a; $R^2 = 0.5975$) with a slope of 0.8216. As many values are less than 8 ppb, some of the scatter may be due to reduced precision as concentrations approach the lower level of detection. The agreement is poorer for site duplicates (Fig. 15b) with considerable scatter in the data and a correspondingly lower R^2 value of 0.2026. This distribution does not include data from sites collected by helicopter and ground-based vehicle. For twenty-two analyses with detectable gold by aqua regia digest/ICP, a second determination by electrothermal atomisation (ETA) shows good agreement (Fig. 15c; $R^2 = 0.8135$) over a concentration range of about 30 ppb. Both methods have the same lower level of detection (LLD) of 1 ppb.

For the <50 µm fraction of the forty samples analysed by a second laboratory, there is a reasonable agreement (Fig. 15d; $R^2 = 0.6761$). At concentrations less than about 5 ppb, there appears to be more scatter in the data for determinations at Ultratrace than those determined at Genalysis.

Regolith geochemistry of the <50 µm fraction

A compilation of analytical data for regolith from the east Wongatha area can be downloaded using GSWA's GeochemExtract web-based application <http://www.dmp.wa.gov.au/geochem>. Summary statistics (Table 2) show that for six elements (Ag, Cd, Hg, Pd, Pt, Se, and Ta), between 69 and 99.9% of the 835 analysed samples returned a concentration of less than the lower level of detection (i.e. the data are censored; Sanford et al., 1993). Four elements (Au, Ge, Te, and W) have censored data for a smaller number of samples (36 and 49% of all samples).

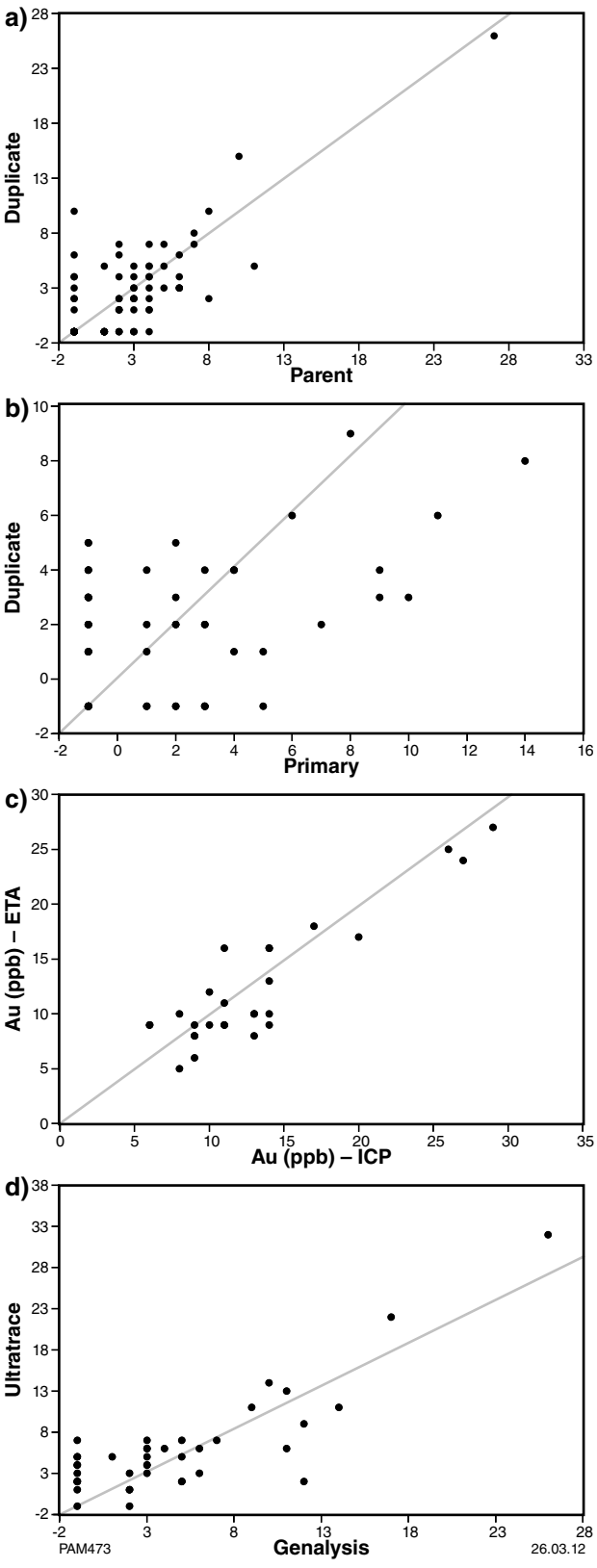

Figure 15. Scatter plots comparing results of gold assay analyses: a) Duplicate sample analyses; b) duplicate site analyses; c) comparison of concentration analysed by two methods; d) gold analysis by two laboratories.

In order to statistically analyse data, it is necessary to substitute a value for each censored data item. There is no agreement on how the value is determined (e.g. Grunsky, 2010; Reimann et al., 2010), but a common practice (and one adopted here) is to substitute a value equal to half of the LLD. These data are referred to as replaced values. Clearly, the validity of any statistical analysis diminishes as the number of replaced values increases, and both Reimann et al. (2010) and Sanford et al. (1993) have recommended replacement of a maximum 10–20% of censored data in order to maintain some statistical integrity. An alternative approach is to use algorithms to predict how data will behave at concentrations less than the detection level, and make substitutions accordingly, but this approach relies on data being normally distributed, which is usually not the case for regional geochemical exploration datasets (Grunsky, 2010).

Due to the high proportion of censored data, statistical analysis has not been undertaken for Ag, Cd, Hg, Pd, Pt, Se, and Ta. As 301 samples (36% of all samples) returned <1 ppb Au, the effects of replacing more than one-third of the data should be borne in mind when evaluating statistical data.

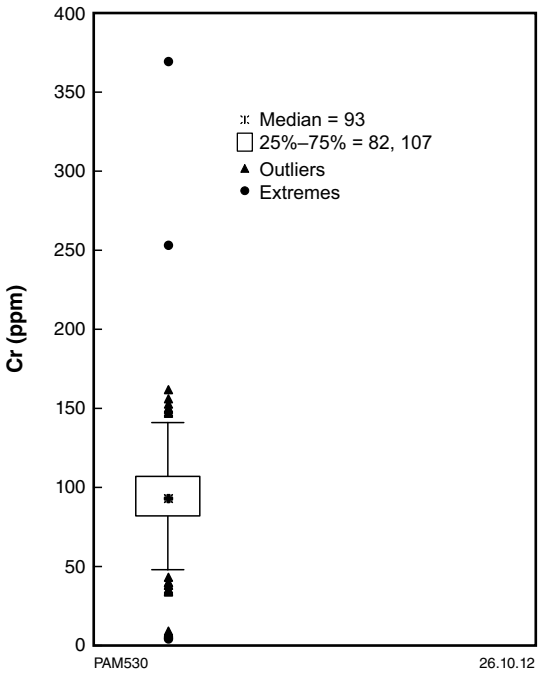

Figure 16. Box and whisker plot (Tukey, 1977) for Cr in regolith from the east Wongatha area (range 4–369 ppm; LLD = 2 ppm; mean = 95 ppm, median = 93 ppm).

Determination of background and anomalous concentrations

One of the main purposes of geochemical exploration is to identify samples with anomalous concentrations of either economic elements, or elements that may be indicative of mineralization (i.e. pathfinder elements). Identification of anomalous samples requires knowing the range of naturally occurring element concentrations (i.e. the background range; Hawkes and Webb, 1962). A commonly used approach has been to limit the background range to concentrations that fall within the mean ± 2SD (i.e. 95th percentile). Concentrations falling in the top or bottom 5% of these distributions are then termed anomalously high or low. The validity of this approach relies on data being normally distributed, which is usually not the case for geochemical datasets, in that they have a higher proportion of lower concentrations, and are therefore positively skewed (Grunsky, 2010). In these cases, the background range can be strongly influenced by a few large or small values, and this approach has received little support (see Reimmann et al., 2010).

In this study, samples with anomalous concentrations are identified using a box and whisker plot (boxplot of Tukey, 1977), whereby the data are ranked then divided into four equal parts based on quantiles (Reimann et al., 2010; Fig. 16). This plot type is largely insensitive to the effects of either extremely high or extremely low values (wild data), or to different types of data distribution (Reimann et al., 2010). The spread of data is shown by the width of the box in the y-axis direction (upper and lower boundaries are the 75th and 25th percentiles respectively), and the degree of skewness is indicated by the position of the median in the box and the extent of the whiskers. The kurtosis ('flatness' of the data distribution) is shown by the relative length of the whiskers and the box. Thus, for chromium in regolith from the east Wongatha area (range from 4–369 ppm; LLD = 2 ppm), the symmetry of the box and whiskers around the median value of 93 ppm (Fig. 16) indicates a broadly normal distribution, which is consistent with the similarity of the median and the mean (95 ppm; Table 2). Anomalously high values are identified as either outliers (concentration >145 ppm; i.e. 75th percentile ± [1.5 x IQR], where IQR is the interquartile range), or extremes (concentration >182 ppm; i.e. greater than 75th percentile ± [3 x IQR]).

Bubble Plots

Concentration variations for a variety of elements are summarized in relation to regional bedrock interpretation (Spaggiari et al., 2011) and geophysical data. For elements that have been statistically treated, concentrations within the background range are shown by circles (bubbles; e.g. Fig. 18) whose diameter is scaled according to concentration. Divisions have been determined according to the quartile range. Anomalous concentrations are shown as either smaller pink stars (outlier values) or larger red stars (extreme values).

Aluminium, iron, calcium, and manganese

Of the 55 elements analysed, aluminium, iron, calcium, and manganese are found at relatively high concentrations in most samples (Table 2).

Table 2. Statistics for analytical data of <50 micron fraction of regolith from the east Wongatha area.

	Valid N	*Unit*	*LLD*	*Mean*	*SD*	*Median*	*Minimum*	*Maximum*	*Range*	*25 pctl*	*75 pctl*	*IQR*	*Skew*	*Kurt*	*Censored*	*% censored*
Ag	835	ppm	0.05	-0.04	0.036	-0.05	-0.050	0.33	0.38	-0.05	-0.05	0.00	3.9	19.7	764	91.5
AgHDL	835	ppm	0.05	0.03	0.018	0.03	0.025	0.33	0.31	0.03	0.03	0.00	8.6	116.1		0.0
Al	835	ppm	20	26123	9560	24422	2075	56560	54485	19132	31997	12865	0.6	0.1	0	0.0
As	835	ppm	1	4	1	4	-1	20	21	3	5	2	2.4	19.2	3	0.4
AsHDL	835	ppb	1	4.2	1.4	4.0	0.5	20.0	19.5	3.0	5.0	2.0	2.6	19.8		0.0
Au	835	ppb	1	2	3	2	-1	29	30	-1	4	5	2.0	8.6	301	36.0
AuHDL	835	ppb	1	2.7	2.9	2.0	0.5	29.0	28.5	0.5	4.0	3.5	2.9	15.0		0.0
Auzero	835	ppb	1	3	3	2	0	29	29	0	4	4	2.6	12.6		0.0
AuNone	534	ppb	1	4	3	3	1	29	28	2	5	3	3.0	15.6		0.0
Ba	835	ppm	1	54	145	26	3	2268	2265	15	51	36	10.8	135.8	0	0.0
Be	835	ppm	0.05	0.70	0.32	0.65	-0.05	2.07	2.12	0.47	0.88	0.41	0.9	0.9	2	0.2
BeHDL	835	ppm	0.05	0.701	0.317	0.650	0.025	2.070	2.045	0.470	0.880	0.410	0.9	0.9		0.0
Bi	835	ppm	0.01	0.24	0.06	0.24	0.01	0.87	0.86	0.21	0.27	0.06	1.7	21.9	0	0.0
Ca	835	%	0.01	0.71	2.27	0.09	-0.01	21.15	21.16	0.04	0.21	0.17	5.4	34.7	7	0.8
CaHDL	835	%	0.010	0.708	2.271	0.090	0.005	21.150	21.145	0.040	0.210	0.170	5.4	34.7		0.0
Cd	835	ppm	0.05	-0.01	0.06	-0.05	-0.05	0.31	0.36	-0.05	0.06	0.11	1.2	0.2	577	69.1
CdHDL	835	ppm	0.050	0.042	0.031	0.025	0.025	0.310	0.285	0.025	0.060	0.035	2.4	9.2		0.0
Ce	835	ppm	0.01	39.34	12.95	38.32	2.06	101.59	99.53	31.29	47.37	16.08	0.5	1.6	0	0.0
Co	835	ppm	0.1	7.4	3.7	6.6	0.9	28.6	27.7	4.8	9.2	4.4	1.4	2.6	0	0.0
Cr	835	ppm	2	95	23	93	4	369	365	82	107	25	2.1	25.4	0	0.0
Cu	835	ppm	1	15	8	13	-1	50	51	10	19	9	1.5	2.7	3	0.4
CuHDL	835	ppm	1.00	15.30	7.70	13.00	0.50	50.00	49.50	10.00	19.00	9.00	1.5	2.7		0.0
Dy	835	ppm	0.01	2.18	0.77	2.11	0.11	5.21	5.10	1.65	2.65	1.00	0.6	0.9	0	0.0
Er	835	ppm	0.01	1.12	0.41	1.09	0.05	2.80	2.75	0.84	1.37	0.53	0.6	1.1	0	0.0
Eu	835	ppm	0.01	0.72	0.25	0.69	0.04	1.80	1.76	0.54	0.87	0.33	0.6	1.2	0	0.0
Fe	835	%	0.01	3.90	0.93	3.92	0.22	7.07	6.85	3.37	4.49	1.12	-0.3	1.0	0	0.0
Ga	835	ppm	0.05	10.43	2.82	10.32	0.59	18.70	18.11	8.63	12.22	3.59	0.0	0.2	0	0.0
Gd	835	ppm	0.01	2.70	0.95	2.62	0.16	6.34	6.18	2.06	3.28	1.22	0.5	0.7	0	0.0
Ge	835	ppm	0.05	0.03	0.07	0.06	-0.05	0.18	0.23	-0.05	0.10	0.15	-0.1	-1.7	355	42.5
GeHDL	835	ppm	0.050	0.064	0.039	0.060	0.025	0.180	0.155	0.025	0.100	0.075	0.4	-1.0		0.0

Table 2. continued

	Valid N	*Unit*	*LLD*	*Mean*	*SD*	*Median*	*Minimum*	*Maximum*	*Range*	*25 pctl*	*75 pctl*	*IQR*	*Skew*	*Kurt*	*Censored*	*% censored*
Hf	835	ppm	0.01	0.50	0.16	0.51	0.03	1.39	1.36	0.41	0.59	0.18	0.3	2.5	0	0.0
Hg	835	ppm	0.2	-0.2	0.0	-0.2	-0.2	0.2	0.4	-0.2	-0.2	0.0	28.9	835.0	834	99.9
HgHDL	835	ppm	0.2	0.1	0.0	0.1	0.1	0.2	0.1	0.1	0.1	0.0	28.9	835.0		0.0
Ho	835	ppm	0.01	0.41	0.15	0.40	0.02	0.98	0.96	0.31	0.51	0.20	0.6	1.0	0	0.0
In	835	ppm	0.01	0.05	0.01	0.05	-0.01	0.08	0.09	0.04	0.05	0.01	-0.5	1.5	4	0.5
InHDL	835	ppm	0.010	0.045	0.012	0.050	0.005	0.080	0.075	0.040	0.050	0.010	-0.3	0.3		0.0
La	835	ppm	0.01	17.05	5.84	16.53	0.89	48.25	47.36	13.21	20.68	7.47	0.6	1.7	0	0.0
Li	835	ppm	0.1	14.8	6.8	13.2	1.2	43.6	42.4	9.9	18.5	8.6	1.0	0.9	0	0.0
Mn	835	ppm	1	155	136	109	18	1293	1275	81	164	83	3.2	14.1	0	0.0
Mo	835	ppm	0.1	0.7	0.2	0.7	-0.1	3.4	3.5	0.5	0.8	0.3	1.8	23.7	3	0.4
MoHDL	835	ppm	0.10	0.68	0.23	0.70	0.05	3.40	3.35	0.50	0.80	0.30	1.9	24.2		0.0
Nb	835	ppm	0.02	0.31	0.09	0.31	0.06	0.98	0.92	0.25	0.36	0.11	0.8	4.5	0	0.0
Nd	835	ppm	0.01	17.40	5.98	16.99	0.96	42.52	41.56	13.38	20.86	7.48	0.5	0.9	0	0.0
Ni	835	ppm	1	22	12	19	-1	103	104	15	26	11	2.0	6.6	1	0.1
NiHDL	835	ppm	1	22.18	11.75	19.00	0.50	103.00	102.50	15.00	26.00	11.00	2.0	6.6		0.0
Pb	835	ppm	1	11	3	11	-1	27	28	9	14	5	0.3	1.1	1	0.1
PbHDL	835	ppm	1	11.5	3.3	11.0	0.5	27.0	26.5	9.0	14.0	5.0	0.4	1.0		0.0
Pd	835	ppb	10	-8	6	-10	-10	29	39	-10	-10	0	3.5	11.0	776	92.9
PdHDL	835	ppb	10	6	3	5	5	29	24	5	5	0	4.5	22.5		0.0
Pr	835	ppm	0.005	4.518	1.543	4.401	0.252	11.430	11.178	3.462	5.441	1.98	0.5	1.0	0	0.0
Pt	835	ppb	5	-4	3	-5	-5	9	14	-5	-5	0	3.9	13.8	788	94.4
PtHDL	835	ppb	5	2.7	0.9	2.5	2.5	9.0	6.5	2.5	2.5	0.0	4.6	20.9		0.0
Rb	835	ppm	0.02	24.07	12.40	20.44	1.92	81.09	79.17	15.03	30.69	15.66	1.3	1.9	0	0.0
Sb	835	ppm	0.02	0.22	0.05	0.22	-0.02	0.41	0.43	0.19	0.24	0.05	-0.5	2.3	1	0.1
SbHDL	835	ppm		0.22	0.05	0.22	0.01	0.41	0.40	0.19	0.24	0.05	-0.5	2.0		0.0
Sc	835	ppm	1	9	3	9	-1	20	21	8	11	3	0.1	0.7	2	0.2
ScHDL	835	ppm	1	9.3	2.7	9.0	0.5	20.0	19.5	8.0	11.0	3.0	0.1	0.5		0.0
Se	835	ppm	1	-1	1	-1	-1	3	4	-1	-1	0	2.4	4.2	718	86.0
SeHDL	835	ppm	1	0.7	0.5	0.5	0.5	3.0	2.5	0.5	0.5	0.0	3.1	8.8		0.0

Table 2. continued

	Valid N	*Unit*	*LLD*	*Mean*	*SD*	*Median*	*Minimum*	*Maximum*	*Range*	*25 pctl*	*75 pctl*	*IQR*	*Skew*	*Kurt*	*Censored*	*% censored*
Sm	835	ppm	0.01	3.42	1.15	3.36	0.17	7.88	7.71	2.65	4.10	1.45	0.5	0.9	0	0.0
Sn	835	ppm	0.05	1.70	0.83	1.54	0.19	9.51	9.32	1.32	1.83	0.51	3.9	23.1	0	0.0
Sr	835	ppm	0.02	37.18	178.16	10.49	1.76	2977.32	2975.56	6.17	21.44	15.27	13.4	198.7	0	0.0
Ta	835	ppm	0.01	-0.01	0.00	-0.01	-0.01	0.05	0.06	-0.01	-0.01	0.00	15.5	285.4	828	99.2
TaHDL	835	ppm	0.01	0.005	0.002	0.005	0.005	0.050	0.045	0.005	0.005	0.000	23.7	614.4		0.0
Tb	835	ppm	0.005	0.379	0.134	0.366	0.021	0.916	0.895	0.286	0.458	0.172	0.5	0.9	0	0.0
Te	835	ppm	0.05	0.04	0.08	0.06	-0.05	0.49	0.54	-0.05	0.09	0.14	0.6	1.3	333	39.9
TeHDL	835	ppm	0.05	0.043	0.068	0.060	-0.025	0.490	0.515	-0.025	0.090	0.115	1.1	3.3		0.0
Th	835	ppm	0.01	11.59	2.95	11.83	0.48	21.57	21.09	9.83	13.49	3.66	-0.5	0.8	0	0.0
Tl	835	ppm	0.01	0.19	0.08	0.18	0.01	1.02	1.01	0.15	0.23	0.08	2.8	21.6	0	0.0
Tm	835	ppm	0.01	0.15	0.05	0.15	-0.01	0.37	0.38	0.12	0.18	0.06	0.6	1.2	3	0.4
TmHDL	835	ppm	0.01	0.152	0.054	0.150	0.005	0.370	0.365	0.120	0.180	0.060	0.6	1.2		0.0
U	835	ppm	0.01	1.01	0.48	0.95	0.14	7.61	7.47	0.76	1.16	0.40	5.8	64.7	0	0.0
V	835	ppm	2	83	21	83	-2	228	230	72	96	24	0.3	4.3	1	0.1
VHDL	835	ppm	2	83	21	83	1	228	227	72	96	24	0.3	4.2		0.0
W	835	ppm	0.05	0.02	0.07	0.05	-0.05	0.25	0.30	-0.05	0.07	0.12	0.3	-1.2	409	49.0
WHDL	835	ppm	0.05	0.053	0.034	0.050	0.025	0.250	0.225	0.025	0.070	0.045	1.5	3.5		0.0
Y	835	ppm	0.02	10.30	4.04	9.83	0.45	25.80	25.35	7.56	12.66	5.10	0.7	0.9	0	0.0
Yb	835	ppm	0.01	0.96	0.34	0.93	0.05	2.51	2.46	0.73	1.15	0.42	0.7	1.5	0	0.0
Zn	835	ppm	1	19	12	15	-1	97	98	11	22	11	2.2	6.6	2	0.2
ZnHDL	835	ppm	1	18.6	11.5	15.0	0.5	97.0	96.5	11.0	22.0	11.0	2.2	6.6		0.0
Zr	835	ppm	0.1	18.3	5.1	18.3	1.5	50.6	49.1	15.6	21.0	5.4	0.5	4.6	0	0.0
50micron-percent	835		2.130	1.562	1.678	0.000	14.351	14.351	1.111	2.668	1.558	2.4	9.1	0	0.0	

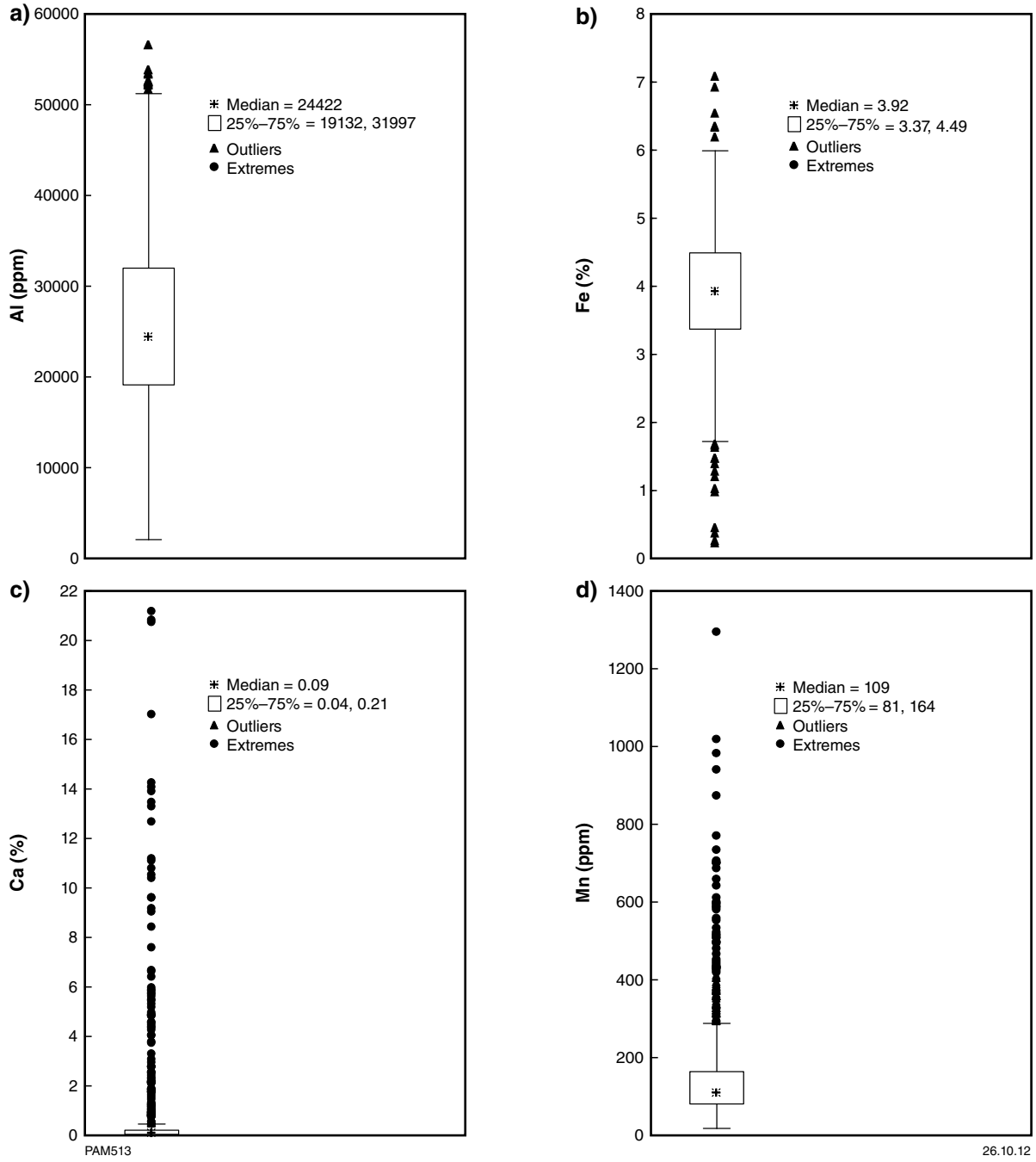

Figure 17. Box and whisker plots for elements analysed in the <50 µm fraction of regolith from the east Wongatha area: a) Al (ppm); b) Fe (%); c) Ca (%); d) Mn (ppm); e) Sr (ppm); f) La (ppm); g) Ce (ppm); h) Zr (ppm); i) Y (ppm); j) U (ppm); k) Th (ppm); l) Ni (ppm; censored data replaced by half LLD); m) Co (ppm); n) Sc (ppm; censored data replaced by half LLD); o) V (ppm; censored data replaced by half LLD); p) As (ppm; censored data replaced by half LLD); q) Bi (ppm); r) Mo (ppm; censored data replaced by half LLD); s) Sb (ppm; censored data replaced by half LLD); t) Cu (ppm; censored data replaced by half LLD); u) Pb (ppm; censored data replaced by half LLD); v) Zn (ppm; censored data replaced by half LLD); w) Au (ppb; censored data set at zero); x) Au (ppb; censored data replaced by half LLD).

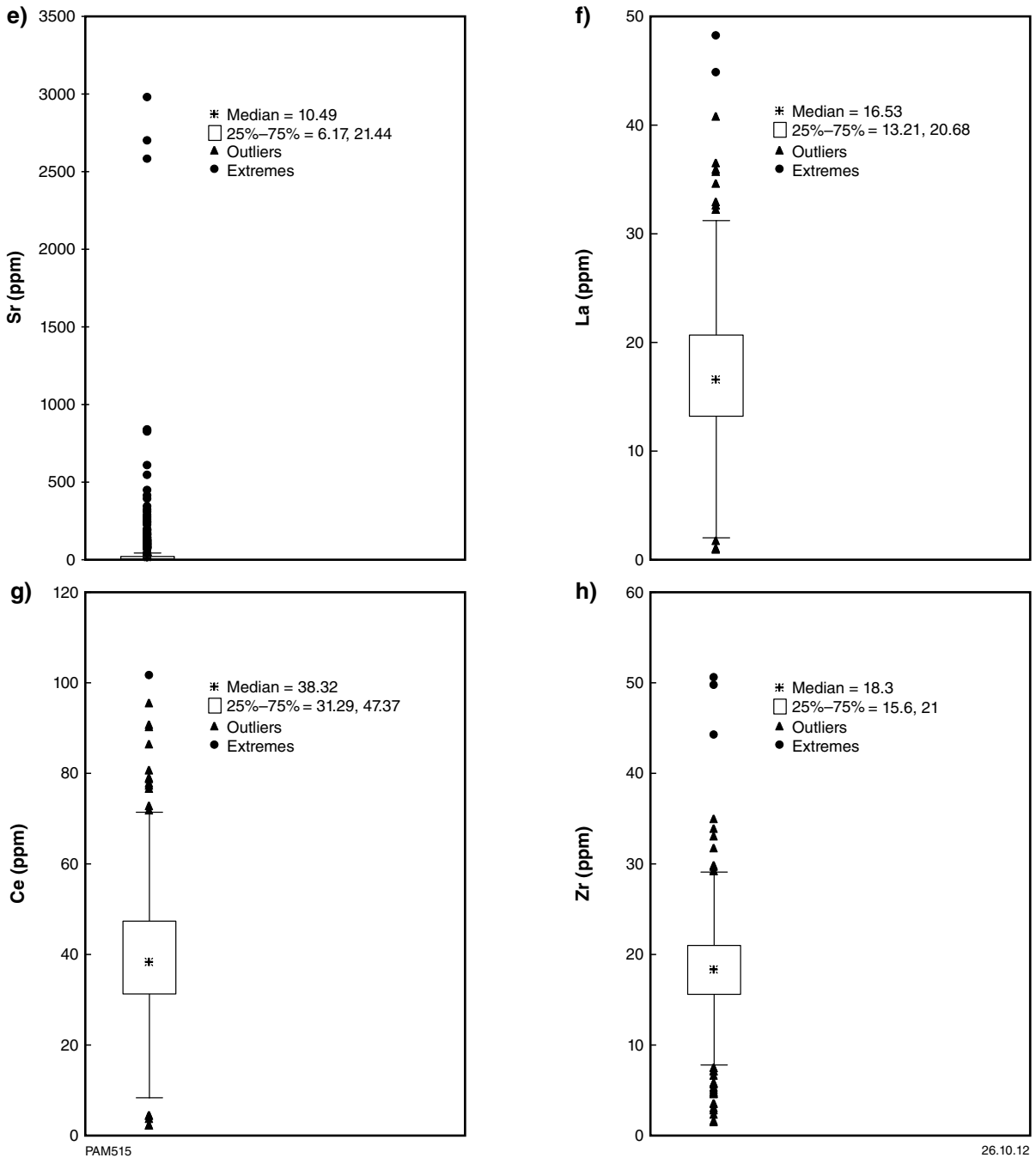

Figure 17. continued

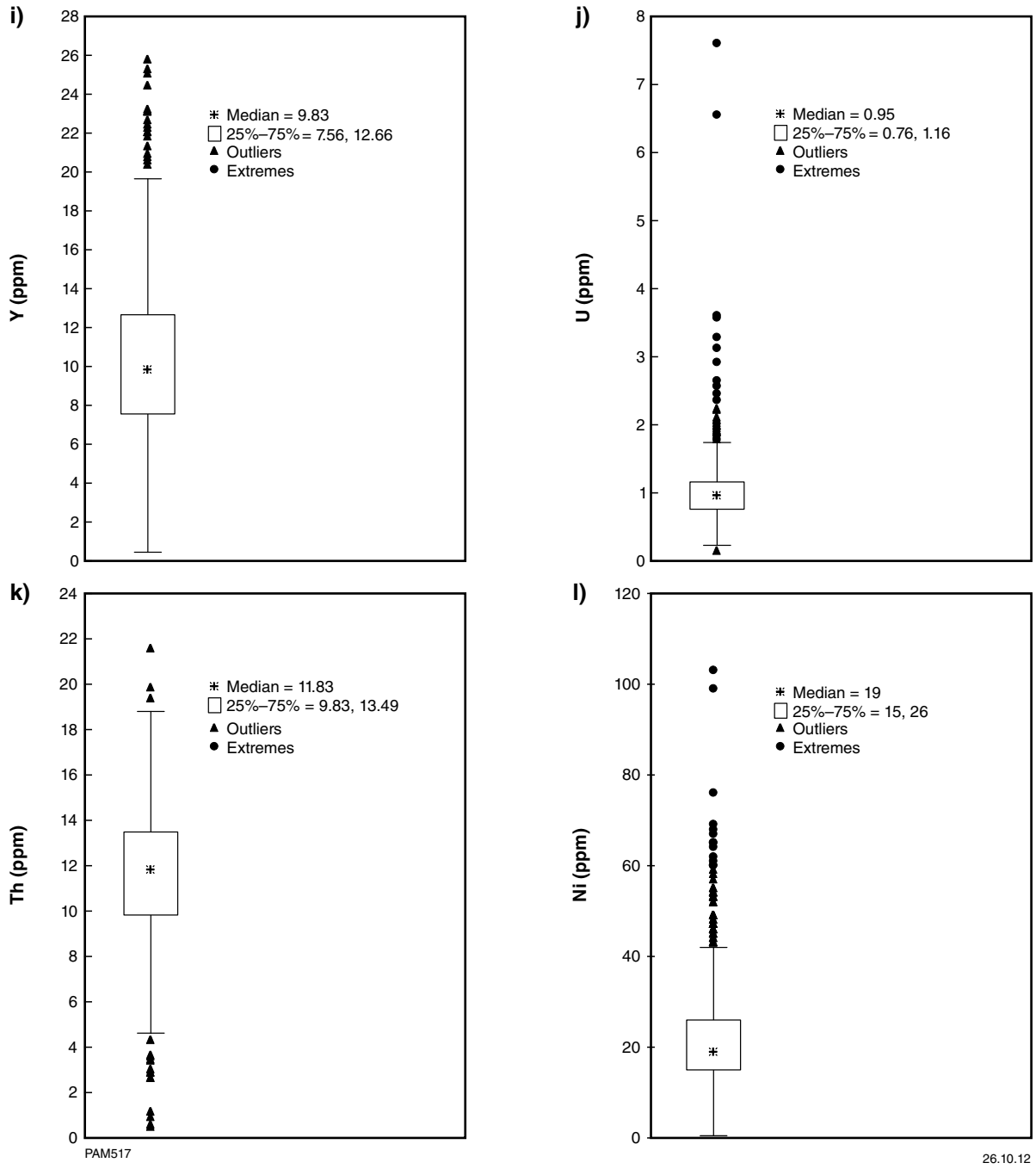

Figure 17. continued

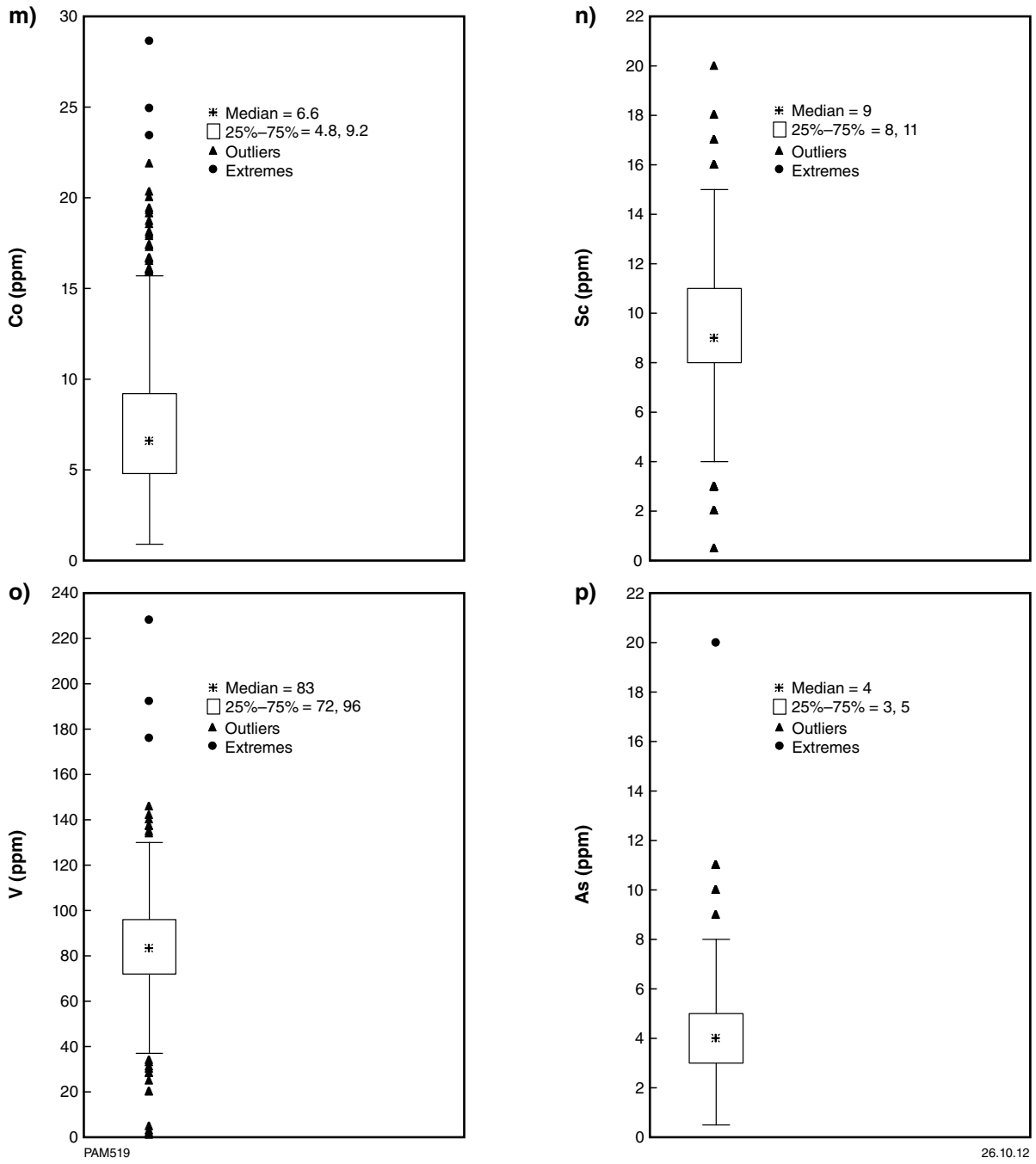

Figure 17. continued

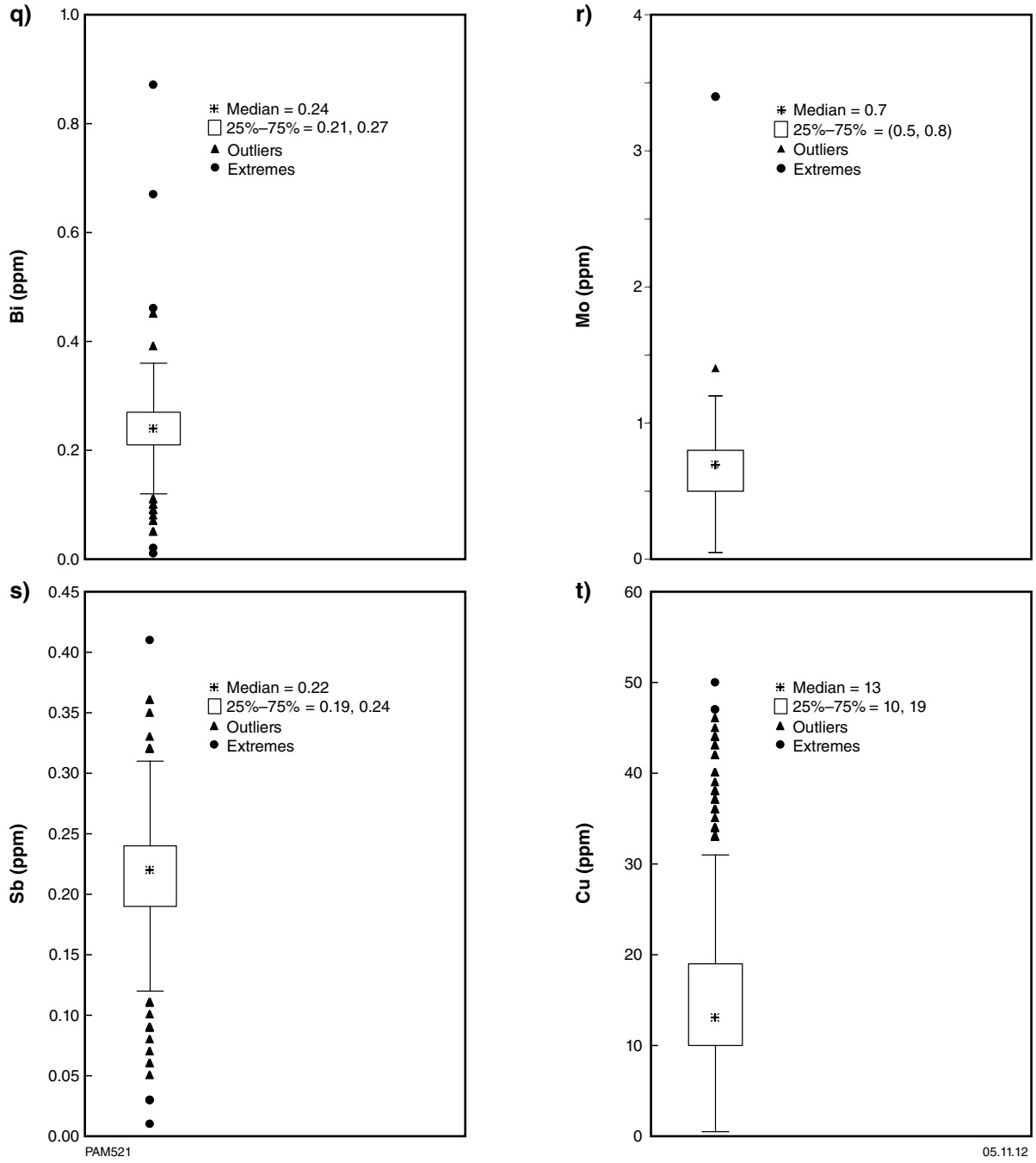

Figure 17. continued

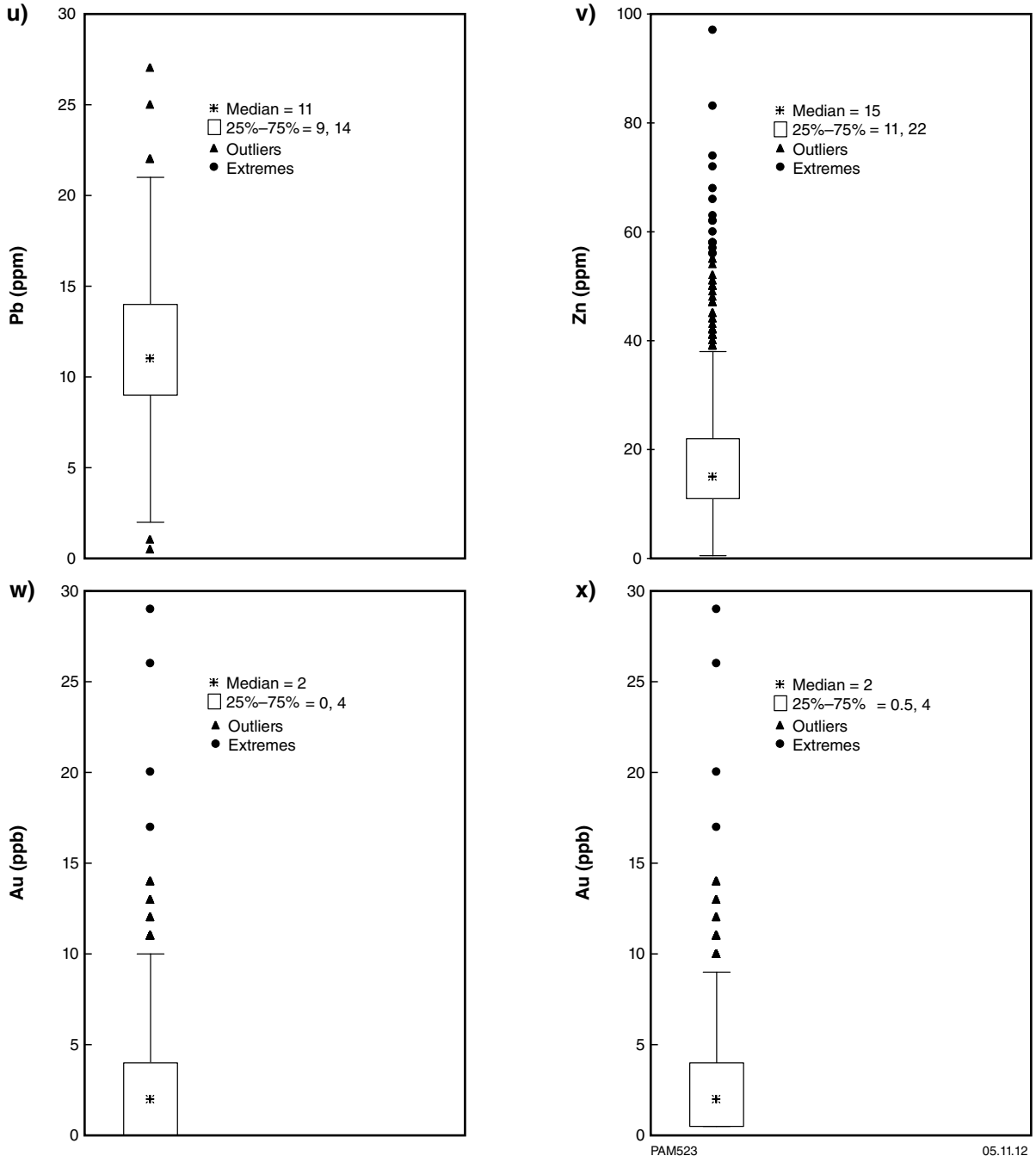

Figure 17. continued

Aluminium ranges from 2075–56 560 ppm (i.e. 0.39 – 10.69% Al_2O_3), and Fe ranges from 0.22 – 7.07% (i.e. 0.31 – 10.11 Fe_2O_3). Calcium (as Ca%) shows a wide concentration range from less than LLD (0.01%; seven samples) to 21.15 (i.e. <0.014 – 29.59% CaO), whereas Mn shows a relatively limited range from 18–1293 ppm (i.e. up to 0.17% MnO).

Both Al and Fe show close to normal distributions (Figs 17a,b), but Ca and Mn are strongly negatively skewed (Figs 17c,d). Consistent with a more normal distribution, there are few samples with anomalous Al (Fig. 18a), and most of these are found over the Yilgarn Craton. Aluminium concentrations appear lower in regolith from over the Gunbarrel Basin. Similarly to Al, there are few samples with anomalous Fe (Fig. 18b), and there is no clear relationship between Fe content of the fine fraction of regolith and tectonic unit; however, the majority of samples with low Fe contents are found in regolith from the Gunbarrel Basin and in lake sediment samples in the northwest of Minigwal. Samples with anomalously high concentrations of Ca are found over most of the Yilgarn Craton on Minigwal, or over Fraser Zone lithologies on Bowden (Fig. 18c). The Fraser Zone rocks include gabbro and metamorphosed mafic rocks. Scattered samples with anomalous concentrations of Ca are also found in parts of the Gunbarrel Basin, and there are a few samples with higher Ca concentrations spatially related to more magnetised bedrock on the Meinya–Kakarook boundary.

Manganese (Fig. 18d) shows a similar distribution to Ca, with elevated concentrations in regolith over parts of the Yilgarn Craton and Fraser Zone mafic rocks. There are a few anomalous samples from the Gunbarrel Basin, as well as on or near to the Meinya–Kakarook boundary.

Lithophile elements

Lithium (maximum 43.6 ppm; Fig. 19a) is found in higher concentrations in regolith from parts of the Yilgarn Craton (cf. Al; Fig. 18a), and in some samples over the Albany–Fraser Orogen. There are few samples with anomalously high rubidium concentrations, and these are mostly found over parts of the Yilgarn Craton and Albany–Fraser Orogen (Fig. 19b). There is a strong positive correlation between Li and Al (Fig. 20a; $R^2 = 0.74$), and between Rb and Al (Fig. 20b; $R^2 = 0.69$), but poor agreement of any of these three elements with the amount of the <50 µm fraction (e.g. Al, Fig. 20c; $R^2 = 0.08$). This indicates that Li, Al, and Rb behave similarly in the silt to clay fraction of regolith, but their concentration is not controlled by the amount of this fine fraction in each sample.

Strontium values range from 1.8 to 2977 ppm, with a strong positively skewed distribution (Fig. 17e). The majority of anomalous values are found in regolith over the Yilgarn Craton (cf. Ca and Mn; Fig. 18c,d), but there is no clear relationship with either granite or greenstone (Fig. 21). Other anomalous samples are found over parts of the Albany–Fraser Orogen, particularly close to the Fraser Zone and on the Meinya–Kakarook boundary. Of the eight samples with >500 ppm Sr, all but one are found in or close to lake systems in the northwest part of Minigwal. If these samples are excluded, there is a positive correlation between Ca and Sr (Fig. 22; $R^2 = 0.75$), although there is some scatter at higher concentrations.

The light rare earth elements (LREE) lanthanum and cerium show a weak positive skewness with a few outlier and extreme values (Fig. 17f,g). The few samples with anomalous concentrations of either element are found on or close to greenstones of the Yilgarn Craton and over parts of the Albany–Fraser Orogen on northeast Bowden (Fig. 23a,b). Zirconium is more normally distributed than either La or Ce (Fig. 17h). Most samples have <30 ppm Zr, and some have anomalously low concentrations of <8 ppm. There is no clear relationship between Zr content and any tectonic unit, although a group of samples with elevated Zr concentrations is found over the Gunbarrel Basin on the Narnoo–Kakarook boundary (Fig. 23c). Low Zr concentrations could reflect the both low zircon content of regolith and the resistance of zirconium to digestion by aqua regia.

Yttrium is weakly positively skewed (Fig. 17i), but only a few samples have anomalous concentrations. These are found on or close to Yilgarn Craton greenstones in the southwest part of Minigwal, or close to Fraser Zone lithologies in the northeast part of Bowden (Fig. 23d). The concentration of uranium in regolith ranges from 0.14 – 7.61 ppm (median = 0.95 ppm; Fig. 17j). Most samples with anomalous U concentrations are found in or close to lake systems in the north-western part of Minigwal (Fig. 23e). One sample with anomalous U in the southeast part of NARNOO is found over a sliver of Yilgarn Craton granite on the Gunbarrel Basin margin (GSWA 200023; 2.91 ppm U). The sample with the highest U content of 7.61 ppm (GSWA 200848) is found in the central part of Meinya amongst samples with generally low U contents.

Thorium concentrations range from 0.5 – 21.6 ppm (median = 11.8 ppm; Fig. 17k), and although three samples have anomalous Th contents (>19 ppm), these are outliers rather than extremes. These samples are found over parts of the Gunbarrel Basin in the northern part of Narnoo (Fig. 23f).

Siderophile elements

Chromium in regolith ranges from 4–369 ppm (median = 93 ppm; Fig. 16), whereas nickel shows a more limited concentration range of <1 to 103 ppm (median = 19 ppm; 1 censored sample; Fig. 17l). Cobalt reaches a maximum of 28.6 ppm, and has a median value of 6.6 ppm (Fig. 17m). All three element distributions are positively skewed.

The maximum Cr value of 369 ppm is found in GSWA 200325 over part of the Biranup Zone on the western part of Bowden (Fig. 24a), a unit dominated by granitic gneiss and paragneiss. Low Cr concentrations are found in regolith over parts of the Gunbarrel Basin and Albany–Fraser Orogen, and in or close to lake areas in the northwest part of Minigwal. A few samples with anomalously high Cr concentrations are found in close proximity to Yilgarn Craton greenstones, and two samples with anomalous Cr contents are found in regolith in

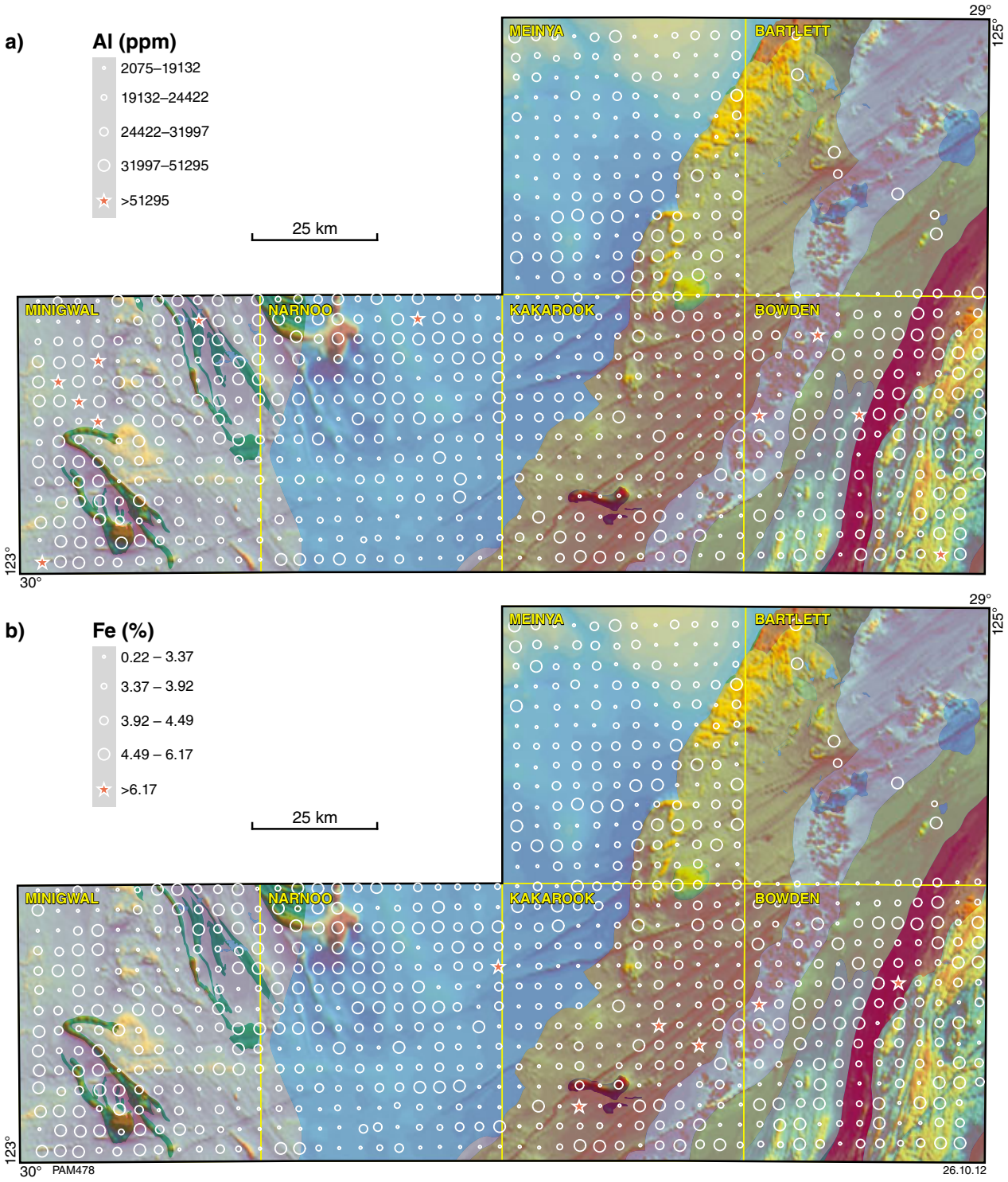

Figure 18. Bubble plots for major components of east Wongatha <50 micron regolith: a) Al (ppm); b) Fe (%); c) Ca (%; censored data set at half LLD); d) Mn (ppm).

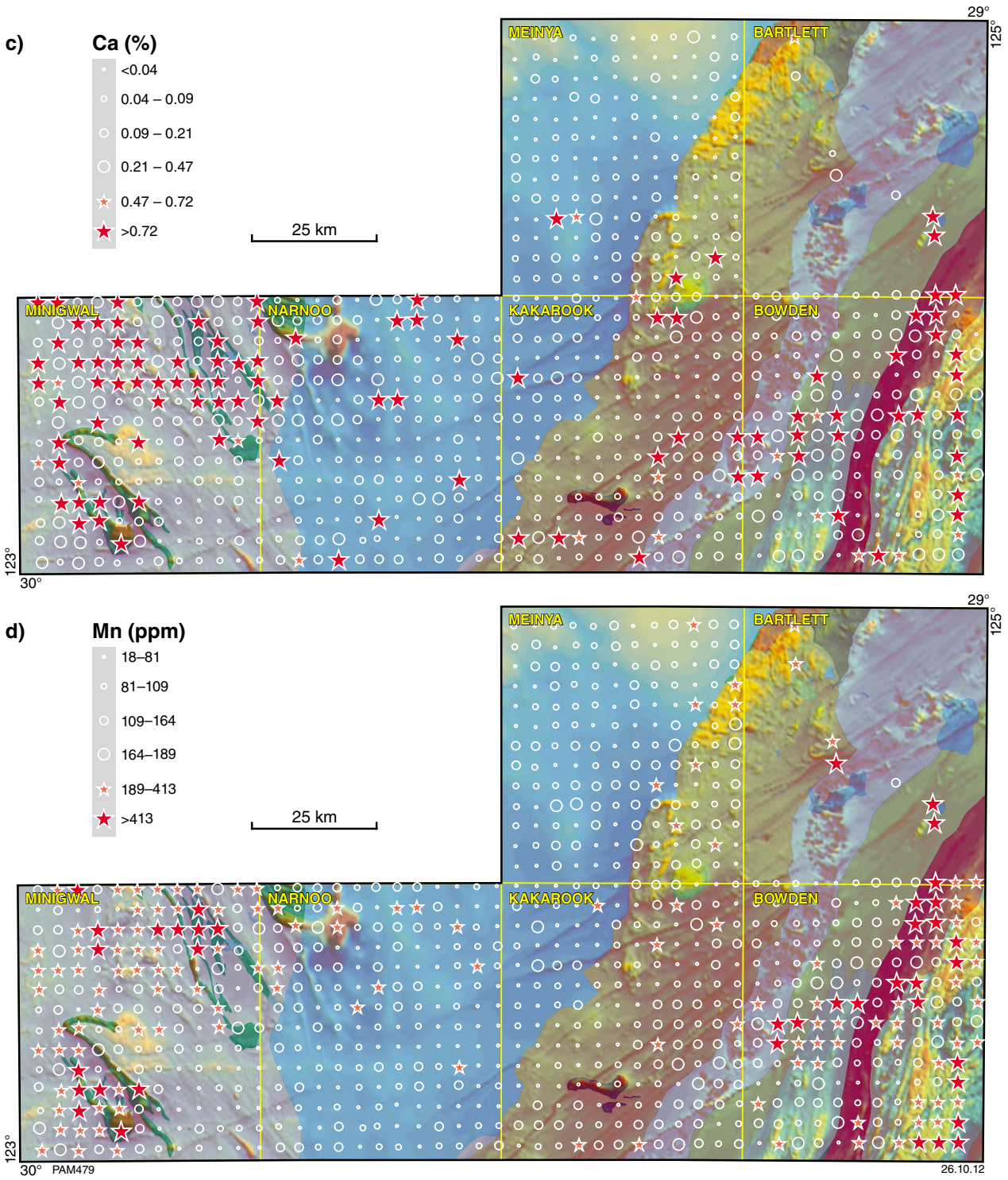

Figure 18. continued

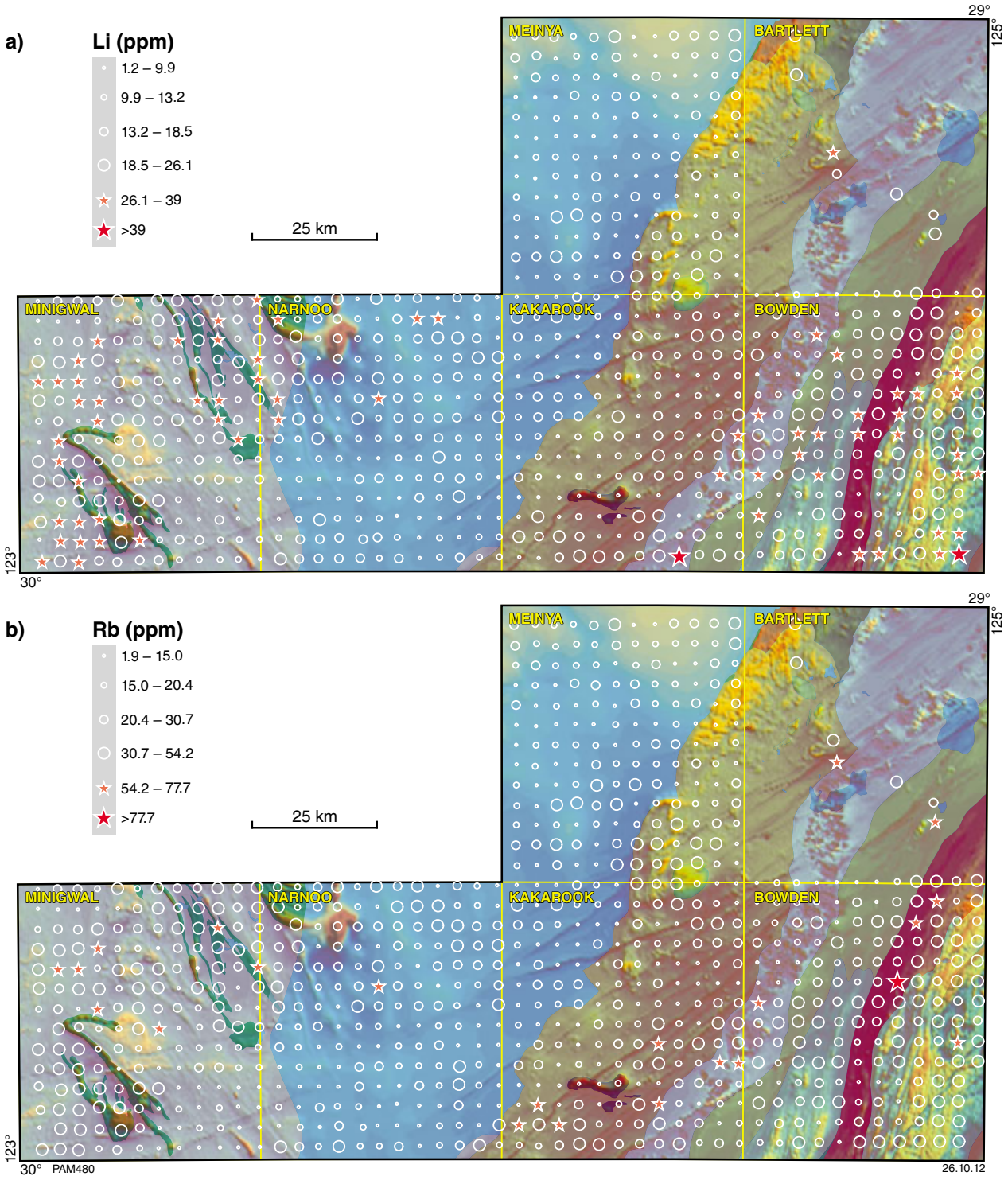

Figure 19. Bubble plots for lithophile elements in the <50 micron fraction of east Wongatha area regolith; a) Li (ppm); b) Rb (ppm).

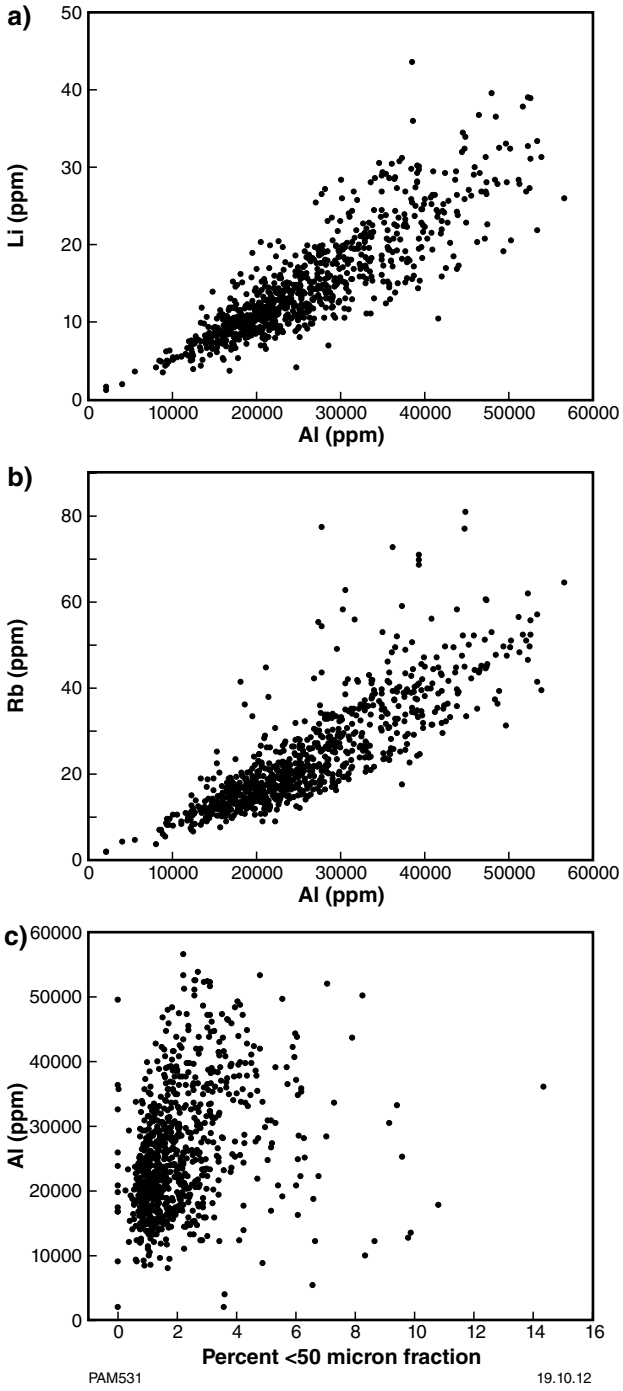

Figure 20. Bivariate plots for components of the <50 µm fraction of regolith from the east Wongatha area; a) Li vs Al (ppm); b) Rb vs Al (ppm); c) Al (ppm) vs Al (%) of <50 µm fraction.

the western parts of the Gunbarrel Basin, on or close to northwest-trending magnetic anomalies extending into the basin from the Yilgarn Craton.

The distribution of Ni in regolith shows a well-developed spatial relationship with Yilgarn Craton greenstones (Fig. 24b). There are a few samples over the Albany–Fraser Orogen with anomalous Ni, including GSWA 200325, which has the highest concentration of both Ni (103 ppm) and Cr (369 ppm) in regolith.

Like Cr, samples with anomalous Co are found on or close to Yilgarn Craton greenstones, with a few anomalous concentrations also found in samples from parts of the Albany–Fraser Orogen (Fig. 24c). Two samples with anomalous Co are found close to the boundary of the Albany–Fraser Orogen with the Gunbarrel Basin in the southern part of NARNOO, where there is selvedge of Yilgarn Craton granite.

Scandium ranges from <1 (two samples) to 20 ppm (median = 9 ppm). The data show a weak positive skewness with no extremely anomalous concentrations (Fig. 17n). Vanadium ranges from <2 to 228 ppm (median = 83 ppm), with several anomalously high values (Fig. 17o).

The few anomalously high Sc values are found on or to the northwest of greenstones in the southwest part of MINIGWAL (Fig. 24d). Several anomalously high vanadium values are also found on or close to Yilgarn Craton greenstones (Fig. 24e), and there is a group of anomalously high values in the western part of the Gunbarrel Basin close to the southeast extension of the Stella Range – Irwin Hills greenstone belt in the northwest part of NARNOO. Several other anomalously high vanadium values are found over parts of the Albany–Fraser Orogen, and in regolith over the Gunbarrel Basin on MEINYA.

Chalcophile elements

Chalcophile elements (e.g. As, Ag, Bi, Cd, Sb, Mo, Se, and W) are those commonly associated with sulphides. Smith et al. (1989) showed that the chalcophile element chemistry of laterite from part of the Yilgarn Craton can be used to indicate zones of potential mineralization ('chalcophile corridors'). Chalcophile element data from the <50 µm fraction of regolith from the east Wongatha area is more difficult to assess than that for most other element groups because there is a high percentage of censored data for Ag (92% of samples), Cd (69%), Se (86%), and W (49%), and data for these elements have not been treated statistically.

Arsenic reaches a maximum concentration of 20 ppm, with three censored values, and a median value of 4 ppm. The data are only weakly positively skewed and there are few anomalous concentrations (Fig. 17p). Although the concentration of bismuth is low in all regolith samples analysed (maximum 0.87 ppm; LLD = 0.01 ppm, median = 0.24 ppm), there are no censored data (Fig. 17q).

Samples with anomalous As concentrations (i.e. ≥8 ppm) are largely found in regolith in the southeast part of KAKAROOK over older (Northern Foreland) rocks of the Albany–Fraser Orogen. These rocks appear to be more strongly magnetized than adjacent lithologies (Fig. 25a). The maximum As concentration of 20 ppm is found in lake sediment sample GSWA 200577 in the northwest part of MINIGWAL. Anomalously high Bi (≥0.36 ppm) is

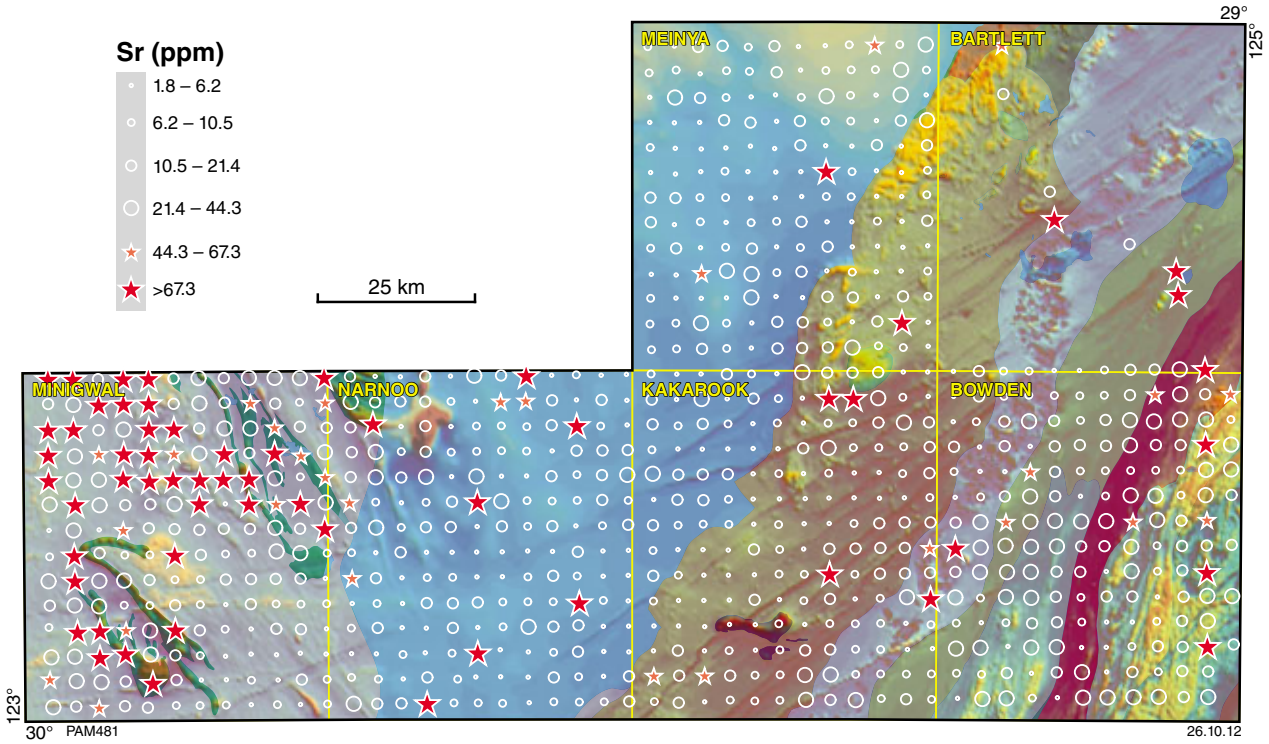

Figure 21. Bubble plot for Sr (ppm) in the <50 micron fraction of east Wongatha area regolith.

found in samples overlying variably magnetized rocks on parts of Bowden, including sample GSWA 200184 from the southwest part of Bowden, with the maximum Bi concentration of 0.87 ppm (Fig. 25b). Sample GSWA 200172 (0.46 ppm Bi) coincides with Proterozoic mafic intrusive rocks forming a distinct magnetic anomaly about 11 km long in the southern part of Kakarook.

Molybdenum reaches a maximum concentration of 3.4 ppm, with a median value of 0.7 ppm (Fig. 17r). There are three censored values. Samples with low Mo contents are found in the sandplain-dominated northern part of Meinya (Fig. 25c). The highest value of 3.4 ppm is in lake sediment sample GSWA 200577, which also has anomalously high As.

There are samples with both anomalously high and low concentrations of antimony (Fig. 17s), which has a maximum concentration of 0.41 ppm. There are few anomalous values, and no clear relationship between Sb concentrations and lithology, although low Sb concentrations are mostly found in regolith over the Gunbarrel Basin, or spatially associated with lake systems in northwest Minigwal (Fig. 25d).

Base metals

Data for copper in three samples are censored (i.e. <1 ppm), with a population median of 13 ppm, and a maximum concentration of 50 ppm. Samples with Cu ≥33 ppm are anomalous (Fig. 17t). Only one sample returned censored data for lead, which has a median value of 11 ppm and a maximum concentration of 27 ppm (Fig. 17u).

Most elevated Cu values are found on or close to areas of greenstone in the southwest part of Minigwal (Fig. 26a), but two anomalous values (including a concentration of 47 ppm in GSWA 200325) are found in regolith over parts of the Albany–Fraser Orogen. Of the few samples

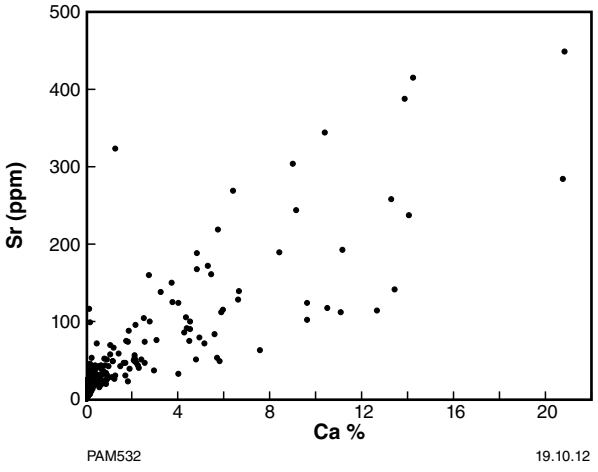

Figure 22. Bivariate plot of Sr (ppm) vs Ca (%; censored data set at half LLD) in <50 micron fraction of regolith from the east Wongatha area for samples with <500 ppm Sr (excludes samples in or close to lake systems).

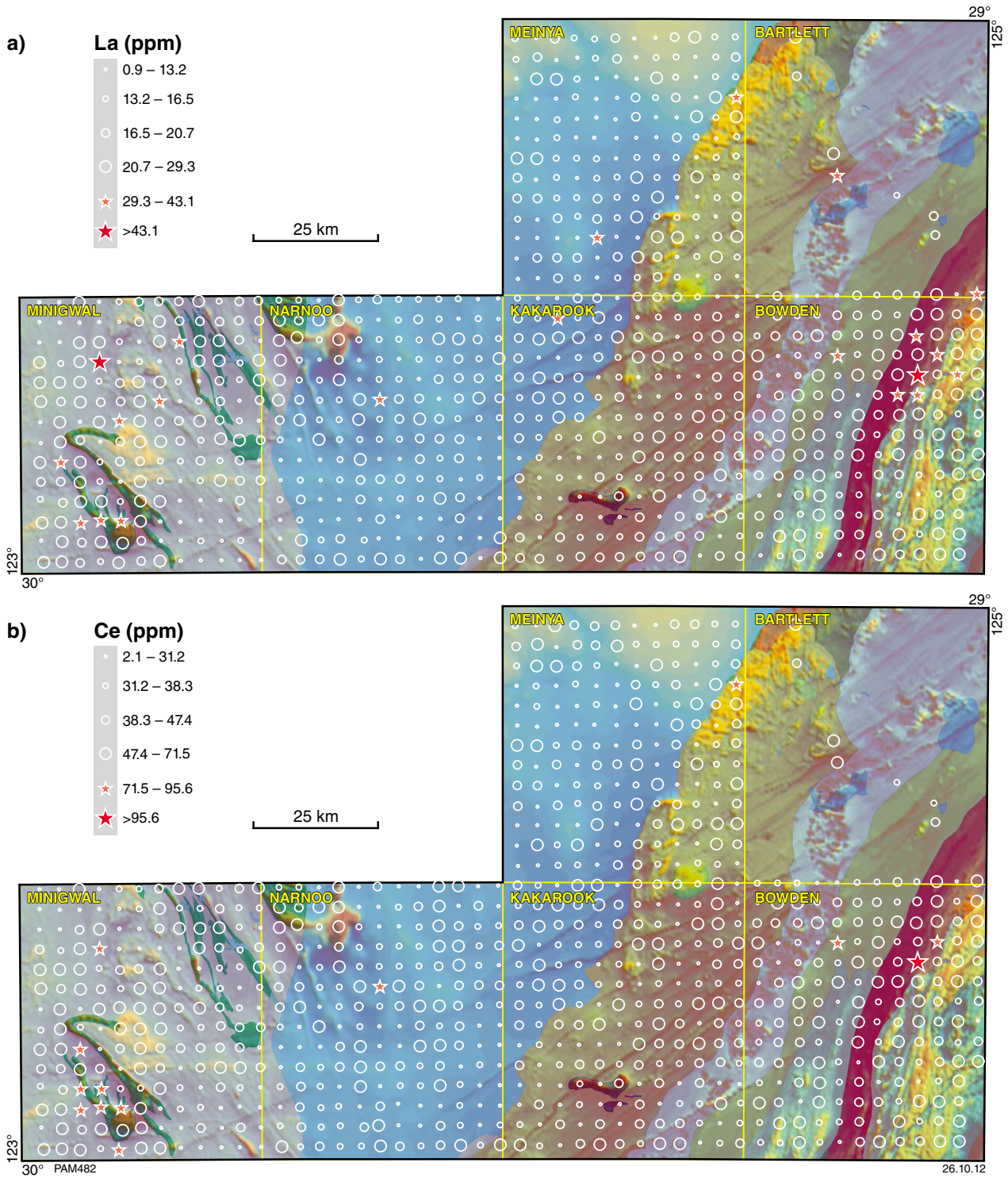

Figure 23. Bubble plots for elements analysed form the <50 µm fraction of regolith from the east Wongatha area: a) La (ppm); b) Ce (ppm); c) Zr (ppm); d) Y (ppm); e) U (ppm) f) Th (ppm).

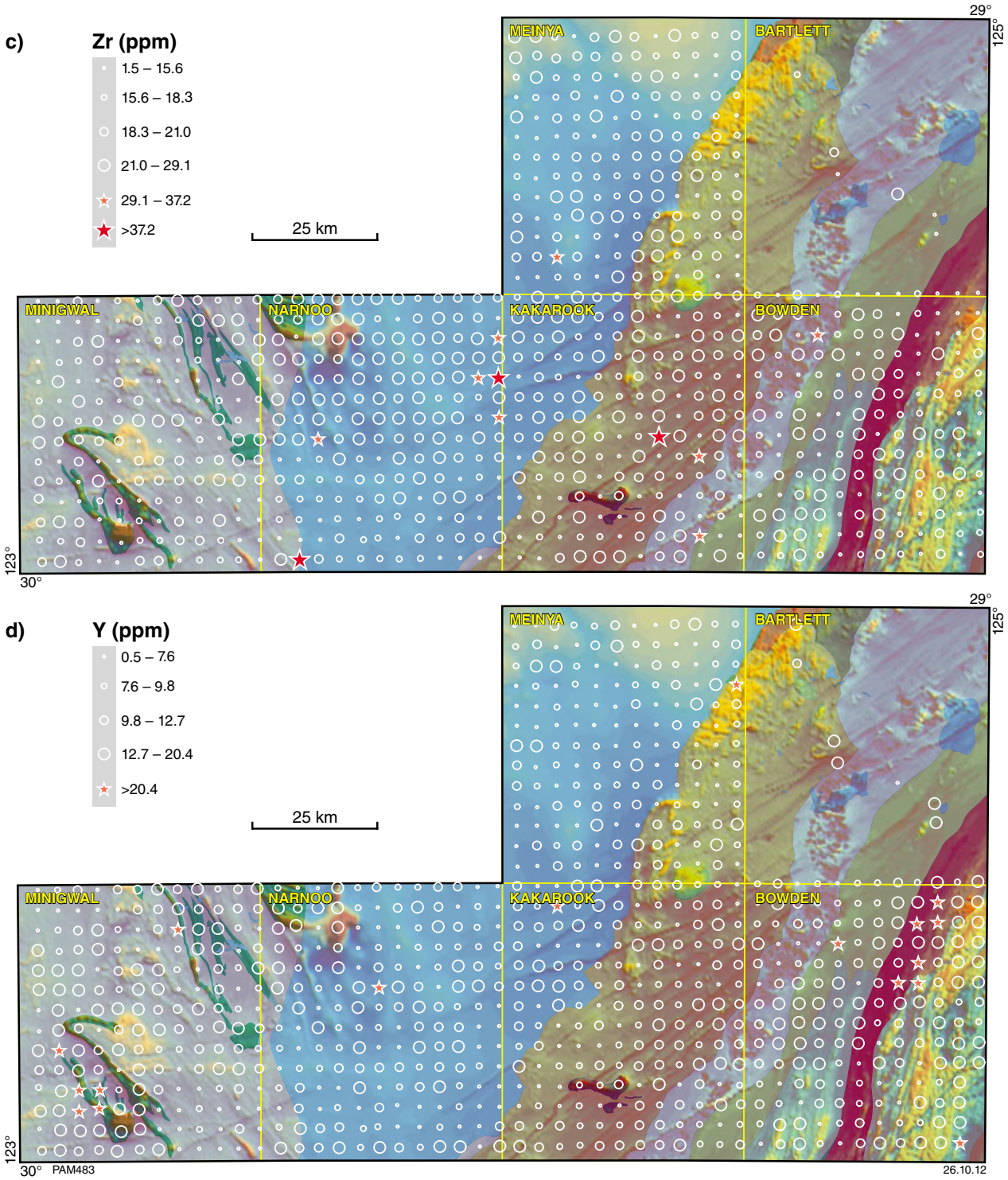

Figure 23. continued

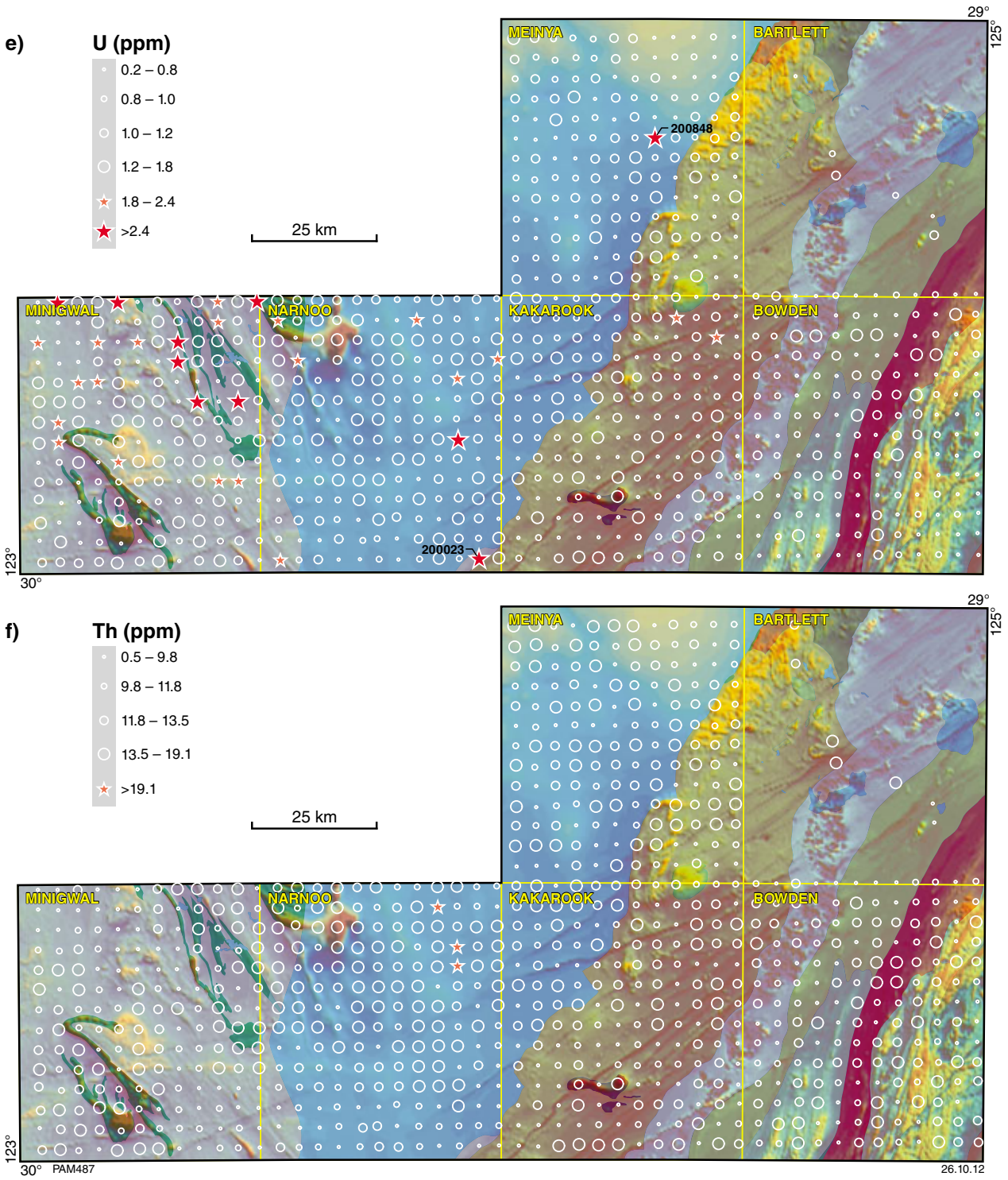

Figure 23. continued

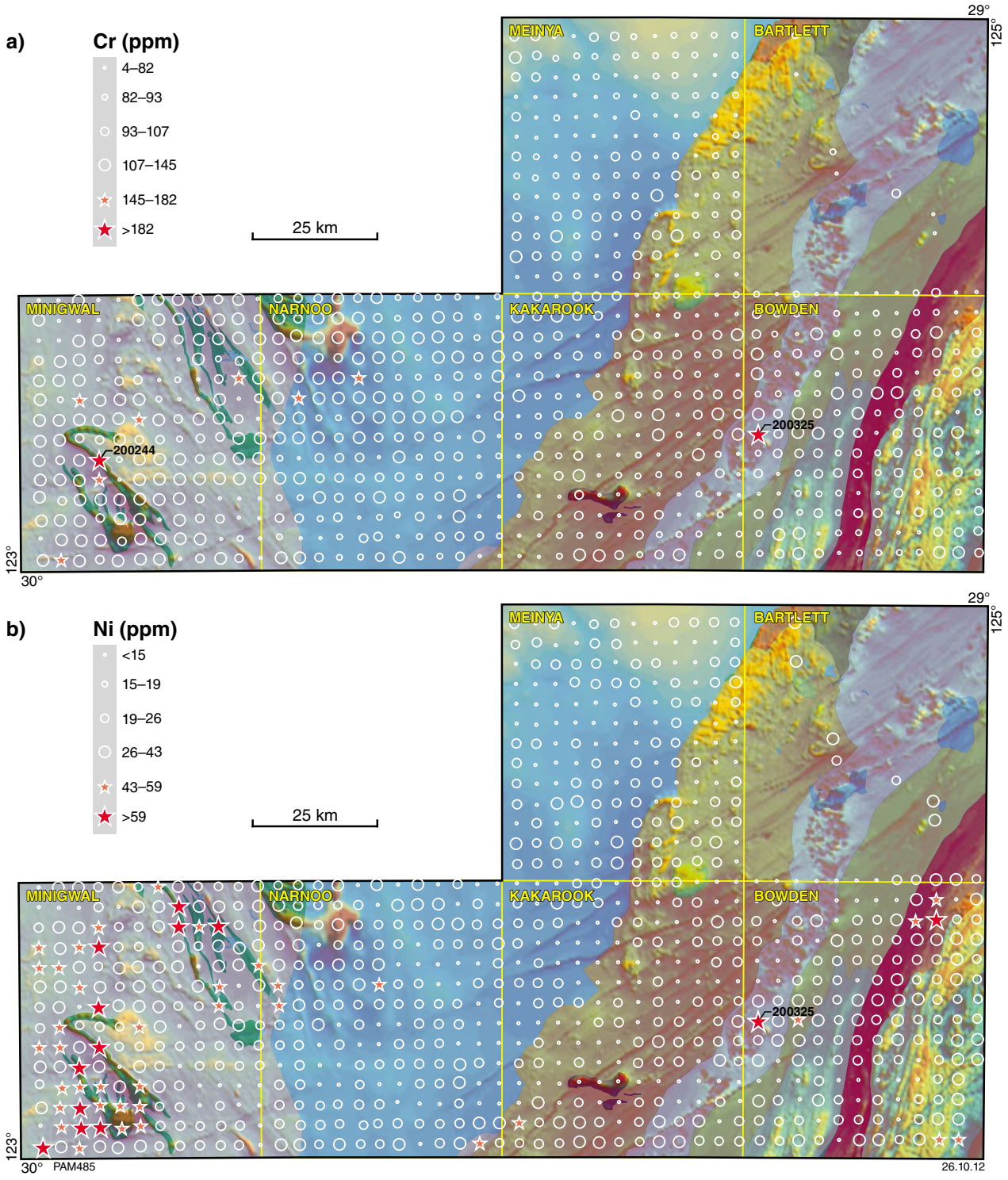

Figure 24. Bubble plots for elements analysed from the <50 µm fraction of regolith from the east Wongatha area: a) Cr (ppm); b) Ni (ppm; censored data set at half LLD); c) Co (ppm); d) Sc (ppm; censored data set at half LLD); e) V (ppm; censored data set at half LLD).

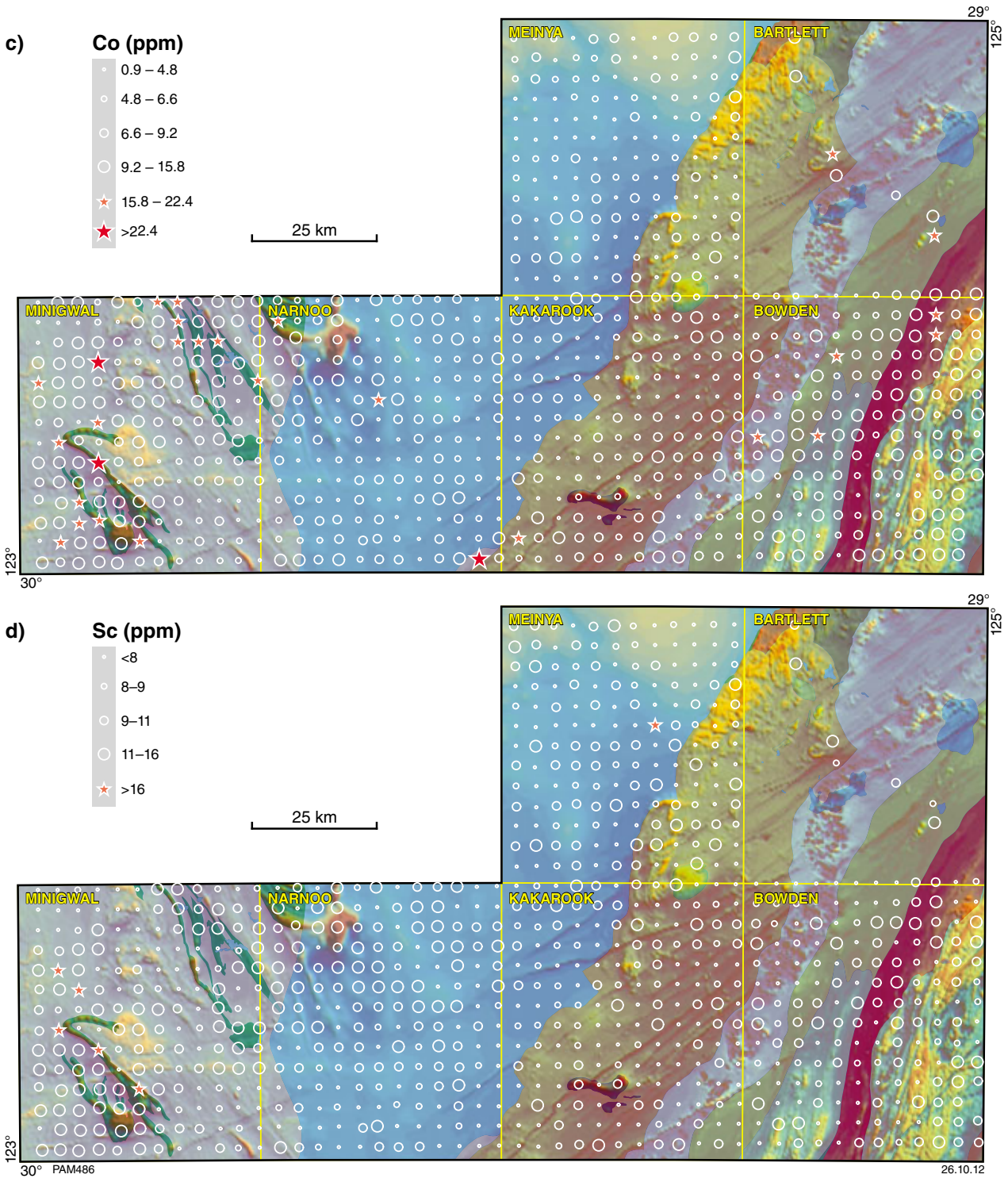

Figure 24. continued

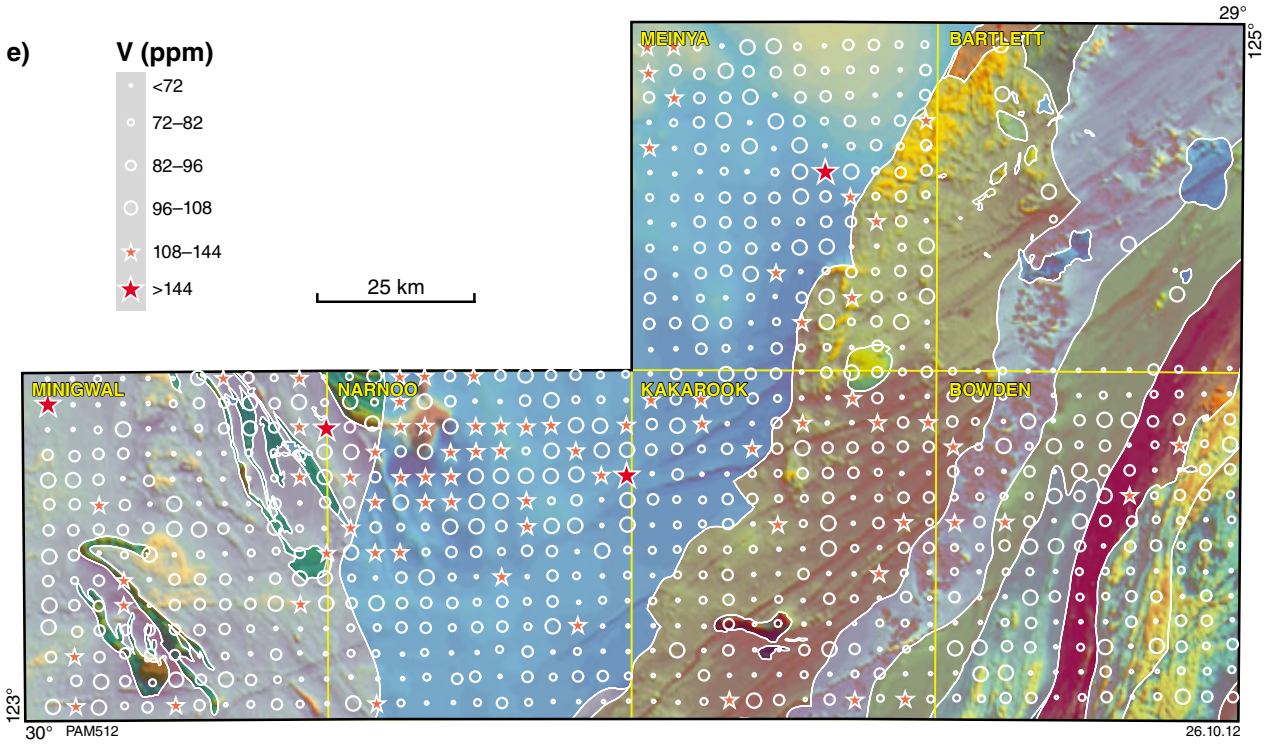

Figure 24. continued

with anomalous Pb concentrations (Fig. 26b), most are found on or close to Yilgarn Craton greenstones (cf. Cu), although one anomalous sample (GSWA 200118; 25 ppm Pb) plots close to the Albany–Fraser Orogen – Gunbarrel Basin margin on Narnoo. Lead values are generally low in samples from over the Gunbarrel Basin.

The box and whisker plot for zinc (Fig. 17v) shows that there are a number of anomalously high values. The maximum Zn concentration of 97 ppm is found in GSWA 200484, clustered with a group of three other extreme values in the northwest part of Minigwal (Fig. 26c). Most of the remaining anomalously high samples are found over the southeast part of Bowden. Here, Albany–Fraser Orogen rocks are dominated by metagabbro, although the proximity of the Eucla Basin could mean that higher Zn is related to higher carbonate in regolith (cf. Fig. 18c). Other, scattered high-Zn values are found elsewhere over parts of the Albany–Fraser Orogen.

Gold, palladium, and platinum

Of the 835 samples analysed in this study, 301 (36%) returned values of less than the LLD (1 ppb) for gold. Box plots and derived statistics for Au were plotted with censored data reported as zero (Fig. 17w), and with censored data reported as 0.5 ppb (half the LLD; i.e. replaced data) (Fig. 17x). Both approaches produce similar median values of 2 ppb, but different thresholds (i.e. the upper background level). Anomalous values and the outlier–extreme boundary with censored data replaced by zero are 10 and 16 ppb respectively, whereas these values are slightly lower (9 and 15 ppb respectively) when censored data are substituted by half the LLD. According to these different approaches, the number of anomalous values are eight and nine respectively.

Replacement of censored data by a value equal to half the LLD (0.5 ppb in this study) is a common practice (Reimann et al., 2010), and the behaviour of these data is discussed below. The distribution of Au for replaced data (Fig. 27a) shows a strong spatial relationship of anomalous Au values with Yilgarn Craton greenstones, including the maximum Au concentration of 29 ppb in GSWA 200150. Some anomalous values, including a value of 20 ppb, are found in regolith samples on northwest strike extensions of greenstones on Minigwal, and on magnetic anomalies indicative of greenstones extending beneath the western part of the Gunbarrel Basin. Other anomalous samples are found on or close to the margins of the Gunbarrel Basin with either the Albany–Fraser Orogen or Yilgarn Craton, but these samples are not spatially related to aeromagnetic anomalies.

Elsewhere in the project area, there are fewer samples with anomalous Au concentrations. On the 11-km long east–west magnetic anomaly corresponding to intrusive, Proterozoic mafic rocks (Spaggiari et al., 2011) on the southern part of Kakarook, sample GSWA 200172 has 11 ppb Au, and three other samples over the Albany–Fraser Orogen have 11 or 12 ppb gold. In general, Au concentrations appear lower in regolith over the Gunbarrel Basin, especially on Meinya.

Due to the high proportion of censored data for silver (91.5% or 764 samples), no statistical analysis was carried out. A bubble plot (Fig. 27b), using natural breaks in the data to determine class sizes, shows that the maximum Ag concentration of 0.33 ppm (LLD = 0.05 ppm) is found in GSWA 200821, in the central part of Meinya in the Gunbarrel Basin. A relatively high proportion of samples with elevated Ag concentrations are found in regolith on or close to greenstones in the southwestern part of Minigwal. There is also measurable Ag in some samples from parts of the Albany–Fraser Orogen, and over the southern part of the Gunbarrel Basin on Narnoo.

There are few samples with measurable palladium; 92.9%, or 776 samples, returned concentrations less than the LLD of 10 ppb. The maximum concentration is 29 ppb, found in GSWA 200568, along with a group of samples with elevated Pd concentrations over part of the Albany–Fraser Orogen, in the northern part of Bowden (Fig. 27c). Similarly, most platinum data are censored (94.4% or 788 samples), with an LLD of 5 ppb. The distribution of samples with measurable Pt is quite different to that for Pd (Fig. 27d). Of those samples that returned measurable Pt, there are few over the Yilgarn Craton, and most are found over the Gunbarrel Basin on Meinya, including the maximum Pt concentration of 9 ppb in GSWA 200751. Sample GSWA 200282, from over the Albany–Fraser Orogen on Bowden, also has 9 ppb Pt.

Element additive indices

The behaviour of several elements that show some chemical affinity can be sumarized by using an additive index approach. Smith et al. (1989) used a chalcophile (CHI-6*X) and pegmatite (Peg-4) index to identify areas of potential chalcophile and pegmatite mineralization in parts of the Yilgarn Craton. They weighted some components of each index to account for lower elements concentrations. Thus, their CHI-6*X index is: As + 3Sb + 10Bi + 3Mo + 30Ag + 30Sn +10W + 3Se.

Reid et al. (2010) have compiled several multi-element indices to target both mineralization and bedrock types using biogeochemical data from the northern Yilgarn Craton. Data were scaled from 0 to 1 based on the 1st to 99th percentile, and then summed to create indices. For example, their Au Min 1 index (Au + Ag + As) aims to detect regional gold targets, whereas the Lithol1 index (V + Cr – (2*U)) aims to separate granite and greenstone.

Several element indices were used in GSWA's regional regolith geochemistry project (Morris and Verren, 2001). In order to take account of the relative concentration, concentration range, and whether or not data were censored, a set procedure was followed. Firstly, censored values were taken as zero, then ten was added to all concentrations. Secondly, the log of each value was calculated, which reduces the effects of extremely high or low values. Thirdly, all data were expressed as standard normal deviates (i.e. data were standardized), which allows direct comparison of element abundance independent of concentration (Rock, 1988). Standard scores were then summed to create additive indices. This approach has been adopted here, although scores have been calculated using the log of the censored data where values less than the LLD have been replaced by half the detection level (i.e. censored data not set to zero and 10 not added to all values).

Base metal index

A bubble plot for a base metal index (BMI: summed standard scores for Cu, Pb, Zn, Sb, As, Bi, Sn) shows a number of anomalously high values over most of the Yilgarn Craton, and extending southeast from the Irwin Hills – Stella Range greenstone belt over parts of the Gunbarrel Basin (Fig. 28). Samples with anomalous values are also found over most of the Albany–Fraser Orogen, although there are fewer elevated values over magnetic rocks in the southeastern part of Meinya. The lowest scores are found over the Gunbarrel Basin. A scatterplot of Cr (ppm) versus BMI (Fig. 29) shows a crude positive correlation (R^2 = 0.486), with two samples lying off the main trend at elevated Cr concentrations (GSWA 200325 from the Albany–Fraser Orogen with 369 ppm Cr, and GSWA 200244 from an area of Yilgarn Craton greenstone on the southern part of Minigwal with 253 ppm Cr; Fig. 24a).

Carbonate index

In this study, a carbonate index is the summed standard score for Ca and Sr. High values for this index are found over Yilgarn Craton greenstones and parts of the Albany–Fraser Orogen (Fig. 30). There is generally poor agreement between gold and the carbonate index (Fig. 31). The three highest gold concentrations found in samples from over the Yilgarn Craton (GSWA 200150 at 29 ppb; GSWA 200100 at 26 ppb; GSWA 197879 at 20 ppb; Fig. 27a) have a high carbonate index, but other samples with Au concentrations >10 ppb show a range in carbonate index values, indicating no consistent relationship between Au and carbonate content.

Chalcophile index

A chalcophile index (CHALCO: summed standard scores for As, Bi, Mo, Sb; Fig. 32) shows a broadly similar distribution to the base metal index (Fig. 28), but there are more anomalous chalcophile index values over the Gunbarrel Basin. There is poor agreement between gold and CHALCO (Fig. 33), with some samples that contain elevated Au concentrations having CHALCO values close to zero.

Ferroalloy index

A ferroalloy index (Ferroalloy: summed standard scores for Ni, Cr, Mo, Co, V) predictably has higher values for samples on or close to Yilgarn Craton greenstones (Fig. 34). Elevated values are also found over parts of the Gunbarrel Basin in the northern part of Narnoo (cf. base metal index, Fig. 28) extending to the east and southeast of the Irwin Hills – Stella Range greenstone belt. There are also higher values over parts of the Albany–Fraser Orogen. Unlike the base metal index, there are several anomalous Ferroalloy values that extend southwest from magnetized

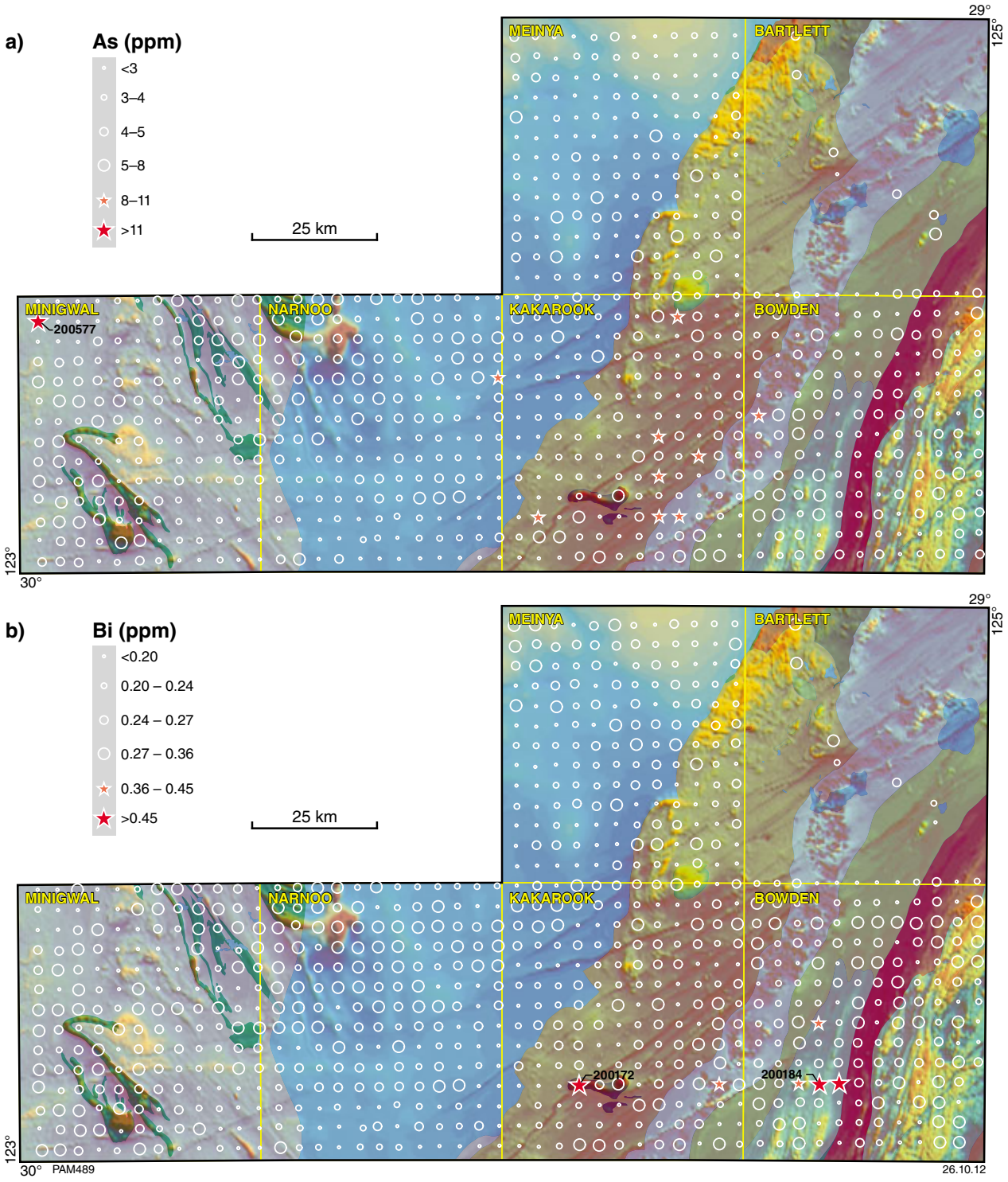

Figure 25. Bubble plots for elements analysed form the <50 µm fraction of regolith from the east Wongatha area; a) As (ppm; censored data set at half LLD); b) Bi (ppm); c) Mo (ppm; censored data set at half LLD); d) Sb (ppm; censored data set at half LLD).

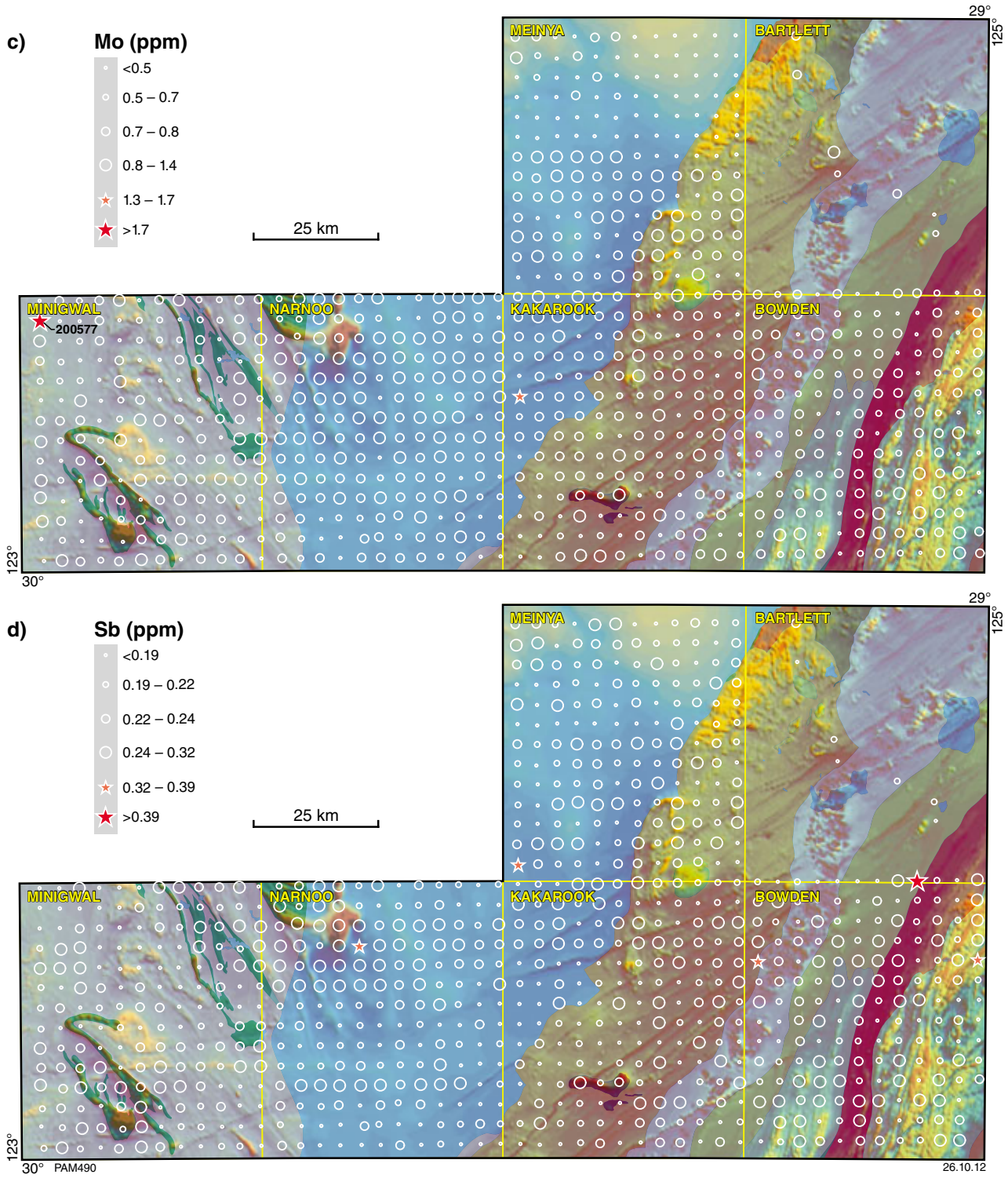

Figure 25. continued

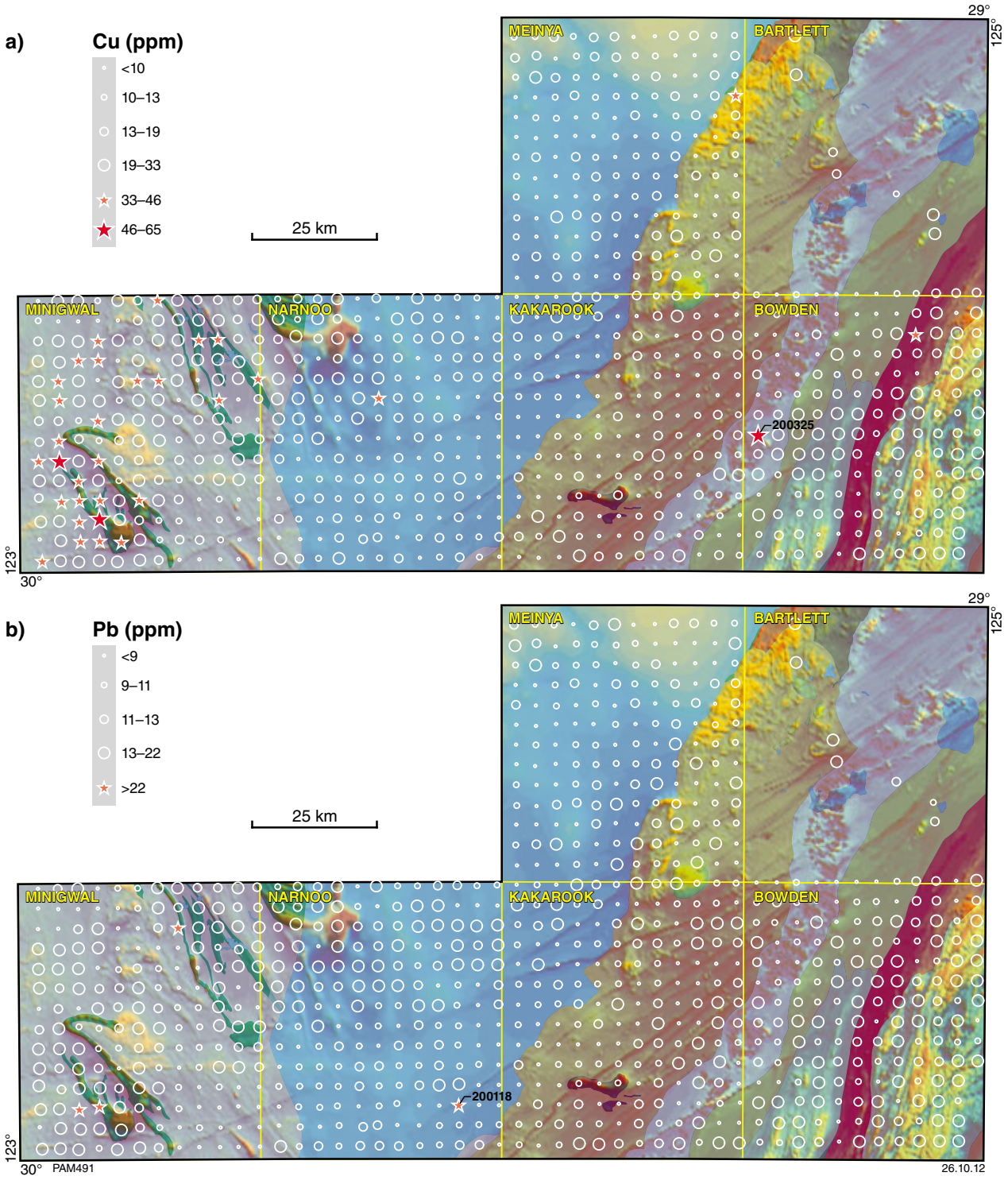

Figure 26. Bubble plots for elements analysed form the <50 µm fraction of regolith from the east Wongatha area: a) Cu (ppm; censored data set at half LLD); b) Pb (ppm; censored data set at half LLD); c) Zn (ppm; censored data set at half LLD).

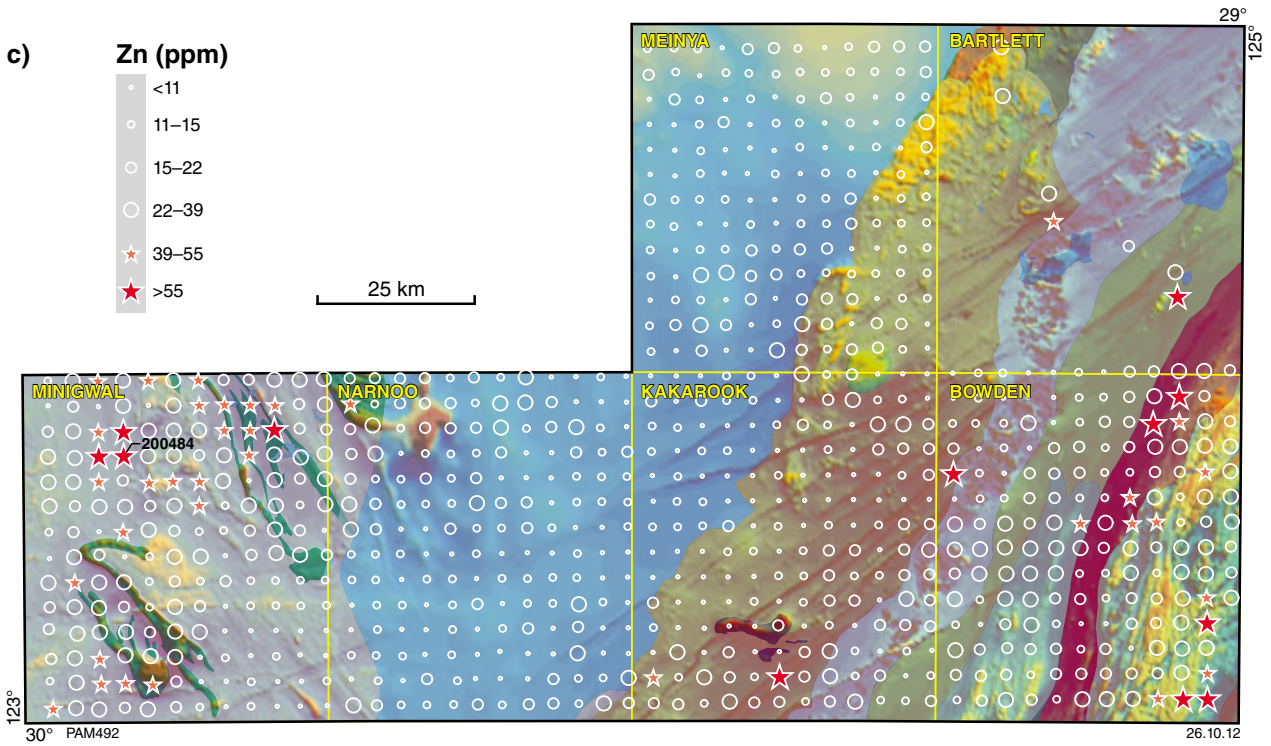

Figure 26. continued

rocks of the Albany–Fraser Orogen into the Gunbarrel Basin on Meinya. The basement here is a heterogeneous assemblage of quartzofeldspathic gneiss, amphibolites, metagranitic rock, and BIF, and it is possible that the Ferroalloy index traces the extension of mafic rocks or BIF beneath the Gunbarrel Basin cover, similar to Yilgarn Craton greenstones in the western part of Narnoo.

Discussion

The relative concentrations of several elements in the fine-fraction of regolith can be used to trace the distribution of bedrock units beneath thick regolith cover. Similarly, there is a correlation between elevated gold concentrations in the fine fraction of regolith with greenstones and known areas of unconformity-hosted mineralization.

Both manganese and calcium are found in higher concentrations in regolith over the Yilgarn Craton and over areas of mafic bedrock of the Albany–Fraser Orogen. Manganese in particular appears to be in high concentration in regolith on or close to mafic rocks found in both the Yilgarn Craton (greenstones) and parts of the Albany–Fraser Orogen (Fig. 18d). Despite their relatively high concentrations in most analysed samples, Fe and Al show little relationship to particular bedrock types, although both elements tend to be less concentrated in regolith from over the Gunbarrel Basin. Some care must be taken in relating the concentrations of elements such as calcium with the distribution of bedrock. Although calcium in regolith tends to be higher on or close to mafic bedrock, regolith-landform mapping (McGuinness, 2010) has shown that elevated calcium is influenced by the distribution of pedogenic carbonate in some paleodrainages (Fig. 6) and lake sediments, such as in the northwest part of Minigwal. The concentrations of uranium and strontium are also higher in or close to saline lake deposits.

Higher concentrations of nickel, cobalt, chromium and scandium are found on or close to Yilgarn Craton greenstones. Notably, nickel, cobalt, and yttrium appear to be more concentrated on or close to the Minigwal and Wongatha greenstone belts in the southwest part of Minigwal. This suggests that regolith chemistry may be capable of picking out the more mafic or ultramafic components of individual greenstone belts. As elevated nickel and cobalt concentrations are found along strike and adjacent to greenstones, it may be that greenstones are more extensively developed than currently mapped. The relationships between nickel and cobalt in regolith to the distribution of mafic rocks is not well demonstrated in the Albany–Fraser Orogen (such as over Fraser Zone rocks). This may indicate that individual bodies of mafic rocks are smaller than those found over the Yilgarn Craton. Although these siderophile elements are usually in lower concentrations in regolith over the Gunbarrel Basin, a few regolith samples in the western part of the basin, southeast of the Stella Range – Irwin Hills greenstone, belt have anomalous concentrations of nickel, chromium, cobalt, and especially vanadium. Some of these samples coincide with linear magnetic anomalies representing greenstone extensions beneath Gunbarrel Basin sedimentary rocks. If the elevated concentrations of these elements in regolith are derived from greenstones, then the elements must

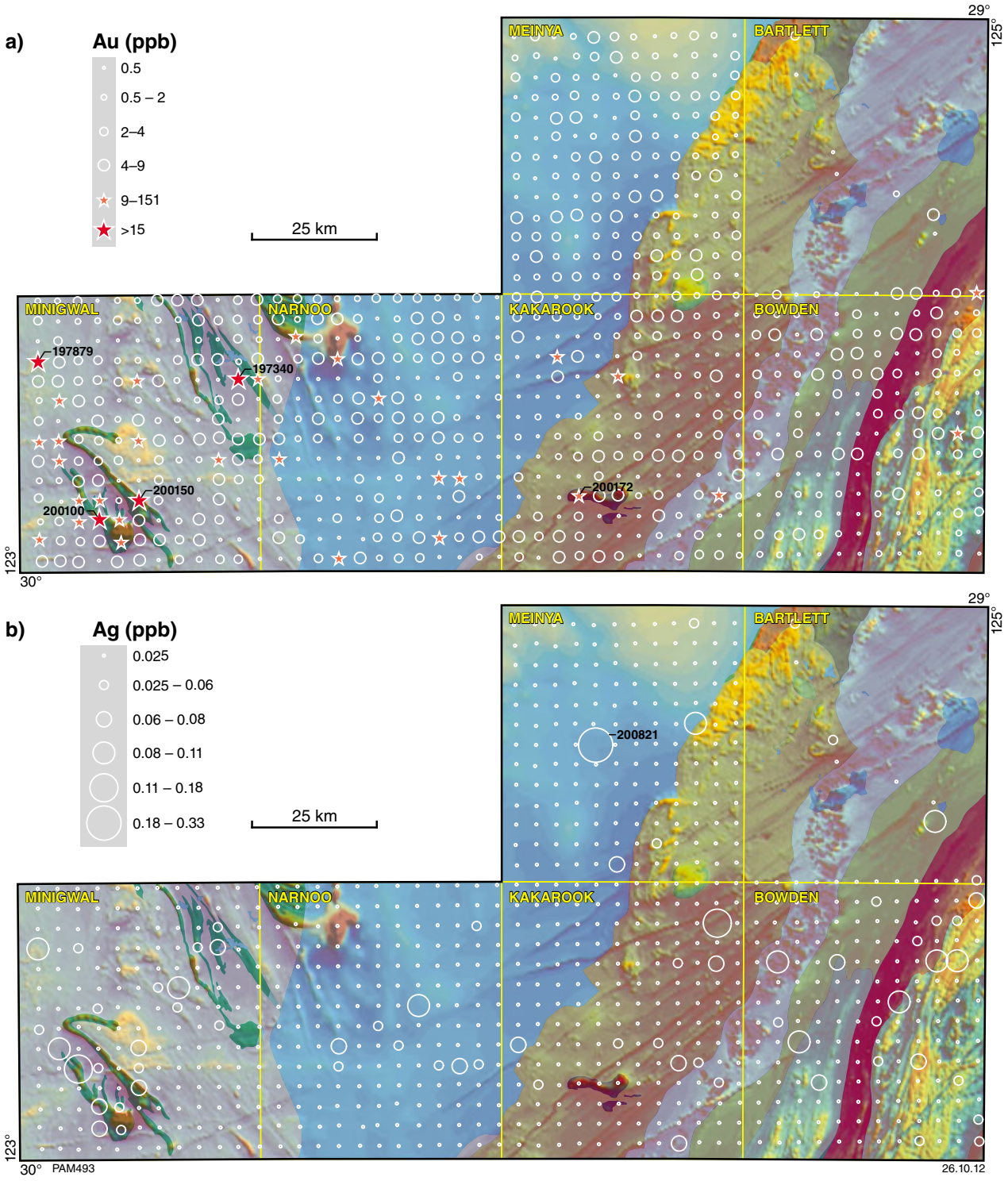

Figure 27. **Bubble plots for elements analysed form the <50 µm fraction of regolith from the east Wongatha area: a) Au (ppb; censored data set at half LLD); b) Ag (ppm; symbol size selected according to natural breaks; c) Pd (ppb; symbol size selected according to natural breaks); d) Pt (ppb; symbol size selected according to natural breaks).**

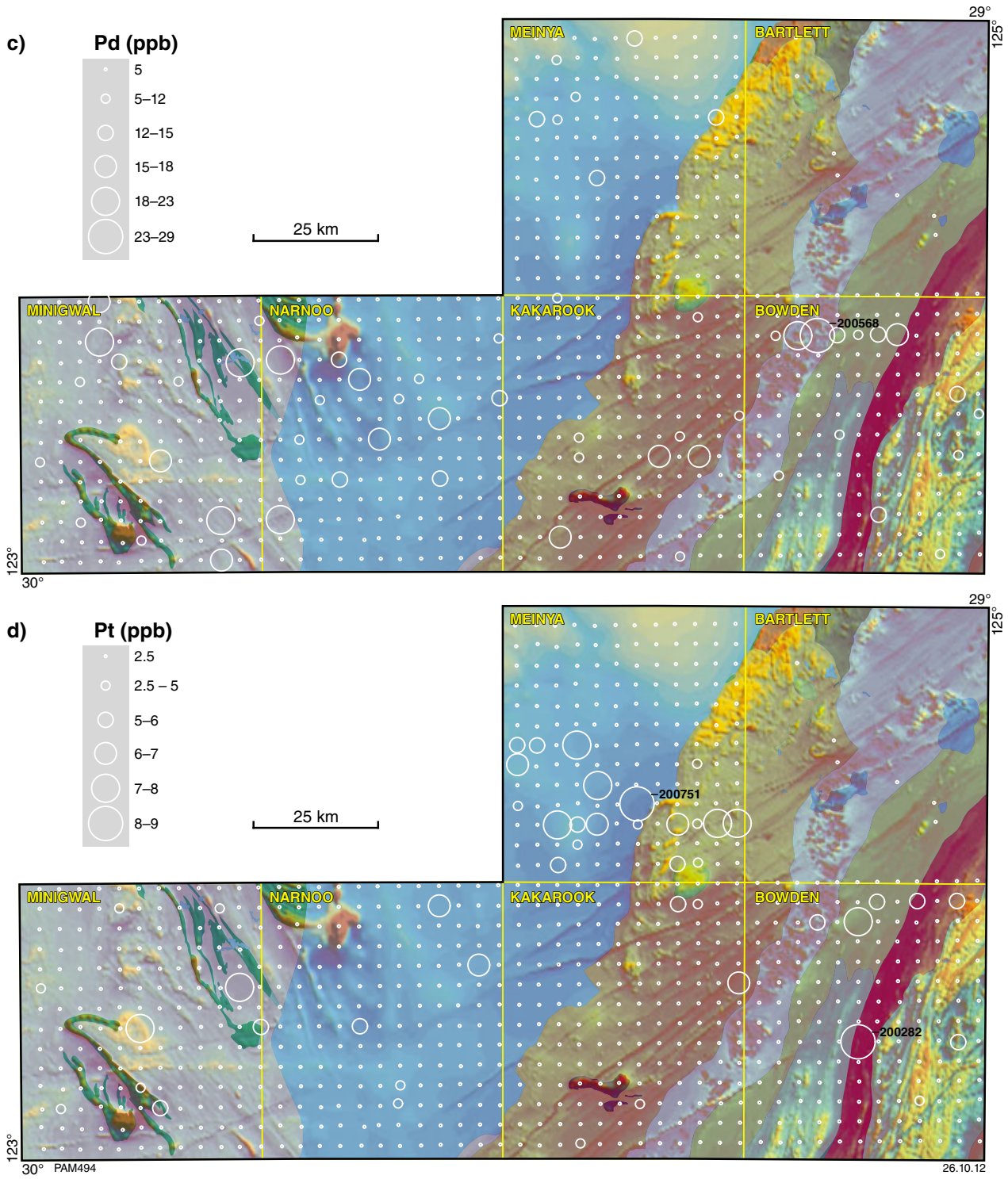

Figure 27. continued

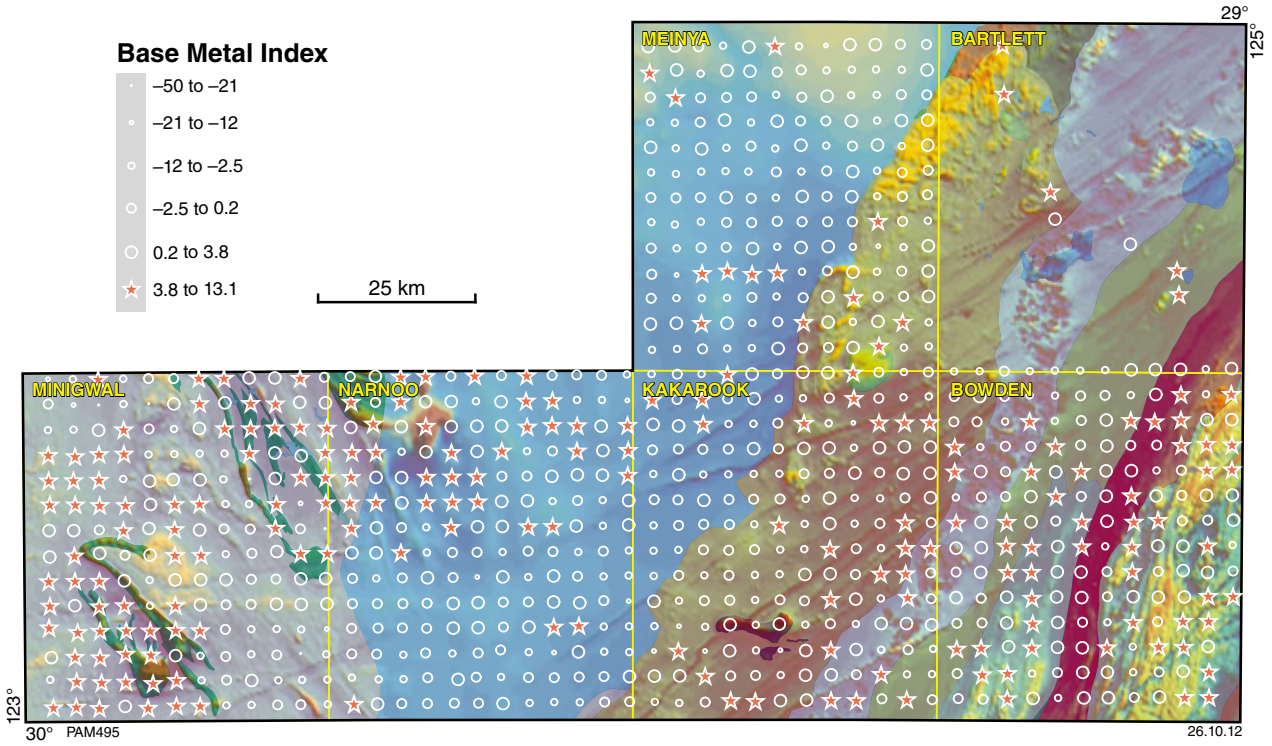

Figure 28. Bubble plot for Base Metal Index (i.e. summed standard scores for Cu, Pb, Zn, Sb, As, Bi, Sn) in <50 µm fraction of regolith from the east Wongatha area.

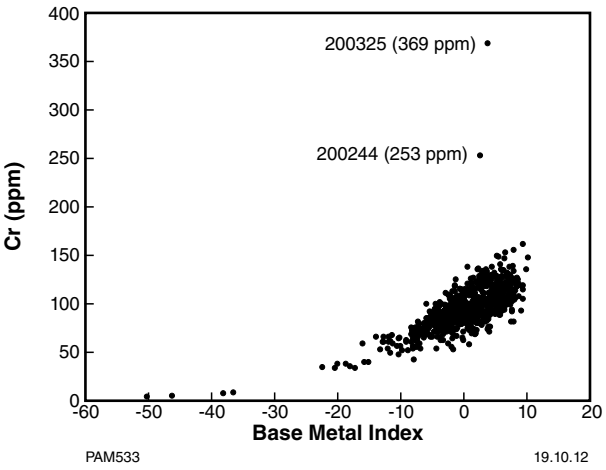

Figure 29. Bivariate plot of Cr (ppm) versus Base Metal Index for the <50 µm fraction of regolith from the east Wongatha area.

have migrated through both Gunbarrel Basin sedimentary rocks and regolith. The thickness of Gunbarrel Basin sedimentary rocks is not well known, but data from drillhole Minigwal 2A drilling data (Perincek, 1998) recorded >400 m of sedimentary rocks capped by about 8 m of regolith.

Lithophile elements are generally in lower concentrations in regolith over the Gunbarrel Basin. Lanthanum and cerium are slightly higher over Yilgarn Craton greenstones, although, for the most part, lithophile element concentrations cannot be tied to bedrock types.

Excluding lake sediments in the northwest part of Minigwal, regolith samples with the highest concentrations of chalcophile elements are generally found over parts of the Albany–Fraser Orogen, although no one group of lithologies has a consistently high chalcophile element content. An exception is found over the 11-km long east–west oriented magnetic belt of rocks in the southern part of Kakarook (interpreted by Spaggiari et al. (2011) as a Proterozoic mafic intrusion). Of the three regolith samples over this intrusion, GSWA 200172 has anomalous concentrations of gold (11 ppb) and bismuth (0.46 ppm).

Regolith samples with statistically anomalous gold concentrations are mainly found in the western part of the project area. There is a well-developed spatial relationship of gold and Yilgarn Craton greenstones, and some samples with anomalous concentrations extend along strike (coincident with magnetic anomalies), suggesting a greater extent of greenstones than evident on the ground. Similarly, some regolith samples with elevated and anomalous gold concentrations coincide with extensions of greenstone beneath the Gunbarrel Basin, shown by magnetic anomalies (Fig. 27a). Thus, similar to siderophile element distribution discussed above, it is possible that gold from greenstone-hosted gold mineralization is evident in the fine-fraction of regolith.

However, in this western part of the Gunbarrel Basin, it is apparent that some samples with anomalous gold in regolith do not coincide with magnetic anomalies.

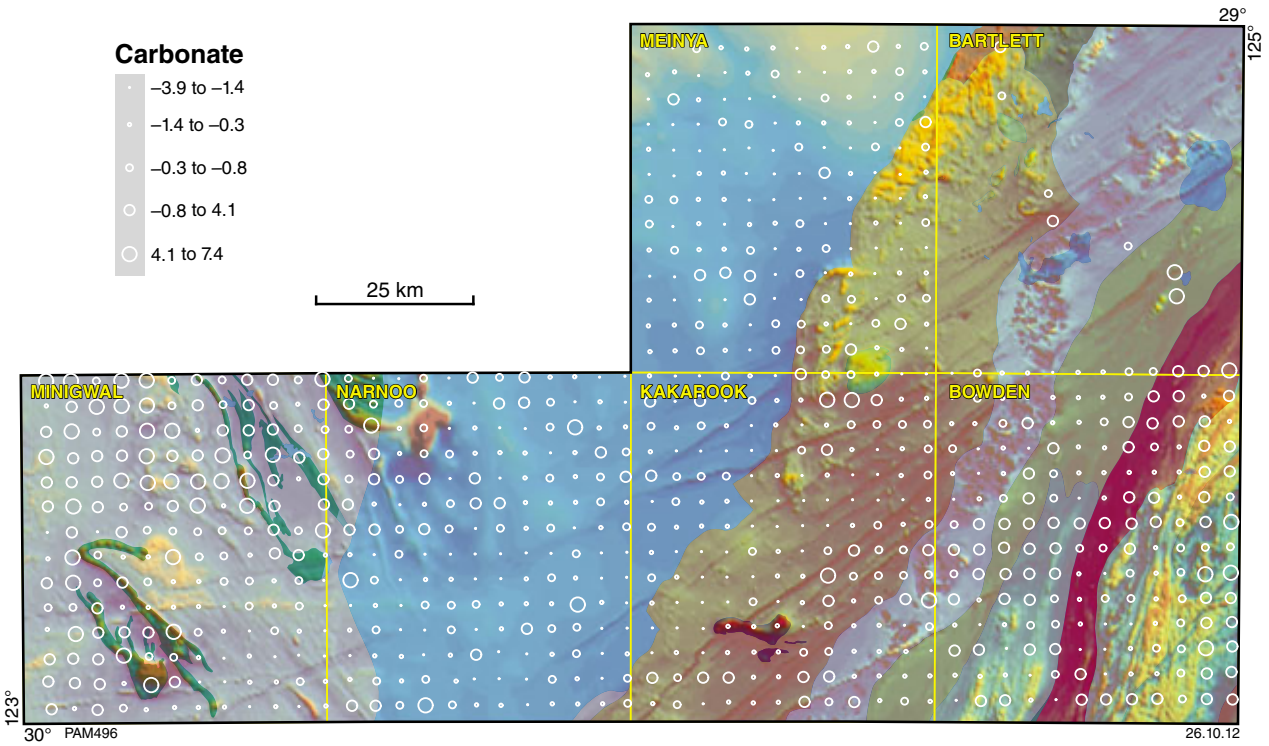

Figure 30. Bubble plot for Carbonate Index (i.e. summed standard scores for Ca and Sr) in <50 µm fraction of regolith from the east Wongatha area.

These samples are found in relatively shallow parts of the Gunbarrel Basin, close to its margin with either the Albany–Fraser Orogen or Yilgarn Craton (Fig. 27a). For example, unconformity-hosted uranium, base metal and gold mineralization have been reported from the Mulga Rock area (Energy and Minerals Australia, 2010b).

The high proportion of censored data for silver (91.5%) means that the data have not been statistically analysed, but samples that returned concentrations above detection level are predominantly found close to areas of Yilgarn Craton greenstones (Fig. 27b).

Of the 32 samples with statistically anomalous gold concentrations (Table 2), 18 have anomalous concentrations of calcium, about six samples have anomalous concentrations of some REE, and a few have anomalous concentrations of barium, beryllium, copper, manganese, nickel, lead, and zinc. Overall, there is no consistent relationship of anomalous gold with either carbonate-rich regolith or chalcophile element abundance. An exception is the association of gold and chalcophile elements over the Proterozoic mafic intrusion on KAKAROOK. Similarly, no samples with anomalous gold have anomalous iron concentrations.

Aqua regia digestion and subsequent analysis of the <50 µm fraction of regolith has demonstrated a relationship between some elements and bedrock, and mineralization. To better understand this relationship (especially the behaviour of gold), two size fractions of 50 samples with variable aqua regia gold concentrations have been further analysed. The <50 µm fraction was digested with deionized water and then analysed by ICP-MS for 12 elements (except for zinc, which was determined by atomic absorption spectrometry or AAS). The <2 to >0.475 mm (fine to medium sand) fraction was dry-screened, then gold, platinum and palladium were selected for by lead-collection fire assay and analysed by ICP-MS.

Deionized water digestion and analysis of the <50 µm fraction

The maximum gold concentration following this approach is 11.78 ppb, with a median value of 0.24 ppb. A similar proportion of samples (36% or 18 samples) to those analysed following aqua regia digestion returned censored values (Table 2). In contrast to aqua regia digestion, only 11 samples (22%) returned censored silver data following deionized water digestion, but more than 50% of samples returned censored data for copper, nickel, lead, platinum, and mercury.

Most samples with elevated gold concentrations (including the maximum value of 11.78 ppb in GSWA 200100) are found in regolith either on or along strike from the Minigwal and Wongatha greenstone belts (Fig. 35a). Other samples with high concentrations are found southeast

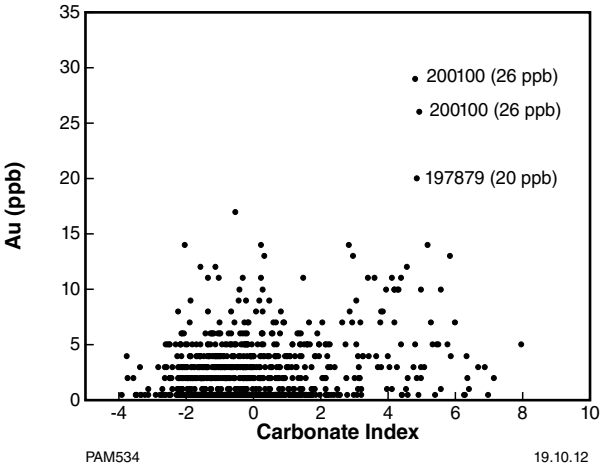

Figure 31. Bivariate plot of Au (ppb) versus Carbonate Index for the <50 µm fraction of regolith from the east Wongatha area.

of the Irwin Hills – Stella Range greenstone belt in the Gunbarrel Basin (GSWA 200444; 4.75 ppb Au), and close to the Yilgarn Craton – Gunbarrel Basin margin in the southern part of NARNOO (GSWA 200016; 4.77 ppb Au). Samples from the central part of MEINYA returned less than detection level gold, and those from the Albany–Fraser Orogen show variable gold concentrations up to 2.82 ppb in GSWA 200672 on the boundary of BARTLETT and BOWDEN.

The distribution of silver is similar to that of gold (Fig. 35b), with higher concentrations found in samples close to Yilgarn Craton greenstones, generally low concentrations in regolith samples from sandplain-dominated areas on MEINYA, and variable concentrations in regolith over the Albany–Fraser Orogen, with concentrations of 0.76 ppb (GSWA 200671) and 0.83 ppb (GSWA 200672), respectively, found in samples on the BARTLETT–BOWDEN boundary. There is a weak positive correlation of gold and silver (Fig. 36; $R^2 = 0.4254$).

There are no censored data for uranium, which shows a similar distribution to gold and silver, with higher concentrations over parts of the Yilgarn Craton, and variable concentrations over the Albany–Fraser Orogen. Most concentrations are low in regolith over the Gunbarrel Basin (Fig. 37). The correlation between gold and uranium ($R^2 = 0.4769$) is similar to that for gold and silver (Fig. 38).

Similar to data generated following aqua regia digestion, most samples returned censored data for both palladium and platinum. Only two samples have platinum levels above the LLD of 0.05 ppb (GSWA 200395 (0.13 ppb) and GSWA 200488 (0.1 ppb)), both of which are found close to Yilgarn Craton greenstones of the Stella Range – Irwin Hills greenstone belt (Fig. 39a). Samples with elevated concentrations of nickel (LLD = 0.05 ppm) are also found on, or near areas of Yilgarn Craton greenstones, although concentrations are notably higher over the Stella Range – Irwin Hills greenstone belt compared to the Minigwal and Wongatha greenstone belts (Fig. 39b).

Arsenic concentrations range from <0.5 (four samples) to 22.1 ppb. Samples with the highest arsenic contents are found either on or along strike from Yilgarn Craton greenstones (Fig. 39c). Elevated values are also found close to the Yilgarn Craton – Gunbarrel Basin boundary on NARNOO. Sample GSWA 200747 (Gunbarrel Basin on MEINYA) has 17.5 ppb arsenic, and elevated concentrations of silver (0.33 ppb) and gold (1.83 ppb).

The maximum thorium concentration is 2.03 ppb, with all samples returning concentrations above the LLD of 0.02 ppb. There is a broad association of higher thorium values with Yilgarn Craton greenstones (Fig. 39d), but samples with higher thorium contents are also found in the northern part of MEINYA, and over different Albany–Fraser Orogen lithologies on KAKAROOK and BOWDEN. As there are also some elevated concentrations in parts of the Gunbarrel Basin, thorium is not clearly related to any lithology.

Similar to thorium, cerium shows a range in concentration (up to 207.16 ppb in GSWA 200101 over greenstones in the southwest part of MINIGWAL), but there is no clear relationship between cerium and lithology, although concentrations appear to be slightly lower over the Gunbarrel Basin (Fig. 39e). Only one sample returned higher than detection-level concentration for mercury (GSWA 200395) with 0.8 ppb.

In terms of base metals, copper concentrations are low (maximum 0.08 ppm), but only nine samples returned censored data. Most samples with higher concentrations are found either over, or along strike from, Yilgarn Craton greenstones (Fig. 39f). Half of the samples analysed for lead returned censored data, and of the remainder, 12 samples have concentrations equal to the LLD (0.3 ppb). Sample GSWA 200101 has the highest lead concentration of 23 ppb (Fig. 39g), and this sample also has elevated cerium.

Zinc reaches 202 ppb in GSWA 200101 (which also has elevated lead and cerium) and, similarly to nickel and copper, most samples with elevated zinc are found on or close to Yilgarn Craton greenstones, in particular the Stella Range – Irwin Hills greenstone belt (Fig. 39h).

Fire assay determination of Au, Pd and Pt in the <2 to >0.45 mm fraction

All samples returned >1 ppb gold for fire assay/ICP-MS analysis of the <2 to >0.475 mm fraction, although 18 samples (i.e. 36%) returned values of 1 ppb, equal to the LLD. Ninety percent of samples returned censored data for platinum, and 94% of values were censored for palladium.

The maximum gold concentration of 9 ppb is found in GSWA 200150 from the southern part of the Minigwal greenstone belt. A nearby sample (GSWA 200100) has 8 ppb gold. Of the three other samples with elevated

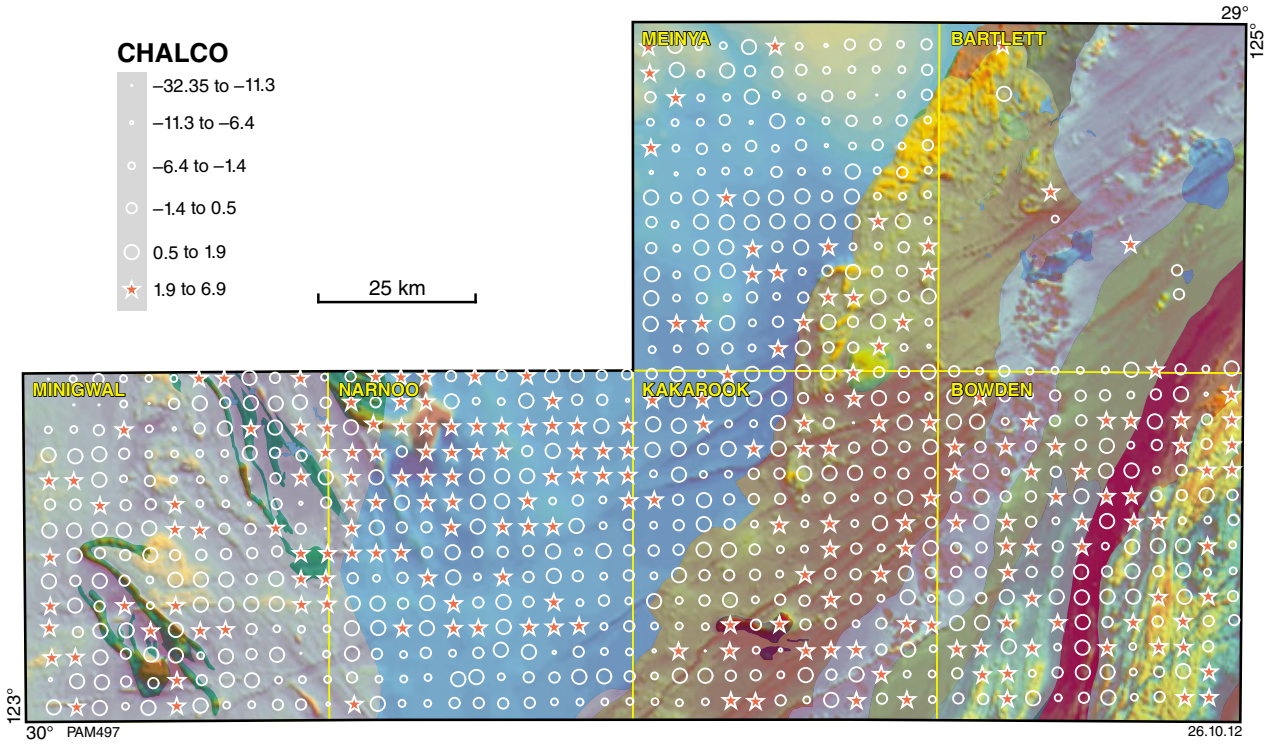

Figure 32. Bubble plot for Chalcophile Index (CHALCO) (i.e. summed standard scores for As, Bi, Mo, Sb) in the <50 µm fraction of regolith from the east Wongatha area.

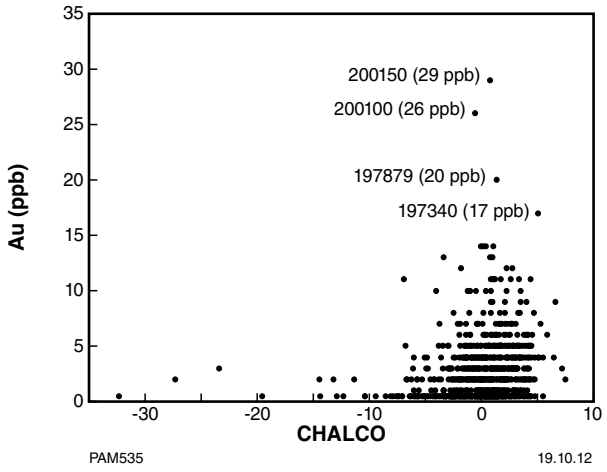

Figure 33. Bivariate plot of Au (ppb) versus Chalcophile Index for the <50 µm fraction of regolith from the east Wongatha area.

gold concentrations, two (GSWA 200214, 8 ppb; GSWA 200016, 6 ppb) are found in the Gunbarrel Basin, and one (GSWA 197340, 5 ppb) is close to the Stella Range – Irwin Hills greenstone belt. Most samples from this western part of the project area record elevated levels of Au (Fig. 40).

A comparison of gold concentrations according to method shows a remarkably good agreement (Fig. 41). Some samples, especially those from on or close to greenstones of the Yilgarn Craton, have high concentrations of gold by all three methods, whereas a few samples from the Gunbarrel Basin southeast of the Stella Range – Irwin Hills greenstone belt show a good response in terms of deionized water digestion compared to both aqua regia digestion of the fine fraction and fire assay analysis of the coarser fraction. Of the three analytical methods, fire assay is the most aggressive, in that all gold in the sample is made available for analysis through fusion and cupellation (Hall and Pelchat, 1994). Aqua regia is less aggressive, as it is largely ineffective in terms of dissolving silicates, whereas deionized water digestion only releases into solution either weakly bound (i.e. water-soluble) gold, or free gold particles.

Summary of results

The positive correlation in gold concentration for samples regardless of method (Fig. 41) suggests that gold may be present in both the coarse and fine grain-size fractions. However, as the <2 to >0.475 mm fraction has been dry screened, it is unclear if the water-soluble gold is coarse grained, or if it is present as finer grained material (silt- to clay-grade) adhered to sand size grains. Regardless of the form of gold, its liberation by a weak digest such as deionized water implies that it is present in a labile or microparticulate form.

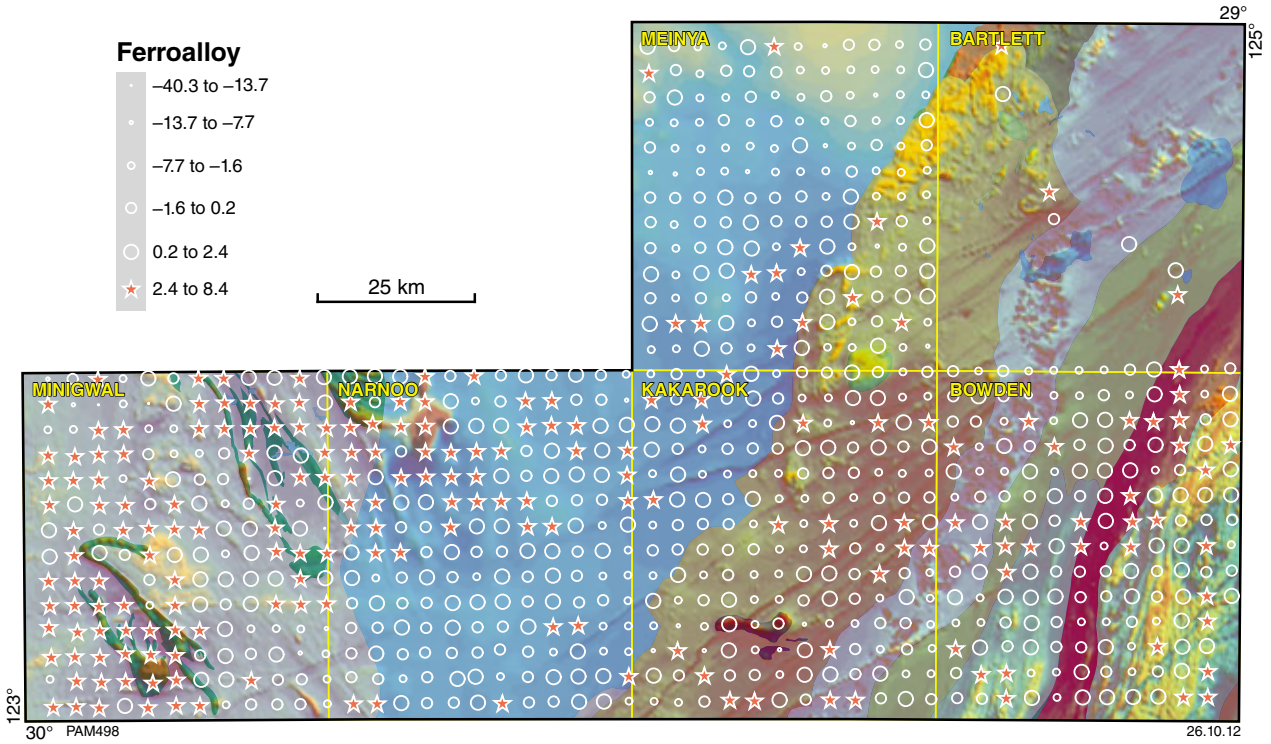

Figure 34. Bubble plot for Ferroalloy Index (i.e. summed standard scores for Ni, Cr, Mo, Co, V) in <50 µm fraction of regolith from the east Wongatha area.

The distribution of some elements in the fine fraction of regolith can be spatially associated with underlying bedrock, for both aqua regia digestion (e.g. nickel, calcium, manganese, yttrium) and deionized water digestion of the <50 µm fraction (e.g. nickel, copper, zinc, silver). Similarly, gold in the fine fraction for both digests shows a strong spatial relationship with either the known or inferred distribution of greenstones.

Chalcophile elements released during deionized water digestion are more common in regolith from areas of greenstone than those resulting from aqua regia digestion. This may indicate the release from sulphates rather than sulfides.

Gold mobility

Available drilling data has shown that regolith in the east Wongatha area is up to at least 120 m thick, and sedimentary rock cover is at least 400 m thick. If some anomalous gold found in the fine fraction of regolith is sourced from greenstones, then vertical migration through several hundreds of metres of rock and regolith has taken place. The release of these elements by deionized water digestion suggests that some or all of the elements analysed for (including gold) must be available in either a native form, or as labile components.

The detection of deeply buried mineralization in the fine fraction of regolith has been discussed elsewhere. Tang et al. (2009) noted that the concentrations of copper and cadmium increased with decreasing grain size in three Chinese soils, and Wang et al. (2007) discussed the distribution of gold in regolith over bedrock-hosted gold deposits in a desert area of northwestern China. In that study, gold was found to not only be enriched lower in the regolith profile close to mineralization, but also in the fine fraction (<125 µm) of samples near the surface directly over mineralization. They concluded that gold must move vertically through the weathering profile and be captured by clays or preserved in oxide coatings on grains. The gold distribution in the regolith profile showed that water-extractactable gold was highest close to bedrock then decreased sharply, whereas total gold associated with oxides was highest both close to the bedrock and to the surface. Silver showed a similar distribution, but was also in higher concentrations close to the surface for water extraction in one profile. Wang et al. (2007) pointed out that as the water table was well below the sampling area, it was unlikely that either water or vegetation contributed to element movement. Instead, they argued that some gold occurred as particles <5 µm diameter, which could be transported vertically by soil gas bubbles. Citing the work of Wu (1998), they also suggested that ultrafine gold particles (<100 nm) could behave as gases rather than solids.

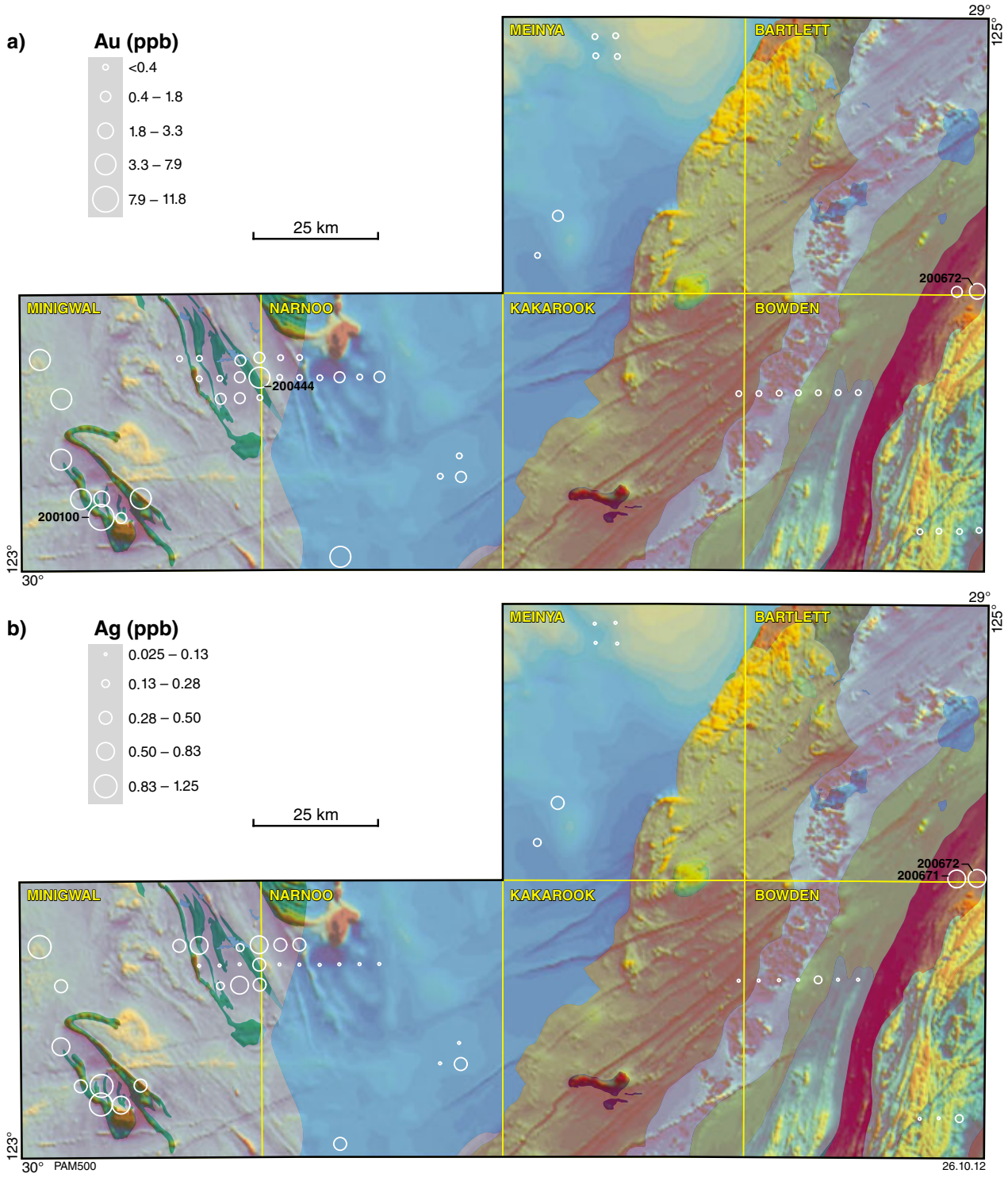

Figure 35. Bubble plots for: a) Au (ppb) and b) Ag (ppb) in the <50 µm fraction of regolith from the east Wongatha area, determined by deionized water digestion and ICP-MS analysis.

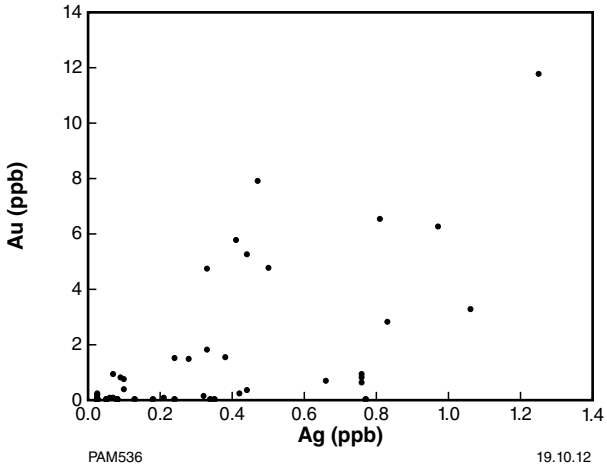

Figure 36. Bivariate plot of Au (ppb) versus Ag (ppb) in the <50 µm fraction of regolith from the east Wongatha area, determined by deionized water digestion and ICP-MS analysis.

Wang (1998) examined the distribution of water-extractable gold in soils from Sichuan Province (China), collected at a density of one sample per 300 km^2. That survey identified a known gold deposit, as well as other areas of potential mineralization. He argued that gold occurred not only as ionic or complexed forms, but also as nanoparticles that were chemically or physically bound to oxides, clay minerals, or carbonates. These particles were transported by soil gas.

Other studies have emphasized the importance of secondary minerals in evaluating gold mobility in areas of thick cover. In a study of two mineral deposits in Nevada covered by 20–100 m of cover, Smee (1998) pointed out a strong concentration correlation of gold, antimony, strontium, boron, and calcium, and suggested that gold was strongly related to secondary carbonate. Similarly, Lintern and Butt (1993) detected gold in pedogenic carbonate through 40 m of overburden. They argued that carbonate resulted from the interaction of Ca^{2+} and HCO_{3-}, where the latter resulted from the reaction of H_2O and CO_2. Carbon dioxide resulted from either an organic source, the atmosphere, or oxidation of the mineral deposit. The correlation of gold with carbonate could mean that gold was transported as an anion, perhaps in a HCO_{3-} complex. Gray and Lintern (1994) suggested that gold in carbonate soils could result from evapotranspiration controlled by surface plants. As noted by Smee (1998) for the Marigold site in Nevada, carbonate sequestering of gold depends on alkaline and oxidising conditions (i.e. an acidic environment), where calcium replaces iron.

The occurrence and origin of nanoparticulate gold has recently been discussed by Hough et al. (2008) and Lintern et al. (2009). Hough et al. (2008) described supergene gold particles ranging in size up to 200 µm (most 40–100 µm) from a gold deposit in Western Australia. They used SEM-EDS to show that these particles were flake-like with thicknesses in the order of 20–50 nm. The spatial association of these particles with halloysite indicated coprecipitation as the result of a drying process. ICP-MS analysis of clay on fracture

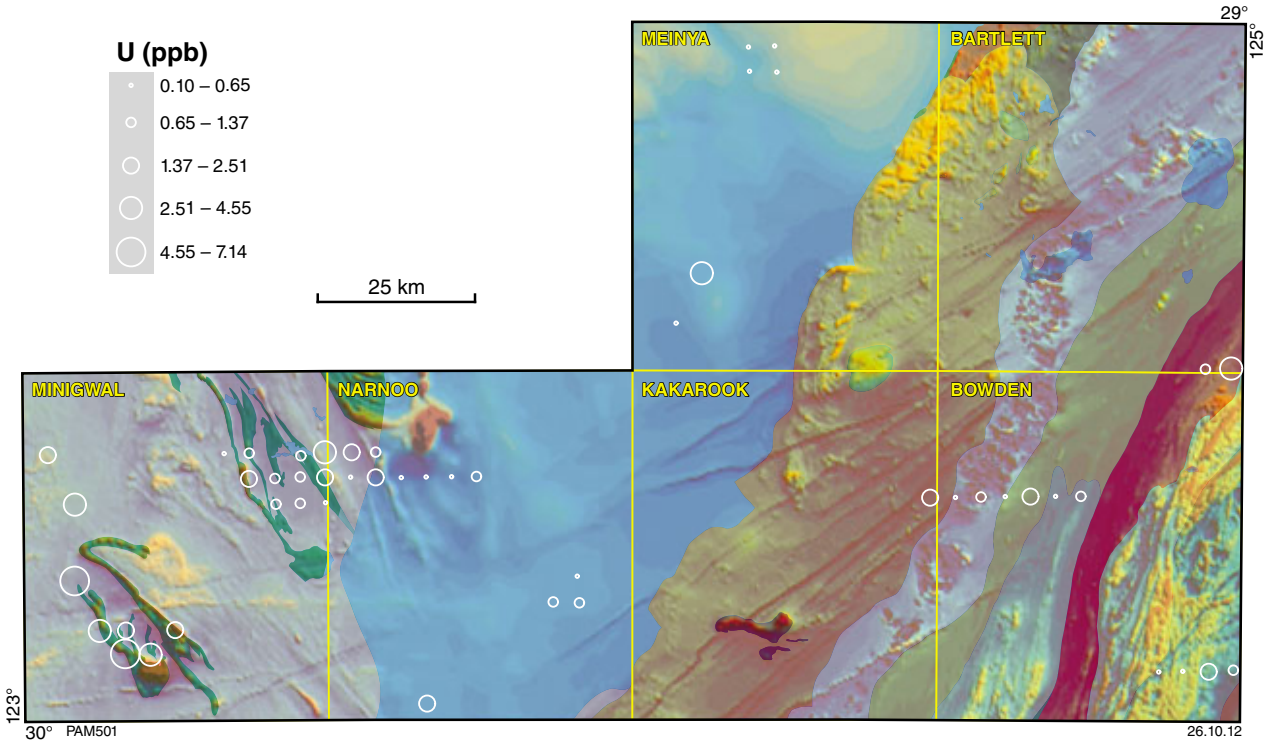

Figure 37. Bubble plot of U (ppb) in the <50 µm fraction of regolith from the east Wongatha area, determined by deionized water digestion and ICP-MS analysis.

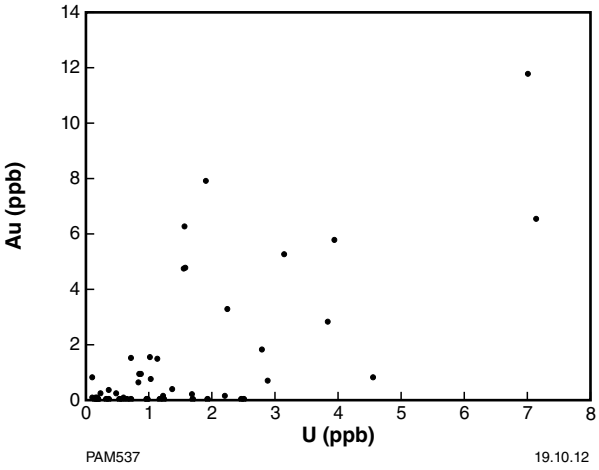

Figure 38. Bivariate plot of Au (ppb) versus U (ppb) for the <50 µm fraction of regolith from the east Wongatha area, following digestion with deionized water and analysis by ICP-MS.

surfaces resulted in gold concentrations of up to 59 ppm, even though gold could not be observed. Hough et al. (2008) drew parallels between industrial production of gold nanoplates by reduction using biological media and the natural occurrence of gold nanoparticles. In nature, the particles result from reduction probably related to dehydration, shown by the association with halloysite.

In their discussion of the relationship between gold and calcrete, Lintern et al. (2009) used synchrotron XRF and micro-X-ray absorption near-edge structure to show that gold is found both as particles and as an ionic species. They noted an association of gold with bromine in a root tubule; this has parallels with Hough et al.'s (2008) observation that the precipitation of gold is associated with dehydration (or evaporation) in a reducing environment. However, Lintern et al. (2009) also pointed out that, although there is a good downhole relationship between gold and calcium (i.e. carbonate content), this relationship is not maintained at the microscopic scale, indicating that gold does not precipitate at the same time as carbonate minerals at this scale. Both Hough et al.'s (2008) and Lintern et al.'s (2009) work suggest the presence of soluble fine-scale gold (as individual nano-scale particles and as ionic species) in soils.

The method of movement of nanoparticles vertically through cover has been discussed on theoretical and experimental grounds by Klussman (2009), who suggested that colloidal-size gold particles (i.e. ≤1 µm) could be moved upward in a soil profile by barometric pumping and soil gas movement. A key point is that the flake-like morphology of the gold inhibits settling. Rates of element migration have been reported on by Goldberg (1998) for Cu–Ni deposits of the Kola Peninsula, where 100-m thick glacial moraine has been dated at 10 000 years, meaning that surface anomalies indicate a vertical migration rate of about 1 cm/year. Goldberg (1998) suggested that observed and estimated rates are higher than those that could be explained by simple diffusion, indicating that another process must be operating.

Effectiveness of the fine fraction of regolith as a sample medium

The results of geochemical programs that use soil- or rock-based media in areas of extensive cover have been questioned by deposit-scale studies, which have argued that the geochemical expression of bedrock mineralization may not be detected through transported regolith thicker than 5–10 m (e.g. Gray et al, 1999; Anand and Butt, 2010). Studies of this type, combined with the necessity to explore for mineralization through thick and commonly transported cover (including 'greenfields' areas), have promoted the use of alternative sample media, such as vegetation (Rogers and Dunn, 1993; Reid et al., 2010), termite mounds (Petts et al., 2009), or groundwater (Gray et al., 2009; Leybourne and Cameron, 2010).

However, greenfields areas, particularly those in Western Australia, are typically arid and characterized by a lack of groundwater, and have only sparse or inhomogeneously distributed vegetation. Thus, there are usually no alternative media for regional geochemistry programs, other than regolith. However, reverting to regolith as a sample medium is often complicated in these areas by the presence of a significant, quartz-rich, eolian sand component, which is not only unrelated to bedrock, but also can act as a dilutant to any bedrock mineralization signature. The influence of this quartz sand component on regolith chemistry needs to be carefully considered for regional geochemistry programs (e.g. Dickson and Scott, 1998; Robertson, 1999; Tate et al., 2007).

Several studies carried out in Chile, the USA, Canada (Cameron et al., 2004, 2010; Hamilton et al., 2004a; Hamilton et al., 2004b), and China (Wang, 1998; Wang et al., 2007) have shown that bedrock-hosted mineralization can be detected through several tens of metres of exotic overburden using surface soil as a sample medium, when coupled with partial or selective digests and analytical techniques capable of detecting low concentrations of either ore or pathfinder elements (Hall, 1998; Mann, 2010). Cameron et al.'s (2004) study, in particular, showed that the exogenic:endogenic ratio varied according to the leach used, the site, and the age of the cover sequence. For sites where metals have taken millions of years to accumulate as an exogenic component in soils, more aggressive leaches such as aqua regia were effective, whereas in areas where cover is only a few thousand years old, the exogenic component is more labile and a less aggressive leach was more effective. Thus, geochemical exploration in greenfields areas using regolith can benefit from some knowledge about the age of different regolith deposits, especially those that are samples for analysis.

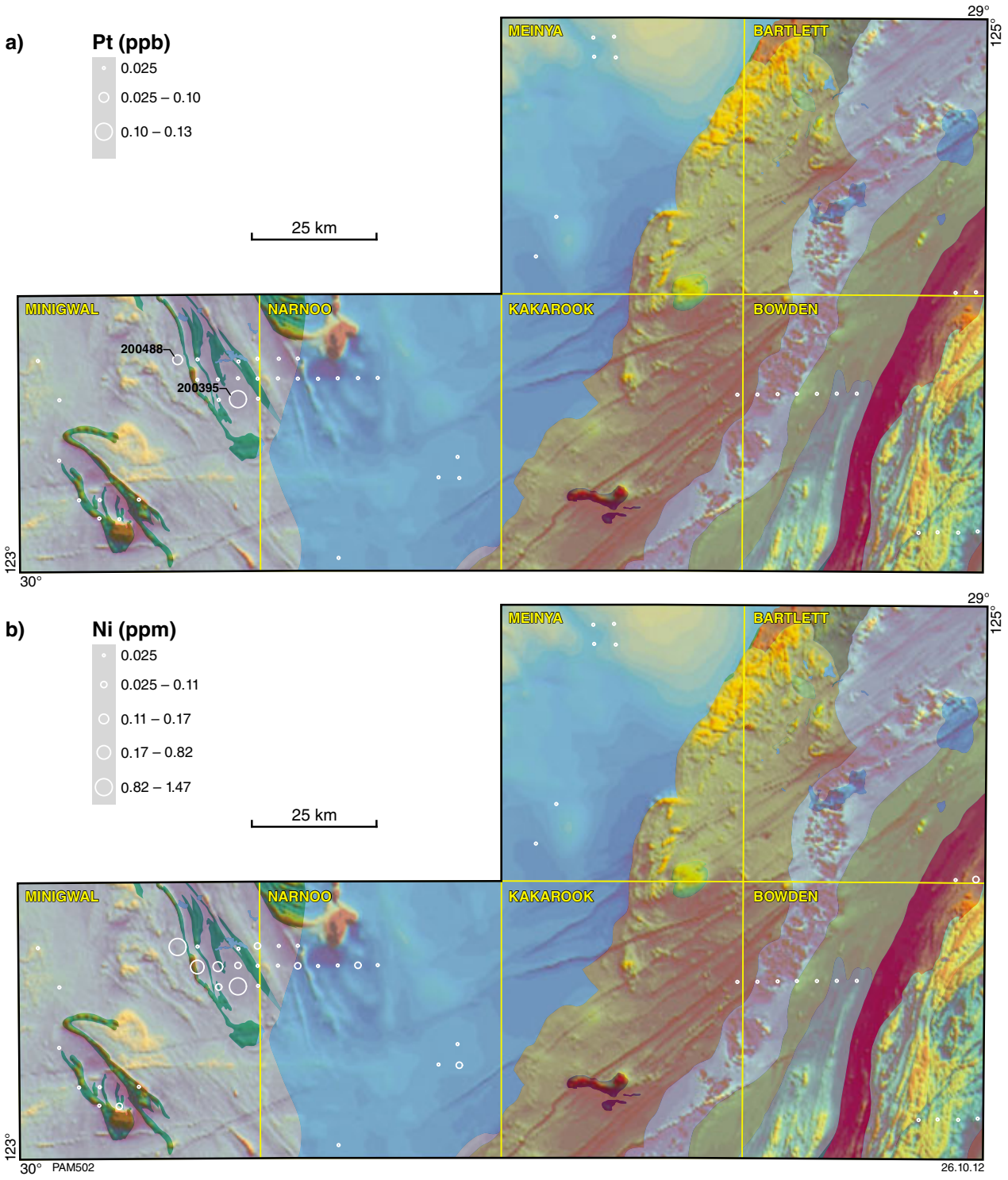

Figure 39. Bubble plots for elements analysed from the <50 µm fraction of regolith from the east Wongatha area following deionized water digestion; a) Pt (ppb); b) Ni (ppm; censored data set at half LLD); c) As (ppb; censored data set at half LLD); d) Th (ppb); e) Ce (ppb); f) Cu (ppm; censored data set at half LLD); g) Pb (ppb; censored data set at half LLD); h) Zn (ppb; censored data set at half LLD).

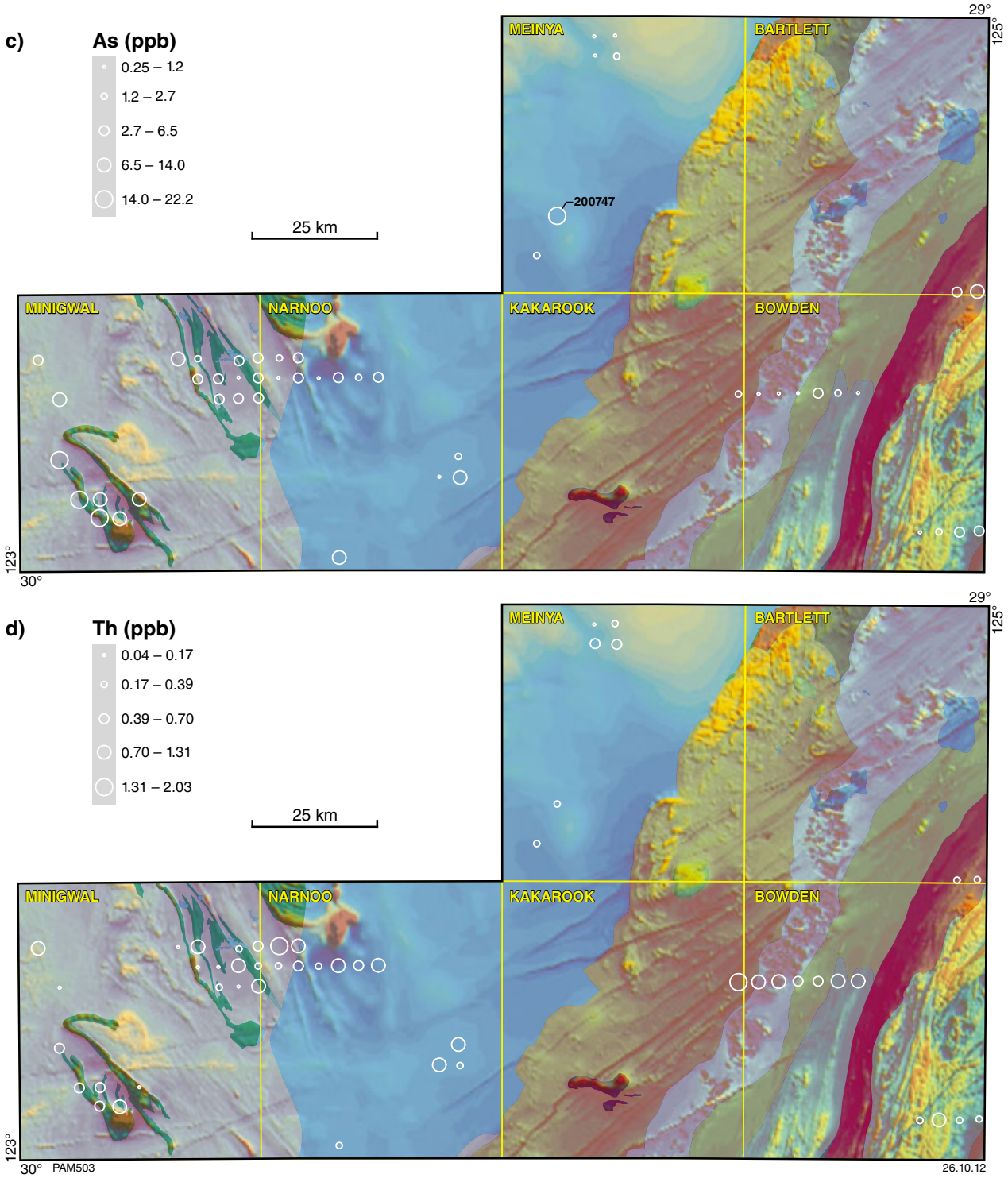

Figure 39. continued

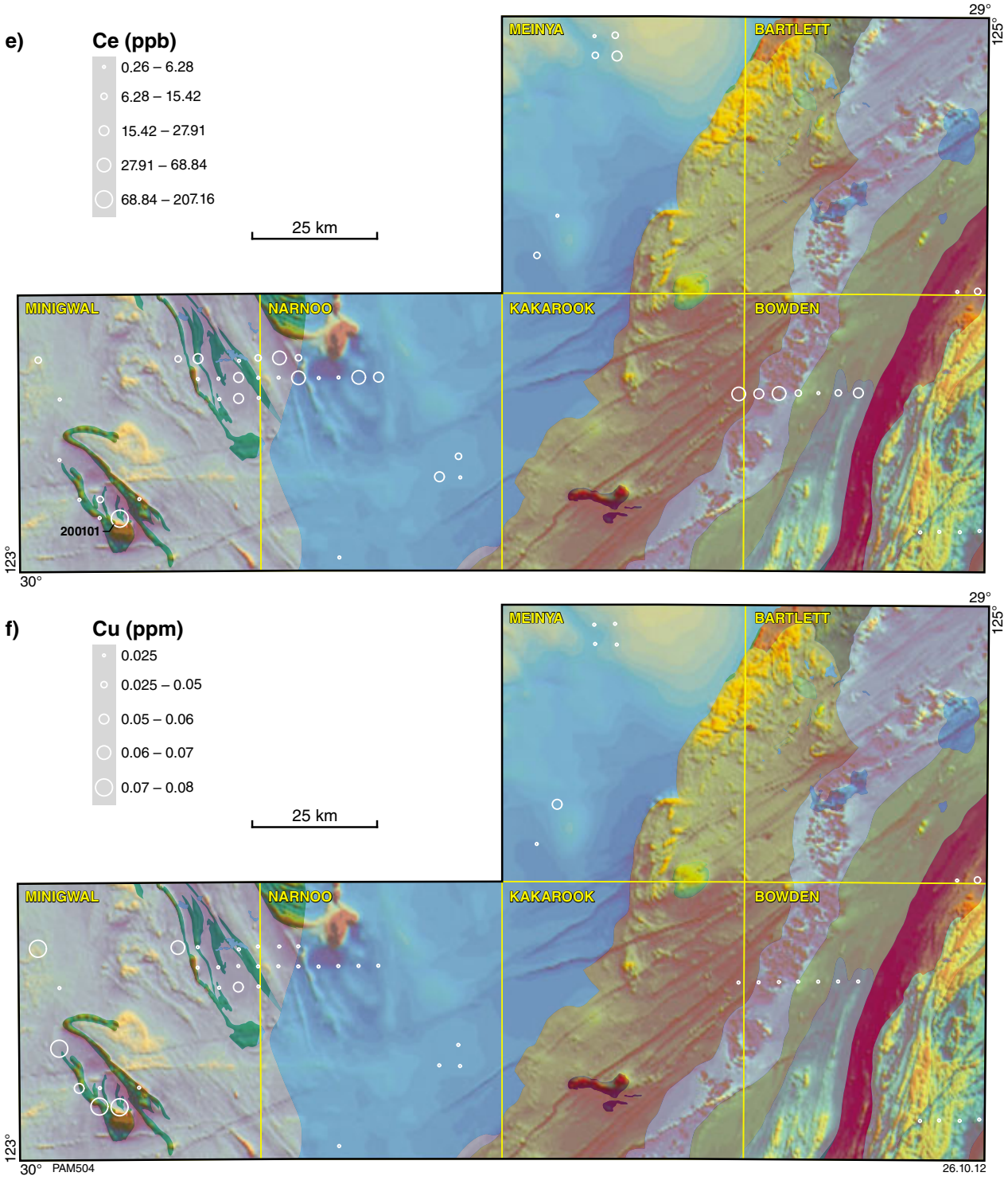

Figure 39. continued

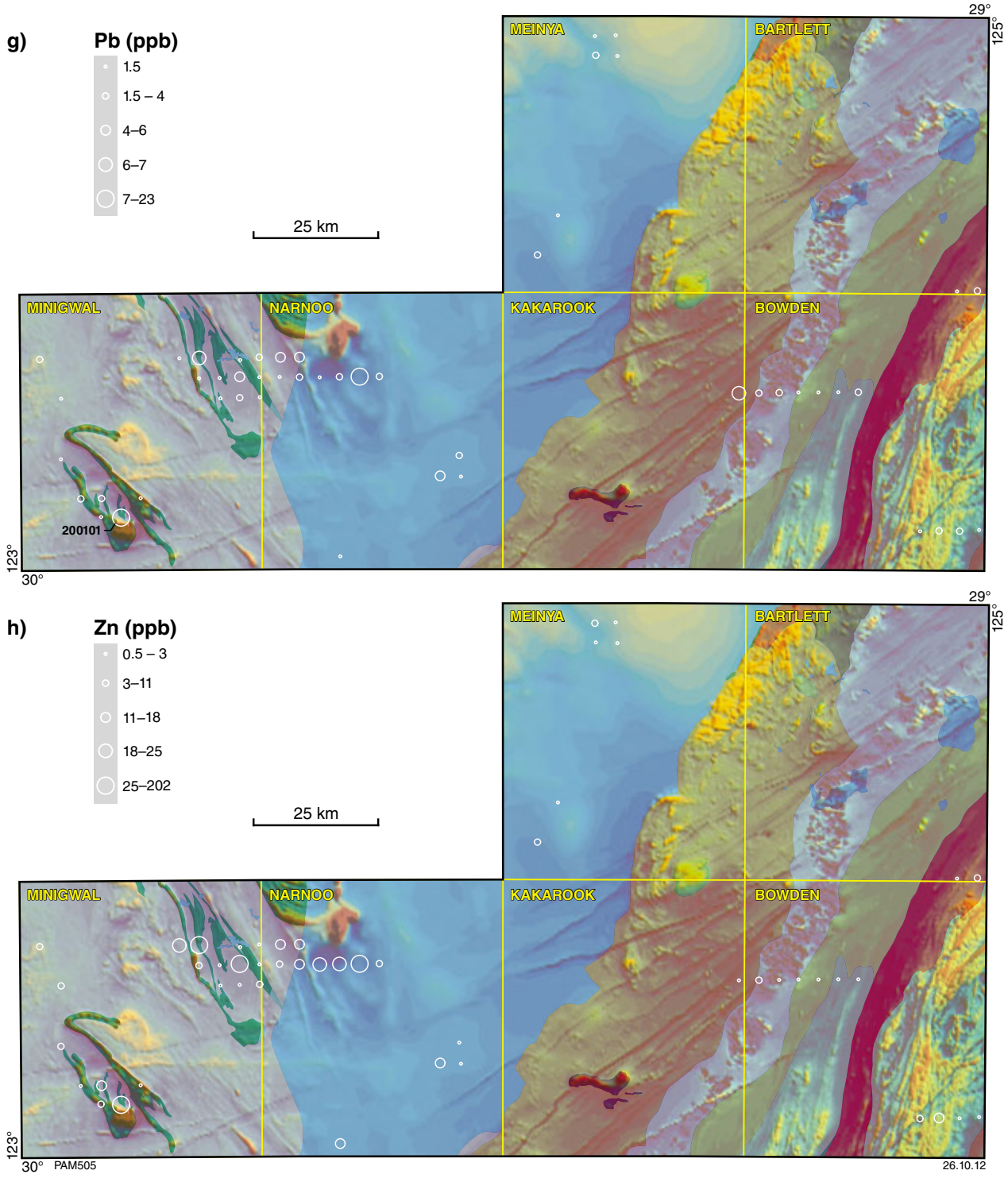

Figure 39. continued

The success of these published studies indicates that elements of economic interest, or related pathfinder elements, have migrated vertically through the thick and exotic cover to the surface. Various mechanisms to account for such vertical element migration have been discussed, including seismic pumping (upward movement of groundwater due to earthquake activity), gas migration through barometric pumping (pressure change), and generation of electrochemical cells above ore bodies by changes in groundwater chemistry through redox and pH changes. In their study of Chilean copper deposits, Cameron et al. (2004) argued that seismic pumping was important for element migration in this earthquake-prone area. At the Spence deposit (Nevada), where cover is 60 m thick, anomalous copper in soil was correlated with the distribution of faults, which presumably acted as conduits. However, in Ontario, mineralization is found in an area where earthquake activity and deformation is not reported, and element migration from the buried ore body was attributed to the vertical migration of elements in a reducing 'chimney' above the ore deposit. Here, reduced material reacts with oxygen at the water table resulting in an acid environment that causes dissolution and redistribution of carbonate originally present in clays (Hamilton et al., 2004a,b). In the east Wongatha area, the margin of the Gunbarrel Basin is known as an area of block-faulted Cenozoic sedimentary rocks, and it is possible that these faults acted as conduits for elements associated with mineralization to migrate vertically and become stabilized in the overlying regolith.

Conclusions

Results of this study in the east Wongatha area show that, despite the well developed (i.e. spatially extensive and thick) cover of exotic regolith over large parts of the project area, the fine fraction of regolith has statistically anomalous concentrations of gold and other elements. The spatial distribution of some of these elements compared with particular bedrock types (e.g. nickel and cobalt cf. greenstones), and evidence for surface expression of known bedrock mineralization styles (e.g. gold and greenstones; gold and unconformity-hosted mineralization), provides some evidence for migration of elements through this thick regolith cover, and even through barren sedimentary rocks. Anomalous gold is locally, but not inevitably, associated with carbonate-rich regolith, but there is no clear association of gold with other elements indicative of secondary processes (e.g. iron). This, combined with the correlation of gold determined following deionized water, as well as aqua regia digestion, suggests that gold and probably other elements are found in regolith as either labile and/or microparticulate native grains. These data show that partial digestion of fine-fraction regolith has potential for detecting bedrock and bedrock-hosted mineralization in areas of thick transported cover.

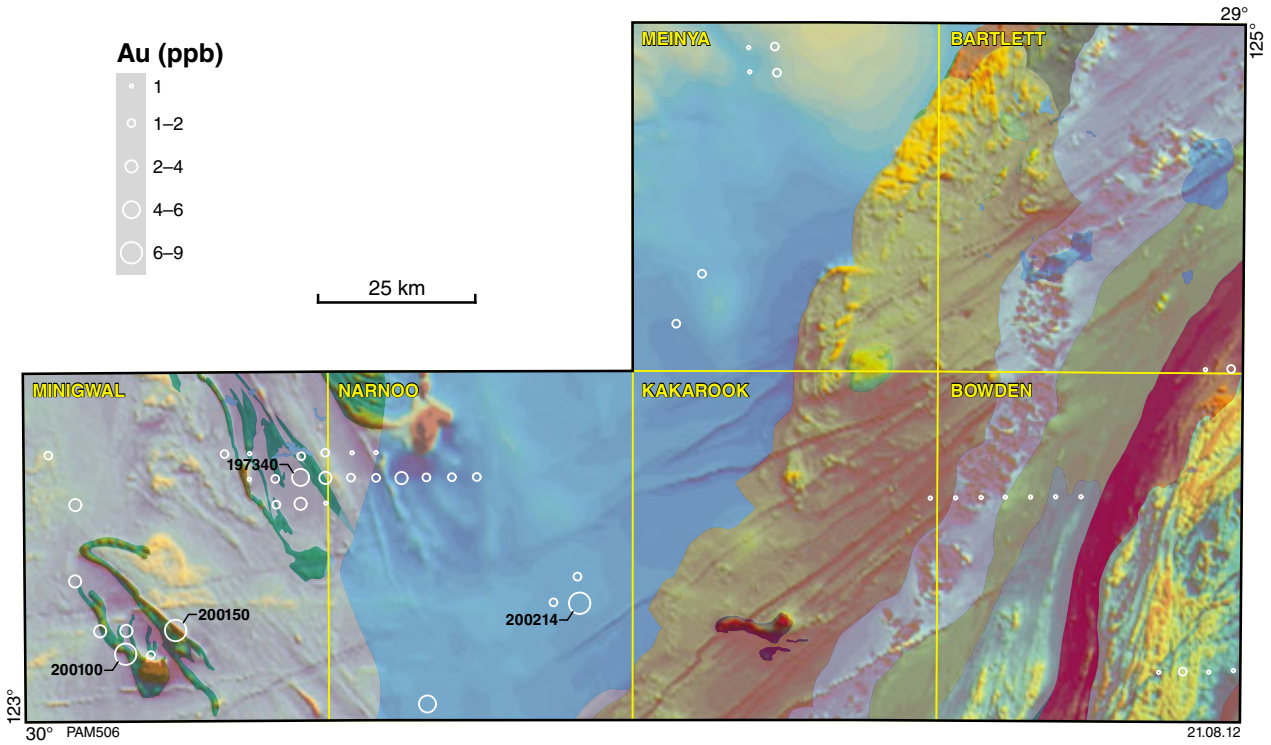

Figure 40. Bubble plot for Au (ppb) analysed from the dry screened <2 to >0.475 fraction of regolith from the east Wongatha area following Pb collection fire assay.

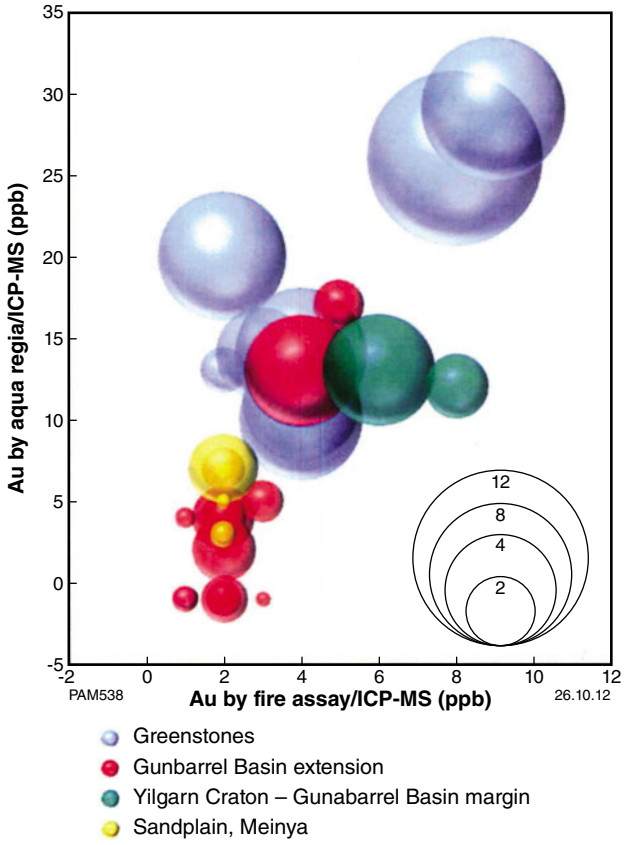

Figure 41. Bivariate plot of Au (ppb) by aqua regia digestion of the <50 µm fraction (y-axis) versus Au (ppb) in the <2 to >0.475 mm fraction by Pb-collection fire assay (x-axis), with symbols scaled according to Au (ppb) in the <50 µm fraction by deionized water digestion.

References

Anand, RR and Butt, CRM 2010, A guide for mineral exploration through the regolith in the Yilgarn Craton, Western Australia: Australian Journal of Earth Sciences, v. 57, p. 1015–1114.

Barley, ME, Krapež, B, Groves, DI and Kerrich, R 1998, The Late Archean bonanza: metallogenic and environmental consequences of the interactions between mantle plumes, lithospheric tectonics and the global cyclicity: Precambrian Research, v. 91, p. 65–90.

Beard, JS 1974, Great Victoria Desert — Explantory Notes to Sheet 3: The University of Western Australia Press, Vegetation Survey of Western Australia, 50p.

Beard, JS 1975, The vegetation of the Nullarbor area — Explanatory Notes to Sheet 4: The University of Western Australia Press, Vegetation Survey of Western Australia, 104p.

Blewett, RS, Henson, PA, Roy, IG, Champion, DC and Cassidy, KC 2010, Scale-integrated architecture of a world-class gold mineral system: the Archean eastern Yilgarn Craton, Western Australia: Precambrian Research, v. 183, no. 2, p. 230–250.

Bunting, JA and Boegli, JC (compilers) 1977, Minigwal, Western Australia: Geological Survey of Western Australia, 1:250 000 Geological Series Explanatory Notes, 19p.

Butt, CRM and Gole, MJ 1985, Helium in soil and overburden as a pathfinder — an assessment: Journal of Geochemical Exploration, v. 24, no. 2, p. 141–173.

Cameron, EM, Hamilton, SM, Leybourne, MI, Hall, GEM and McClenaghan, MB 2004, Finding deeply buried deposits using geochemistry: Geochemistry: Exploration, Environment, Analysis, v. 4, p. 7–32.

Cameron, EM, Leybourne, MI, Reich, M and Palacios, C 2010, Geochemical anomalies in northern Chile as a surface expression of the extended supergene metallogenesis of buried copper deposits: Geochemistry: Exploration, Environment, Analysis, v. 10, p. 157–169.

Cassidy, KF, Champion, DC, Krapež, B, Barley, ME, Brown, SJA, Blewett, RS, Groenewald, PB and Tyler, IM 2006, A revised geological framework for the Yilgarn Craton, Western Australia: Geological Survey of Western Australia, Record 2006/8, 8p.

Chao, TT 1984, Use of partial dissolution techniques in geochemical exploration: Journal of Geochemical Exploration, v. 20, p. 101–135.

Chao, TT and Sanzolone, RF 1992, Decomposition techniques: Journal of Geochemical Exploration, v. 44, p. 65–106.

Dickson, BL and Scott, KM 1998, Recognition of aeolian soils of the Blayney district, NSW: implications for mineral exploration: Journal of Geochemical Exploration, v. 63, p. 237–251.

Douglas, GB, Butt, CRM and Gray, DJ 2003, Mulga Rock uranium and multielement deposits, Officer Basin, W.A.: CRC LEME Monograph, p. 1–3.

Douglas, GB, Butt, CRM and Gray, DJ 2011, Geology, geochemistry and mineralogy of the lignite-hosted Ambassador palaeochannel uranium and multi-element deposit: Mineralium Deposita, v. 46, p. 761–787.

Doyle, MG, Gibbs, D, Savage, J and Blenkinsop, TG 2009, Geology of the Tropicana Gold Project, Western Australia, *in* Smart Science for Exploration and Mining: Economic Geology Research Unit, James Cook University; 10th Biennial SGA Meeting of The Society for Geology Applied to Mineral Deposits, Townsville, Queensland, 17 August 2009; Proceedings v. 1, p. 50–52.

Energy and Minerals Australia 2010a, Sandstone uranium delineated at Mulga Rock: Report to Australian Securities Exchange, 16 March 2010, 21p.

Energy and Minerals Australia 2010b, Additional sandstone hosted uranium mineralisation identified: Report to Australian Securities Exchange, 19 July 2010, 8p.

Energy and Minerals Australia 2010c, Mulga Rocks Ambassador deposit lignite uranium results and confirmation of polymineralic mineralisation: Report to Australian Securities Exchange, 10 May 2010, 58p.

Fletcher, WK 1981, Sample decomposition-solution techniques, *in* Handbook of Exploration Geochemistry *edited by* GJS Govett: Elsevier Scientific Publishing, Amsterdam, The Netherlands, p. 57–95.

Geological Survey of Western Australia 2009, Exploration Geochemistry of Western Australia, June 2009: Geological Survey of Western Australia, digital data product.

Goldberg, IS 1998, Vertical migration of elements from mineral deposits: Journal of Geochemical Exploration, v. 61, p. 191–202.

Gray, DJ 2001, Hydrogeochemistry in the Yilgarn Craton: Geochemistry: Exploration, Environment, Analysis, v. 1, p. 253–264.

Gray, DJ and Lintern, MJ 1994, The solubility of gold in soils from semi-arid areas of Western Australia: CSIRO Division of Exploration and Mining, Exploration and Mining Research News no. 1, p. 8–9.

Gray, DJ, Noble, RRP and Reid, N 2009, Hydrogeochemical mapping of northeast Yilgarn groundwater: Geological Survey of Western Australia, Record 2009/21, 78p.

Gray, DJ, Wildman, JE and Longman, GD 1999, Selective and partial extraction analyses of transported overburden for gold exploration in the Yilgarn Craton, Western Australia: Journal of Geochemical Exploration, v. 67, p. 51–66.

Grunsky, EC 2010, The interpretation of geochemical survey data: Geochemistry: Exploration, Environment, Analysis, v. 10, p. 27–74.

Hall, GEM 1998, Analytical perspective on trace element species of interest in exploration: Journal of Geochemical Exploration, v. 10, p. 27–74.

Hamilton, SM 1998, Electrochemical mass transport in overburden: a new model to account for formation of selective leach geochemical anomalies in glacial terrain: Journal of Geochemical Exploration, v. 63, p. 155–172.

Hamilton, SM, Cameron, EM, McClenaghan, MB and Hall, GEM 2004a, Redox, pH and SP variation over mineralization in thick glacial overburden. Part I: methodologies and field investigation at the Marsh Zone gold property: Geochemistry: Exploration, Environment, Analysis, v. 4, p. 33–44.

Hamilton, SM, Cameron, EM, McClenaghan, MB and Hall, GEM 2004b, Redox, pH and SP variation over mineralization in thick glacial overburden. Part II: field investigation at Cross Lake VMS property: Geochemistry: Exploration, Environment, Analysis, v. 4, p. 45–58.

Hawkes, HE and Webb, JS 1962, Geochemistry in Mineral Exploration: Harper and Row, New York, USA, 415p.

Hocking, RM 1994, Subdivisions of Western Australian Neoproterozoic and Phanerozoic sedimentary basins: Geological Survey of Western Australia, Record 1994/4, 85p.

Hough, RM, Noble, RRP, Hitchen, GJ, Hart, R, Reddy, SM, Saunders, M, Clode, P, Vaughan, D, Lowe, J, Gray, DJ, Anand, RR, Butt, CRM and Verrall, M 2008, Naturally occurring gold nanoparticles and nanoplates: Geology, v. 36, p. 571–574.

Iasky, RP 1990, Officer Basin, in Geology and mineral resources of Western Australia: Geological Survey of Western Australia, Memoir 3, p. 362–380.

Kane, JS 1990, Reference samples for use in analytical geochemistry: their availablity, preparation, and appropriate use: Journal of Geochemical Exploration, v. 44, p. 37–63.

Kirkland, CL, Spaggiari, CV, Wingate, MTD, Smithies, RH and Pawley, MJ 2010, New geochronology from the Albany–Fraser Orogen: implications for Mesoproterozoic magmatism and reworking, *in* Geological Survey of Western Australia Annual Review 2008–09: Geological Survey of Western Australia, p. 58–65.

Klussman, RW 2009, Transport of ultratrace reduced gases and particulate, near-surface oxidation, metal deposition and adsorption: Geochemistry: Exploration, Environment, Analysis, v. 9, p. 203–213.

Leybourne, MI and Cameron, EM 2010, Groundwater in geochemical exploration: Geochemistry: Exploration, Environment, Analysis, v. 10, p. 99–118.

Lintern, MJ and Butt, CRM 1993, Pedogenic carbonate: an important sample medium for gold exploration in semi-arid areas: Association of Applied Geochemists 16th International Geochemical Exploration Symposium, Beijing, China, September 1993; Abstracts, p. 115.

Lintern, MJ, Hough, RM, Ryan, CG, Watling, J and Verrall, M 2009, Ionic gold in calcrete revealed by LA-ICP-MS, SXRF and XANES: Geochimica et Cosmochimica Acta, v. 23, p. 1666–1683.

Mann, AW 2010, Strong versus weak digestions: ligand-based soil extraction geochemistry: Geochemistry: Exploration, Environment, Analysis, v. 10, p. 17–26.

McCuaig, TC, Beresford, S and Hronsky, J 2010, Translating the mineral systems approach into an effective exploration targeting system: Ore Geology Reviews, v. 38, p. 128–138.

McGuinness, SJ, 2010, Regolith-landform mapping of the east Wongatha area (digital data layer) *in* East Albany–Fraser and southeast Yilgarn, 2011 update: Geological Survey of Western Australia, Geological Exploration Package.

Morris, PA and Verren, AL 2001, Geochemical mapping of the Byro 1:250 000 sheet: Geological Survey of Western Australia, 1:250 000 Regolith Geochemistry Explanatory Notes, 53p.

Myers, JS 1990, Albany–Fraser Orogen, in Geology and mineral resources of Western Australia: Geological Survey of Western Australia, Memoir 3, p. 255–263.

Perincek, D 1998, A compilation and review of data pertaining to the hydrocarbon prospectivity of the Officer Basin: Geological Survey of Western Australia, Record 1997/6, 209p.

Petts, A, Hill, SM and Worrall, L 2009, Termite species variations and their importance for termitaria biogeochemistry: towards a robust media approach for mineral exploration: Geochemistry: Exploration, Environment, Analysis, v. 9, p. 257–266.

Reid, N, Lintern, M, Anand, R, Pinchand, T, Gray, D, Noble, R, Sutton, G and Jarrett, R 2010, North East Yilgarn biogeochemistry project (MERIWA): Geological Survey of Western Australia, Record 2010/4, 154p.

Reimann, C, Filzmoser, P, Garrett, RG and Dutter, R 2010, Statistical data analysis explained: John Wiley and Sons, Ltd, Chichester, UK, 343p.

Robertson, IDM 1999, Origins and applications of size fractions of soils overlying the Beasley Creek gold deposit, Western Australia: Journal of Geochemical Exploration, v. 66, no. 1–2, p. 99–113.

Rock, NMS 1988, Numerical geology: Springer-Verlag, Berlin, Germany, 427p.

Rogers, PJ and Dunn, CE 1993, Trace element chemistry of vegetation applied to mineral exploration in eastern Nova Scotia, Canada: Journal of Geochemical Exploration, v. 48, no. 1, p. 71–95.

Sanford, RF, Pierson, CT and Crovelli, RA 1993, An objective replacement method for censored geochemical data: Mathematical Geology, v. 25, no. 1, p. 59–80.

Shaw, WJ, Khosrowshahi, S, Horton, J and Waltho, A 1998, Predicting and monitoring variability in sampling, sample preparation and assaying, *in* More meaningful sampling in the mining industry *edited by* B Davis and SE Ho: Australian Institute of Geoscientists Bulletin 22, p. 11–19.

Smee, BW 1998, A new theory to explain the formation of soil geochemical responses over deeply covered gold mineralization in arid environments: Journal of Geochemical Exploration, v. 61, no. 1–3, p. 149–172.

Smith, RE, Birrell, RD and Brigden, JF 1989, The implications to exploration of chalcophile corridors in the Archaean Yilgarn Block, Western Australia, as revealed by laterite geochemistry: Journal of Geochemical Exploration, v. 32, p. 169–184.

Spaggiari, CV, Kirkland, CL, Pawley, MJ, Smithies, RH, Wingate, MTD, Doyle, MG, Blenkinsop, TG, Clark, C, Oorschot, CW, Fox, LJ and Savage, J 2011, The geology of the east Albany–Fraser Orogen — a field guide: Geological Survey of Western Australia, Record 2011/23, 97p.

Spaggiari, CV, Kirkland, CL, Pawley, MJ, Wingate, MTD, Smithies, RH and Howard, HM 2010, Building the Proterozoic Albany–Fraser Orogen on the Yilgarn Craton margin: setting the scene for Tropicana, *in* GSWA 2010 extended abstracts: promoting the prospectivity of Western Australia: Geological Survey of Western Australia, Record 2010/2, p. 30–32.

Tang, Z, Wu, L, Luo, Y and Christie, P 2009, Size fraction and characterization of nanocolloidal particles in soil: Environmental Geochemical Health, v. 31, p. 1–10.

Tate, SE, Greene, RSB, Scott, KM and McQueen, KG 2007, Recognition and characterisation of the aeolian component in soils in the Girilambone Region, north western New South Wales, Australia: Catena, v. 69, p. 122–133.

Tukey, JW 1977, Exploratory data analysis: Addison-Wesley, Reading, Massachusetts, USA, 506p.

Van De Graaff, WJE and Bunting, JA (compilers) 1977, Plumridge, Western Australia: Geological Survey of Western Australia, 1:250 000 Geological Series Explanatory Notes, 28p.

Wang, X 1998, Leaching of mobile forms of metals in overburden: development and application: Journal of Geochemical Exploration, v. 61, p. 39–55.

Wang, X, Wen, X, Rong, Y, Liu, Z, Sun, B, Zhao, S, Shi, S and Wei, H 2007, Vertical variations and dispersion of elements in arid desert regolith: a case study from the Jinwozi gold deposit, northwestern China: Geochemistry: Exploration, Environment, Analysis, v. 7, no. 2, p. 163–171.

Wu, B 1998, Nano-technology and new development of solid physics (in Chinese): Modern Scientific Instruments, v. 55–57, p. 34–43.

RECORD 2012/13

Fine-fraction geochemistry of regolith from the east Wongatha area, Western Australia: tracing bedrock and mineralization through cover

Morris

This Record is published in digital format (PDF) and is available as a free download from the DMP website at <http://www.dmp.wa.gov.au/GSWApublications>.

Further details of geological products produced by the Geological Survey of Western Australia can be obtained by contacting:

Information Centre
Department of Mines and Petroleum
100 Plain Street
EAST PERTH WESTERN AUSTRALIA 6004
Phone: (08) 9222 3459 Fax: (08) 9222 3444
http://www.dmp.wa.gov.au/GSWApublications